International Journal of Computational Engineering Research

Volume 4, Issue 9, September, 2014

Open Access JOURNAL

International Journal of Computational Engineering Research is an international, peer-reviewed journal publishing an overview of IT research and algorithmic processes that create, describe and transform information to formulate suitable abstractions to model complex systems.

International Journal of Computational Engineering Research under Open Access category aims to provide advance in the study of the theoretical foundations of information and computation and of practical techniques.

International Journal of Computational Engineering Research explicates the complicated aspects of Information Technology & Software Engineering and focusing on research and experience that contributes to the improvement of software development practices. The Journal has a dual emphasis and contains articles that are of interest both to practicing information technology professionals and to university and industry researchers.

International Journal of Computational Engineering Research - Open Access uses online manuscript submission, review and tracking systems for quality and quick review processing. Submit your manuscript at

http://www.ijceronline.com/online-submission.html

Editors & Editorial Board

CONTENTS:

S.No.	Title Name	Page No.
	Version I	
1.	Effect Of Curing Temperature And Curing Hours On The Properties Of Geo-Polymer Concrete **Mohammed Rabbani Nagral, Tejas Ostwal, Manojkumar V Chitawadagi**	01-11
2.	Analysis About Losses of Centrifugal Pump by Matlab **Ravi Shastri, Anjani Kumar Singh, Manish Kumar Singh**	12-22
3.	Design Consideration of Different Volute Casing at Best Efficiency Point for Commercial **Ravi Shastri , Anjani Kumar Singh , Manish Kumar Singh**	23-27
4.	Iterative Determinant Method for Solving Eigenvalue Problems **Owus M. Ibearugbulem, Osasona, E. S. , Maduh, U. J.**	28-31
5.	Efficient Query Evaluation of Probabilistic Top-k Queries in Wireless Sensor Networks **P.Supriya ,M.Sreenivasulu, Me**	32-37
6.	Effect of sintering time on the particle size and dielectric properties of La-doped PbTiO3 ceramic nanoparticles **A. A. Abd El-razek, E. M. Saed, M. K. Gergs**	38-44
7.	Can Digital Drawing Tools Significantly Develop Children's Artistic Ability and Creative Activity? **Aber Salem ABOALGASM ||Rupert WARD**	45-50
8.	Some Other Properties of Fuzzy Filters on Lattice Implication Algebras **Priyanka Singh|| Amitabh Banerjee|| Purushotam Jha**	51-54
9.	Global Domination Set in Intuitionistic Fuzzy Graph **R. JahirHussain || S. Yahya Mohamed**	55-58

ISSN (e): 2250 – 3005 || Vol, 04 || Issue, 9 || September – 2014 ||
International Journal of Computational Engineering Research (IJCER)

Effect Of Curing Temperature And Curing Hours On The Properties Of Geo-Polymer Concrete

Mohammed Rabbani Nagral[1], Tejas Ostwal[2], Manojkumar V Chitawadagi[3]
[1] Graduate Student, Civil Engineering, B. V. B. College of Engineering & Technology, Karnataka, India
[2] UG Student, Civil Engineering, B. V. B. College of Engineering & Technology, Karnataka, India
[3] Professor, Civil Engineering, B. V. B. College of Engineering & Technology, Karnataka, India

ABSTRACT:
Geopolymer, an inorganic alumina silicate polymer is synthesized predominantly from silicon and aluminum materials or from by-product materials like fly ash. In the present paper the effect of curing temperature, curing hours on Geo-polymer Concrete(GPC) specimens and also the effect of extra water on workability and compressive strength of GPC cubes were studied. Fly ash and GGBS were used as binder, combined with an alkaline solution to form geopolymer paste instead of cement paste to bind the aggregates. The experiments were conducted on GPC cubes for curing temperature of 80° C, 90° C and 100° C with curing period of 12 and 24 hours by adopting hot oven curing method. The constants used in the experiments were alkaline solution to binder ratio taken as 0.45, molarity of NaOH solution as 12M and ratio of sodium silicate to sodium hydroxide as 2.5. All the specimens were kept at one day rest period. The tests were conducted on each sample and results revealed that there is an increase in compressive strength for curing temperature 80°C to 90°C for both 12 and 24 hours of curing of GPC specimens. Maximum strength was obtained at temperature of 90°C for 12 hours of curing period. Beyond this, increase in curing temperature resulted in decrease in compressive strength of GPC specimen. Furthermore the study was continued by varying water to geopolymer solids ratio and addition of extra water to study the workability and compressive strength of GPC specimens at optimum temperature 90°C-12 hours. Results showed that increase in water to geopolymer solids ratio and extra water increased the workability of GPC and decreased the compressive strength of GPC.

KEYWORDS: *Curing hours, Curing strength, Curing temperature, Flyash, GGBS, GPC.*

I. INTRODUCTION

Demand for concrete as a construction material is on the increase so as the production of cement. The production of cement is increasing about 3% annually. The production of one ton of cement liberates about one ton of CO_2 into the atmosphere. Also, Portland cement is the most energy intensive construction material, after aluminum and steel [1]. In recent years, geopolymer has emerged as a novel engineering material in the construction industry [2, 3]. It is formed by the alkali activation reaction between alumina-containing and silica-containing solids and alkali activators. The raw material for geopolymer production normally comes from industrial by-products, for instance, fly ash and blast furnace slag. In India more than 100 million tons of fly ash is produced annually. Out of this, only 17 – 20% is utilized either in concrete or in stabilization of soil. Most of the fly ash is disposed off as a waste material that coves several hectares of valuable land [4]. There are environmental benefits in reducing the use of Portland cement in concrete, and using a by-product material, such as fly ash as a substitute. The industrial by-products can substitute cement clinker by 100% in the system of geopolymer. For this reason, geopolymer is generally considered as an environment-friendly construction material with great potential for sustainable development. Apart from the environmental advantages, pastes and concrete made of geopolymer can exhibit many excellent properties, for example, high early-age strength, low creep and shrinkage, high resistance to chemical attack and good fire resistance [5,6].

The process of geo-polymerization takes place by activating the alumino-silicate waste materials with high alkaline solution. The most crucial aspect which plays an important role in the polymerization process is the curing of freshly prepared geopolymer concrete. Proper curing of concrete has a positive effect on the final properties of the geopolymer concrete.

As the reaction of fly ash-based geopolymeric materials is very slow and usually show a slower setting and strength development, the curing of geopolymer concrete is mostly carried out at elevated temperatures [7]. Previous research has shown that both curing time and curing temperature significantly influence the compressive strength of geopolymer concrete. Several researchers have investigated the effect of curing time and curing temperature on the properties of geopolymer concrete. It is reported by Palomo et al. [8], in their study on fly ash-based geopolymers that the curing temperature and curing time significantly affected the mechanical strength of fly ash-based geopolymers. The results also revealed that higher curing temperature and longer curing time resulted in higher compressive strength. Hardjito et al. [9, 10] studied the influence of curing temperature, curing time and alkaline solution-to-fly ash ratio on the compressive strength. The authors confirmed that the temperature and curing time significantly improves the compressive strength, although the increase in strength may not be significant for curing at more than 60°C. The results also revealed that the compressive strength decreases when the water-to-geopolymer solids ratio by mass is increased. The drying shrinkage strains of fly ash based geopolymer concrete were found to be significant.

The present study was aimed at producing GPC cubes of strength 50MPa by using Fly ash and GGBS as binders for 12M molarity of NaOH solution. Samples were cured at 80ºC, 90ºC and 100°C with curing hours of 12 hours and 24 hours. From these results the optimum temperature and curing hours were obtained corresponding to high compressive strength of geopolymer concrete. Further study was extended to study the effect of extra water on workability and compressive strength of geopolymer concrete cured at optimum temperature and curing hours.

II. MATERIALS

Fly ash which was obtained from Raichur Thermal Power Station, India and GGBS obtained from JSW steel, Bellary, India were having specific gravity of 2.4 & 2.9 respectively. The chemical composition of Flyash & GGBS as obtained by X-ray fluorescence (XRF) is shown in Table-1 & Table-3 respectively. The IS code requirements & composition of Flyash is shown in Table-2. The class F fly ash used here confirms to requirement as per 3812-2003 IS code & shown in Table 2. Locally available Fine aggregate of specific gravity 2.8 & Coarse aggregate of specific gravity 2.7 were used in this experimental work. A combination of 12M sodium hydroxide and sodium silicate in the ratio of 2.5 was used as solution for activation. Sodium hydroxide solution NaOH (97% purity), in the form of pellets were used in this work. Sodium silicate also known as water glass is of industrial grade with SiO_2 as 34.8% by mass and Na_2O as 16.51% & water as 48.69%. Water used for the mix is of potable quality. The plasticizers are used to improve the workability of geopolymer concrete, the addition of super plasticizer, up to approximately 4% of fly ash by mass, improves the workability of the fresh fly ash-based geopolymer concrete; however, there is a slight degradation in the compressive strength of hardened concrete when the super plasticizer dosage is greater than 2% [11]. Hence in the present study dosage of plasticizer (conplast 430) was taken as 1% of Binder.

Table-1: Chemical composition of Fly ash as determined by XRF analysis in (mass %)

Binder	**Fly Ash**
S.Gr	2.4
*LOI	0.90
Al_2O_3	31.23
Fe_2O_3	1.50
SiO_2	61.12
MgO	0.75
SO_3	0.53
Na_2O	1.35
Chlorides	0.05
CaO	3.2

*LOI - Loss on Ignition

Table -2 : Constitution of Flyash and code requirements

Constituents	**Composition in %**	**Requirements as per IS 3812- 2003**
LOI	0.90	Max 5
(Al_2O_3+Fe_2O_3+SiO_2)	93.85	Min 70
SiO_2	61.12	Min 35
MgO	0.75	Max 5
SO_3	0.53	Max 3
Na_2O	1.35	Max 1.5
Chlorides	0.05	Max 0.05

Table -3: Chemical composition of GGBS as determined by XRF analysis in (mass %)

Binder	**GGBS**
S.Gr	2.9
LOI	0.19
Al_2O_3	13.24
Fe_2O_3	0.65
SiO_2	37.21
MgO	8.46
SO_3	2.23
Na_2O	- - -
Chlorides	0.003
CaO	37.2

III. EXPERIMENTAL WORK

3.1 Mix Design

Concrete mix design process is vast and generally based on performance criteria. Initially the density of Geopolymer concrete was assumed as 2400 kg/m^3. The coarse and fine aggregates were taken as 72% of entire mixture by mass as per Lloyd et al [12]. This value is similar to that used in OPC concrete in which it will be in the range of 75% to 80% of the entire mixture by mass. Fine aggregate were taken as 30% of the total aggregates. The remaining mass is the combination of Alkaline solution and Binder (Geopolymer paste). Assuming the Alkaline solution to Binder ratio as 0.45 the masses of Alkaline solution and Binder in kg/m^3 were obtained. Assuming Sodium silicate solution to Sodium Hydroxide Solution ratio as 2.5, mass of Sodium silicate solution and sodium hydroxide solution were obtained in kg/m^3. Assuming the molarity of sodium hydroxide solution as 12M, the geopolymer mix was designed. To study the effect of high temperature curing and to get optimum temperature and curing hours the mix proportions were prepared as listed in Table -4.

Water present in geopolymer concrete is of two types namely, water present in alkaline solution and extra water. Water present in alkaline solution is of very small quantity and hence geoplymer concrete mixes are usually very stiff. Therefore to improve the workability and to make geopolymer mix as a homogeneous mix an extra water is added to the mix, but this water is the main parameter which directly affects the strength of geopolymer concrete. Hence in the present work, the extra water was studied as varying parameter, to study the properties of geopolymer concrete. After obtaining the optimum curing temperature and curing hours the mix proportion details of geopolymer concrete to study the effect of extra water on workability and compressive strength of geopolymer concrete were prepared as shown in Table -5.

3.2 Preparation of fresh Geopolymer concrete

The manufacturing of geopolymer concrete was similar to cement concrete, the process involved preparation of alkaline solution, dry mixing, wet mixing, curing & testing of samples. To prepare sodium hydroxide solution of 12 molarity, 480 g (12 x 40) i.e (molarity x molecular weight) of sodium hydroxide pellets were dissolved in one litre of water. The mass of sodium hydroxide solids in the solution varies depending on the concentration of the solution expressed in terms of molar M. The prepared NaOH solution was added with sodium silicate solution proportionately according to the mix, 24 hours before casting.

Table -4: Mix design trials with different curing temperatures and curing hours

Materials	GPC1	GPC2	GPC3	GPC4	GPC5	GPC6
Coarse Aggregate (kg/m^3)	1123.2	1123.2	1123.2	1123.2	1123.2	1123.2
Fine Aggregate (kg/m^3)	604.8	604.8	604.8	604.8	604.8	604.8
Fly ash (kg/m^3)	231.72	231.72	231.72	231.72	231.72	231.72
GGBS (kg/m^3)	231.72	231.72	231.72	231.72	231.72	231.72
NaOH Solution (kg/m^3)	59.59	59.59	59.59	59.59	59.59	59.59
Molarity of NaOH	12M	12M	12M	12M	12M	12M
Na_2SiO_3 Solution (kg/m^3)	148.96	148.96	148.96	148.96	148.96	148.96
Temperature (ºC)	80	80	90	90	100	100
Curing Period (Hours)	12	24	12	24	12	24
Water to geopolymer solids ratio	0.201	0.201	0.201	0.201	0.201	0.201
Alkaline solution to Binder ratio	0.45	0.45	0.45	0.45	0.45	0.45
Rest period (days)	1	1	1	1	1	1
Extra Water (kg/m^3)	0	0	0	0	0	0
Slump (mm)	0	0	0	0	0	0
Super Plasticizers (Conplast 430) in % of binder	1%	1%	1%	1%	1%	1%

The coarse aggregate, fine aggregate, flyash and GGBS were taken in required amount in a mixing tray and dry mixed manually for about two minutes. The alkaline solution prepared 24 hours before was thoroughly stirred, then the required amount of superplastisizer was mixed with the alkaline solution and was added to the dry mix, addition of solution had to be done in small quantities so that there was no wastage of solution, usually the wet mixing time should be about 10 to 15 minutes or greater. The mixing of total mass was continued until the mixture became homogeneous and uniform in colour. After this the mix was left for 10 to 15 minutes then the extra water was added to the mix, again after mixing homogenously the slump test was carried out.
The fresh geopolymer concrete was casted in cubes of size 150 X 150 X 150 mm to three layers and was compacted by using the standard compaction rod so that each layer received 25 strokes followed by further compaction on the vibrating table. Then the cubes were kept at room temperature for one day rest period.

The casted specimens after one day rest period were demoulded and specimens were kept in oven for 80ºC, 90ºC and 100ºC for the curing period 12 hours and 24 hours as shown in Figure-1, after required curing period the specimens were removed from the oven and were kept open at room temperature until testing as shown in Figure-2.

The specimens were removed from the oven; after the cooling of the samples, the specimens for the required period (3^{rd} day and 7^{th} day) were tested as per IS 516 : 1979 in the Compressive Testing Machine of capacity 2000 kN for obtaining ultimate load of the specimens.

Fig-1: Specimens kept in Oven of 300°C capacity

Fig-2 : Specimens kept at room temperature after removing from oven

Table -5: Mix design trials with different water to geopolymer solids ratio and extra water

Materials	GPC7	GPC8	GPC9	GPC10
Coarse Aggregate (kg/m^3)	1123.2	1123.2	1123.2	1123.2
Fine Aggregate (kg/m^3)	604.8	604.8	604.8	604.8
Fly ash (kg/m^3)	231.72	231.72	231.72	231.72
GGBS (kg/m^3)	231.72	231.72	231.72	231.72
NaOH Solution (kg/m^3)	59.59	59.59	59.59	59.59
Molarity of NaOH	12M	12M	12M	12M
Na_2SiO_3 Solution (kg/m^3)	148.96	148.96	148.96	148.96
Temperature (°C)	90	90	90	90
Curing Period (Hours)	12	12	12	12
Water to geopolymer solids ratio	0.25	0.30	0.35	0.40
Alkaline solution to Binder ratio	0.45	0.45	0.45	0.45
Rest period (days)	1	1	1	1
Extra Water (kg/m^3)	27	55	83	111
Slump (mm)	10	68	126	170
Super Plasticizers (Conplast 430) in % of binder	1%	1%	1%	1%

IV. RESULTS AND DISCUSSIONS

4.1 Effect of Temperature and Curing Hours on Compressive Strength of Geopolymer Concrete

Compressive strength of geopolymer concrete mainly depends on the temperature of curing and corresponding curing hours. In the present investigation, 3rd day and 7th day compressive tests were conducted with concrete cubes of size 150mm X 150mm X 150mm.

Table -6 : Mean compressive strength of GPC specimens at curing temperature of 80°C

Sample Name	Mean Density (kg/m^3)	Mean Compressive Strength (N/mm^2)	Curing Temperature (°C)	Curing Period (hours)	Days Of Testing
GPC1	2468	38.71	80	12	3
GPC1	2387	51.15	80	12	7
GPC2	2450	50.22	80	24	3
GPC2	2505	57.53	80	24	7

Table -7 : Mean compressive strength of GPC specimens at curing temperature of 90°C

Sample Name	Mean Density (kg/m^3)	Mean Compressive Strength (N/mm^2)	Curing Temperature (°C)	Curing Period (hours)	Days Of Testing
GPC3	2430	67.91	90	12	3
GPC3	2434	76.53	90	12	7
GPC4	2398	66.20	90	24	3
GPC4	2462	60.91	90	24	7

Table -8 : Mean compressive strength of GPC specimens at curing temperature of 100°C

Sample Name	Mean Density (kg/m^3)	Mean Compressive Strength (N/mm^2)	Curing Temperature (°C)	Curing Period (hours)	Days Of Testing
GPC5	2357	57.24	100	12	3
GPC5	2499	54.18	100	12	7
GPC6	2505	47.24	100	24	3
GPC6	2481	46.12	100	24	7

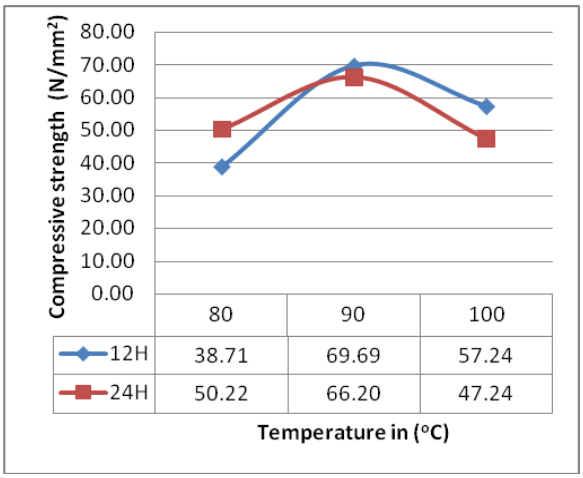

Fig-3 Variation of compressive strength on 3rd day represented graphically

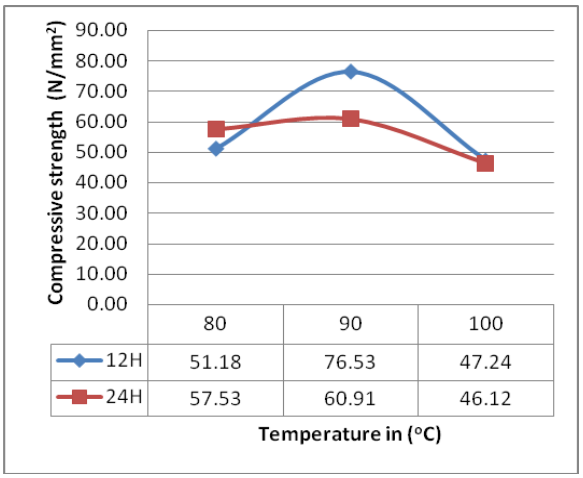

Fig-4 Variation of compressive strength on 7th day represented graphically

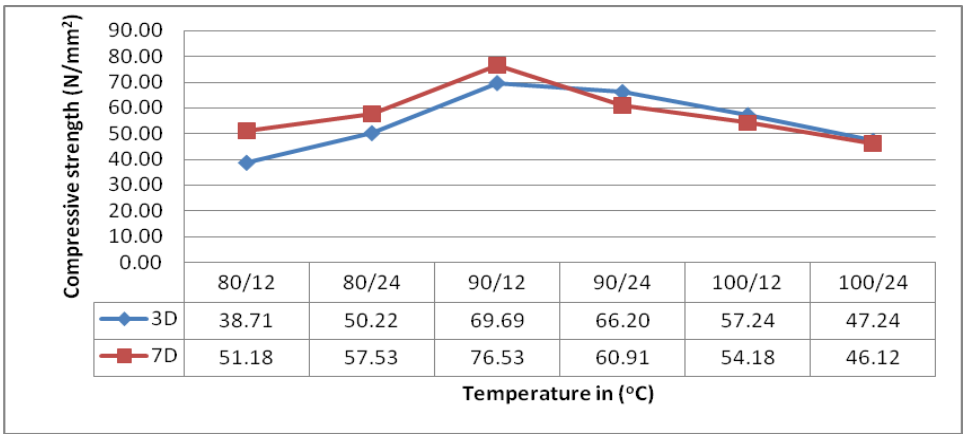

Fig-5 Spread compression strength for all combinations of curing temperatures and curing time

Fig-3 shows the compressive strength of geopolymer concrete specimen at different temperatures and different curing periods on 3rd day. The curing temperature at 90ºC showed better compressive strength than 80ºC and 100ºC. Furthermore 90ºC-12 hour curing produced maximum strength when compared with 90ºC-24 hours curing. This showed that curing hours play an important role in achieving the compressive strength of geopolymer concrete. This was because polymerization process increases with increase in the temperature and at a high temperature the 2D-polymer chains are converted into 3D-polymer chain with strong bond. At the same time the higher temperature results in increase in the rate of development of strength. This was same as observed in [13,14] and using high temperatures 90°C -12 hours produced compressive strength of 69.69MPa on 3rd day as compared to [15] in which 28th day compressive strength was 52MPa. Beyond this optimum temperature, increase in the curing temperature and curing hours reduced the compressive strength of geopolymer concrete specimens. The loss in compressive strength was due to continuous moisture loss from the specimens which produced voids and resulted in strength degradation. Fig-4 shows the compressive strength of geopolymer concrete specimen at different temperatures and different curing periods on 7th day. The curing temperature at 90ºC showed better compressive strength than 80ºC and 100ºC. Furthermore 90ºC-12 hours curing produced maximum strength when compared with 90ºC-24 hours curing. This showed that curing hours play an important role in achieving the compressive strength of geopolymer concrete. This was because polymerization process increases with increase in the temperature and at a high temperature the 2D-polymer chains are converted into 3D-polymer chain with strong bond. At the same time the higher temperature results in increase in the rate of development of strength. This was as same as observed in [13,14] and using high temperatures 90ºC-12 hours produces compressive strength 76.53MPa on 7th day as compared to [15] in which 28th day compressive strength was 52MPa.

Fig-5 shows that the compressive strength of GPC increased with increase in the temperature along with the curing hours from 80ºC to 90ºC for 12 hours curing on 3rd and 7th day of test. From the experiments it was observed that 7th day strength cured at 90ºC-12 hours produced maximum strength, which is the optimum temperature for the further study but when the curing period increased beyond 12 hours the compressive strength of geopolymer concrete decreased, this decrease in compressive strength would have been due to the continuous evaporation of moisture from the specimens. As the water content in geopolymer concrete was very less and when subjected to high temperature, there was loss of moisture on the surface which may have developed surface cracks, hence strength of geopolymer concrete decreased.

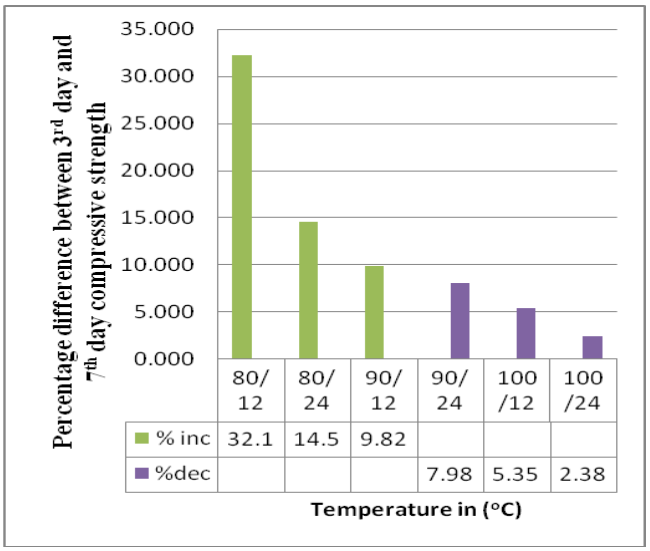

Fig-6 Variation in percentage change of compressive strength of GPC with varying temperatures and curing time

From fig-6 it is derived that, at 80º-12 hours the percentage increase in the strength from 3rd day to 7th day was 32.19%, at 80º-24 hours the percentage increase in the strength from 3rd day to 7th day was 14.55% and at 90º-12 hours the percentage increase in the strength from 3rd day to 7th day was 9.82%. This showed that increase in the temperature resulted in decrease in percentage difference from 3rd day to 7th day and also the increase in temperature up to an optimum temperature increased the rate of development of the strength. This was due to the degree of polymerization which directly depended on the temperature of curing, higher temperature resulted in the increase of degree of polymerization.

4.2 Effect of extra water & water to geopolymer solids ratio on the properties of Geopolymer concrete

In the present study, optimum temperature and curing hours which corresponded to maximum strength were 90^0-12 hours. When the water to geopolymer solids were kept as 0.201 the mix was not workable, but as per [12] when water to geopolymer solids was 0.20 the concrete showed moderate workability. The reason for this would have been the total aggregate to water ratio, coarse aggregate to water ratio and the size of coarse aggregate. As per the tests conducted by [12] the total aggregate to water ratio and the coarse aggregate to water ratio were taken as 21 and 14.7 respectively. But in the present study the total aggregate to water ratio and coarse aggregate to water ratio were taken as 15.31 and 9.96 and moreover half of the binder was replaced by GGBS which was much finer than the fly ash particles, hence these were the reasons for getting lower workability at water to geopolymer solids ratio of 0.201. Hence, further study was carried to make workable mix of geopolymer concrete by addition of extra water, this extra water was calculated by varying the water to geopolymer solids ratio and is tabulated in Table-9. The results of the slump and compressive strength of geopolymer concrete are tabulated in Table-9.

Table -9 : Mean Compressive Strength of GPC Specimens varying with addition of extra water and water to geopolymer solids ratio at an optimum temperature 90^0C-12 hours on 7th day

Sample Name	Density (kg/m^3)	Compressive Strength (N/mm^2)	Water to Geopolymer Solids ratio	Extra Water (kg/m^3)	Optimum Temperature (^{0}C) and optimum curing hours	Slump (mm)	% Decrease in Compressive Strength
GPC3	2434	46.53	0.2	0	90^0/12 hours	0	------
GPC7	2510	70.24	0.25	27	90^0/12 hours	10	8.22%
GPC8	2591	63.64	0.3	55	90^0/12 hours	68	16.84%
GPC9	2548	60.42	0.35	83	90^0/12 hours	126	21.05%
GPC10	2537	55.53	0.4	111	90^0/12 hours	170	27.44%

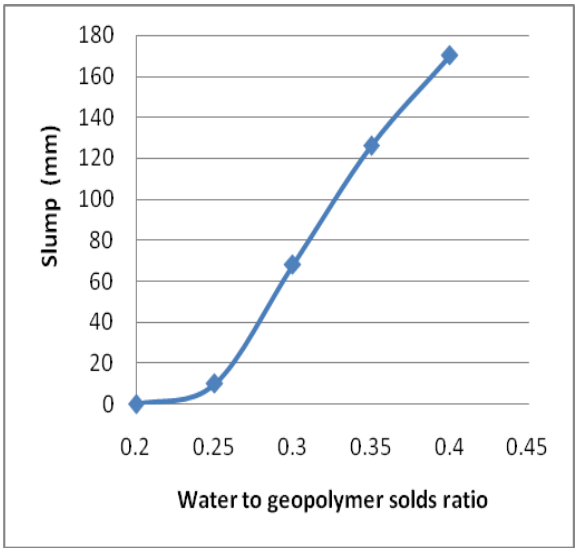

Fig-7 Water to geopolymer solids ratio Vs slump

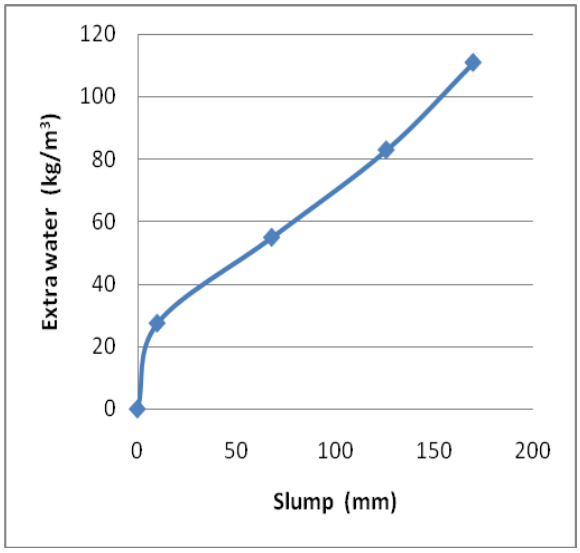

Fig-8 Variation of slump with extra water

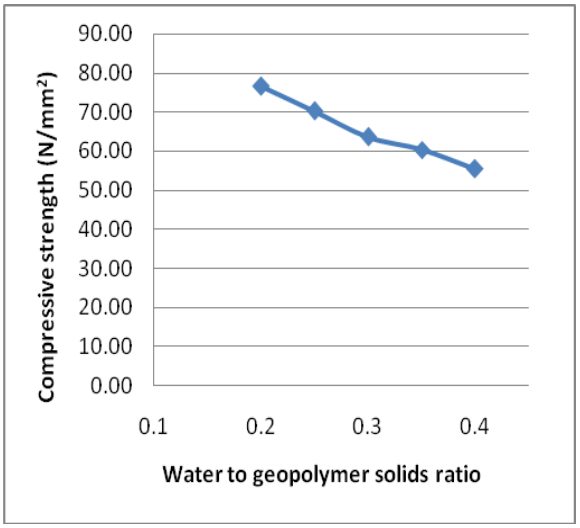

Fig-9 Variation of compressive strength with water to geopolymer solids ratio

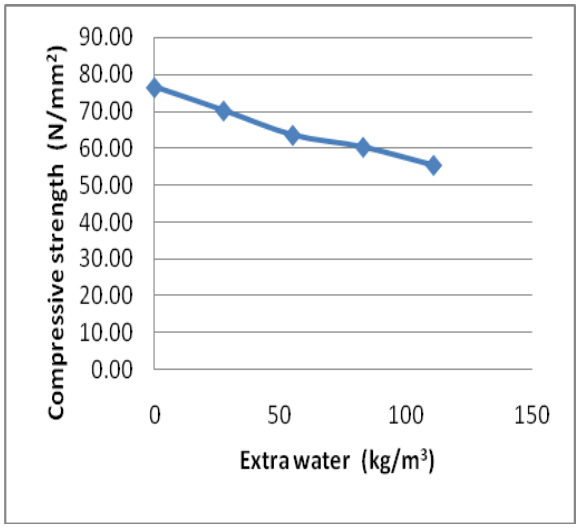

Fig-10 Variation of compressive strength with extra water

4.3 Effect of extra water and water to geopolymer solids ratio on the properties geopolymer concrete

From fig-7 and fig-8 it is clear that by increasing the water to geopolymer solids ratio and addition of extra water the workability of geopolymer concrete had increased as seen in Table-9. When the water to geopolymer solids ratio increased from 0.25 to 0.4 the corresponding slump was from 10 to 170 mm respectively. According to IS 456-2000 when slump is lesser than 25mm the concrete is said to be very low workable and when the slump is greater than 150mm it is said to be very high workable. In this study for water to geopolymer solids ratio of 0.3 slump obtained was 68 mm, hence this can be used for less reinforced concrete work and for water to geopolymer solids ratio of 0.35, the slump obtained was 126 mm, hence this can be used for congested reinforced concrete. Therefore by adjusting the water to geopolymer solids in the range 0.2 to 0.4, the desired slump for the desire work can be obtained.

From fig-9 and fig-10 it is clear that the compressive strength of geopolymer concrete depends on the water to geopolymer solids and extra water. Increasing the water to geopolymer solids ratio and extra water resulted in decrease of compressive strength of geopolymer concrete. This may be due to increase in the water content which resulted in the void formation after evaporation of water during curing process and also the increase in water resulted in the increase of H_2O to Na_2O ratio which further resulted in decrease of strength[13]. Based on the present study it is observed that high strength geopolymer concrete can be produced and strength can be achieved as early as in 7 days as compared to conventional concrete at 28 days. Hence it is much advantageous in fast track constructions.

V. CONCLUSIONS

Following conclusions were drawn from the experimental results of this study by varying curing temperature, curing hour, water to geopolymer solids ratio and extra water to achieve the compressive strength of 50MPa:

- The compressive strength of geopolymer concrete increases with increase in the curing temperature upto an optimum temperature of 90^0C & curing period of 12 hours to achieve the desired strength of 50MPa, beyond which the compressive strength of geopolymer concrete reduces.
- For the geopolymer solids to water ratio of 0.2-0.4, when extra water of 0-111kg/m^3 is added, the slump value increases from 0-170mm, while the compressive strength decreases from 0-27.44% respectively. Hence the design of GPC mix can be made for desired workability and compressive strength at the cost of extra water.

ACKNOWLEDGEMENT : This Research project was supported by B.V.B. College of Engineering & Technology, Hubli, Karnataka, India. The authors are also thankful to the Department of Civil Engineering for promoting this Research.

REFERENCES

[1] J. Davidovits. "Global Warming Impact on the Cement and Aggregate Industries". World Resource review 1995; Vol. 6, no. 2, pp. 263-278.
[2] M. Ahmaruzzaman. "A review on the utilization of fly ash". Progress in Energy and Combustion Science 2010; 36(3):327–363.
[3] P. Duxson, J.L. Provis, G.C. Lukey, J.S.J. van Deventer. "The role of inorganic polymer technology in the development of 'green concrete'". Cement and Concrete Research 2007; 37(12):1590–1597.
[4 V.M. Malhotra, A.A. Ramezanianpour. "Fly ash in concrete". Canada Centre for Mineral and Energy Technology (CANMET) September 1994; pp.1-253.
[5] S.A. Palomo, A. Femandez-Jimenez. "Alkaline activation of fly ashes: NMR study of the reaction products". Journal of the American Ceramic Society 2004; 87(6):1141–1145.
[6] A. Fernández-Jiménez, S.A. Palomo. "Composition and microstructure of alkali activated fly ash binder: effect of the activator". Cement and Concrete Research 2005; 35(10):1984–1992.
[7] B.V. Rangan, D. Hardjito, S.E. Wallah, D.M.J. Sumajouw. "Studies on fly ash-based geopolymer concrete. Geopolymer: green chemistry and sustainable development solutions". Faculty of Engineering and Computing, Curtin University of Technology, GPO Box U 1987, Perth 6845, Australia, pp. 133-138.
[8] A. Palomo, M.W. Grutzeck, M.T. Blanco. "Alkali-activated fly ashes – A cement for the future". Cement and Concrete Research 1999; 29 (8): pp. 1323–1329.
[9] D. Hardjito, S.E. Wallah, D.M.J. Sumjouw and B.V. Rangan, "Properties of Geopolymer Concrete with Fly Ash as Source Material: Effect of Mixture Composition", Seventh CANMET/ACI International Conference on Recent Advances in Concrete Technology, Las Vegas, USA, 26-29 May, 2004.
[10] D. Hardjito, S.E. Wallah, D.M.J. Sumjouw and B.V. Rangan. "Fly ash-Based Geopolymer Concrete, Construction Material for Sustainable Development", Invited paper, Concrete World: Engineering and Materials, American Concrete Institute, India Chapter, Mumbai, India, 9-12 December 2004.
[11] M. F. Nuruddin, S. Demie, M.F.Ahmed, and N. Shafiq. "Effect of super plasticizer and NaOH molarity on workability, compressive strength and microstructure properties of self-compacting geo-polymer concrete". World Academy of Science, Engineering and Technology 2011; Vol. 5, No. 3, pp. 1378–1385.
[12] N. Lloyd, B.V. Rangan. "Geopolymer Concrete with Fly Ash". In Second International Conference on Sustainable Construction Materials and Technologies, Ancona, Italy: UWM Center for By-Products Utilization. Jun 28, 2010.

[13] D. Hardjito, S.E. Wallah, D.M.J. Sumajouw & B.V. Rangan."On The Development of Fly Ash-Based Geopolymer Concrete." ACI Materials Journal 2004; Vol. 101, No. 6, pp 467-472.
[14] D. Hardjito, S.E. Wallah, D.M.J. Sumajouw & B.V. Rangan. "Fly Ash-Based Geopolymer Concrete". Australian Journal of Structural Engineering 2005; Vol. 6, No. 1, pp. 77-85.
[15] N.P. Rajamane, M.C. Nataraja, N. Lakshmanan, J.K. Dattatreya & D. Sabitha. "Sulphuric acid resistant ecofriendly concrete from geopolymerisation of blast furnaceslag". Indian Journal of Engineering & Materials Sciences 2012; Vol. 19, pp. 357-367.

ISSN (e): 2250 – 3005 || Vol, 04 || Issue, 9 || September – 2014 ||
International Journal of Computational Engineering Research (IJCER)

Analysis About Losses of Centrifugal Pump by Matlab

[1]Ravi Shastri, [2]Anjani Kumar Singh, [3]Manish Kumar Singh

[1]*Asst. Prof. Cambridge Institute of Technology, Tatisilway, Ranchi, Jharkhand, India*

[2]*Ph.D. Scholar, Materials and metallurgical Engineering National Institute of Foundry and Forge Technology, Hatia, Ranchi, Jharkhand, India*

[3]*M.Tech Scholar, Materials Science and Engineering, National Institute of Foundry and Forge Technology, Hatia, Ranchi, Jharkhand, India*

ABSTRACT :

Design aids available today might have helped the pump designers to bring about theoretically the most efficient pumps, but the production technology and quality control during manufacture has not kept pace with such achievements in realizing the goals of developing energy efficient pumps. Pump designers often face the problem of selecting and optimizing a number of independent geometrical parameters whilst aiming at the derived efficiency from the pump. The only option is to approximate the theoretical design with experimental findings iteratively until the end result is achieved. It is found that about half of pumps were not performing efficiently, either because the wrong pump had been chosen for the job or because the pump was worn. If the pump is not doing its job, this can increase pumping costs and reduce productivity. To certain costs, use need to monitor energy usage regularly and repair and maintain the pump to operate efficiently. The aim of careful pump design parameter selection and regular pump maintenance is to have the pump performing as efficiently as possible, because this gives the lowest running costs. The pressure and flow that a pump is working at is called the duty. Efficiency changes with the range of possible duties for any specific pump. If one can improve pump efficiency for that the pump was designed to operate at, means reducing pumping costs. Pump efficiency measures hour well the pump converts electrical power to useful work moving the water.In addressing problems related to pumps, beside computing velocities, losses and other variables, the main aim is to study the effects of the various parameters on the performance of the machine and to investigate conditions that minimize losses and brake power, and maximize water power, overall efficiency, and other factors.

KEY WORDS: *Euler Equation, MATLAB*

I. INTRODUCTION

Pumps are used in a wide range of industrial and residential applications. Pumping equipment is extremely diverse, varying in type, size, and materials of construction. There have been significant new developments in the area of pumping equipment. They are used to transfer liquids from low-pressure to high pressure in this system, the liquid would move in the opposite direction because of the pressure difference.Centrifugal pumps are widely used for irrigation, water supply plants, stream power plants, sewage, oil refineries, chemical plants, hydraulic power service, food processing factories and mines. Moreover, they are also used extensively in the chemical industry because of their suitability in practically any service and are mostly used in many applications such as water pumping project, domestic water raising, industrial waste water removal, raising water from tube wells to the fields. A centrifugal pump delivers useful energy to the fluid on pump-agelargely through velocity changes that occur as this fluid flows through the impeller and the associated fixed passage ways of the pump. It is converting of mechanical energy to hydraulic energy of the handling fluid to get it to a required place or height by the centrifugal force of the impeller blade. The input power of centrifugal pump is the mechanical energy and such as electrical motor of the drive shaft driven by the prime mover or small engine. The output energy is hydraulic energy of the fluid being raised or carried. In a centrifugal pump, the liquid is forced by atmospheric or other pressure into a set of rotating vanes. A centrifugal pump consists of a set of rotation vanes enclosed within a housing or casing that is used to impart energy to a fluid through centrifugal force [1-3].

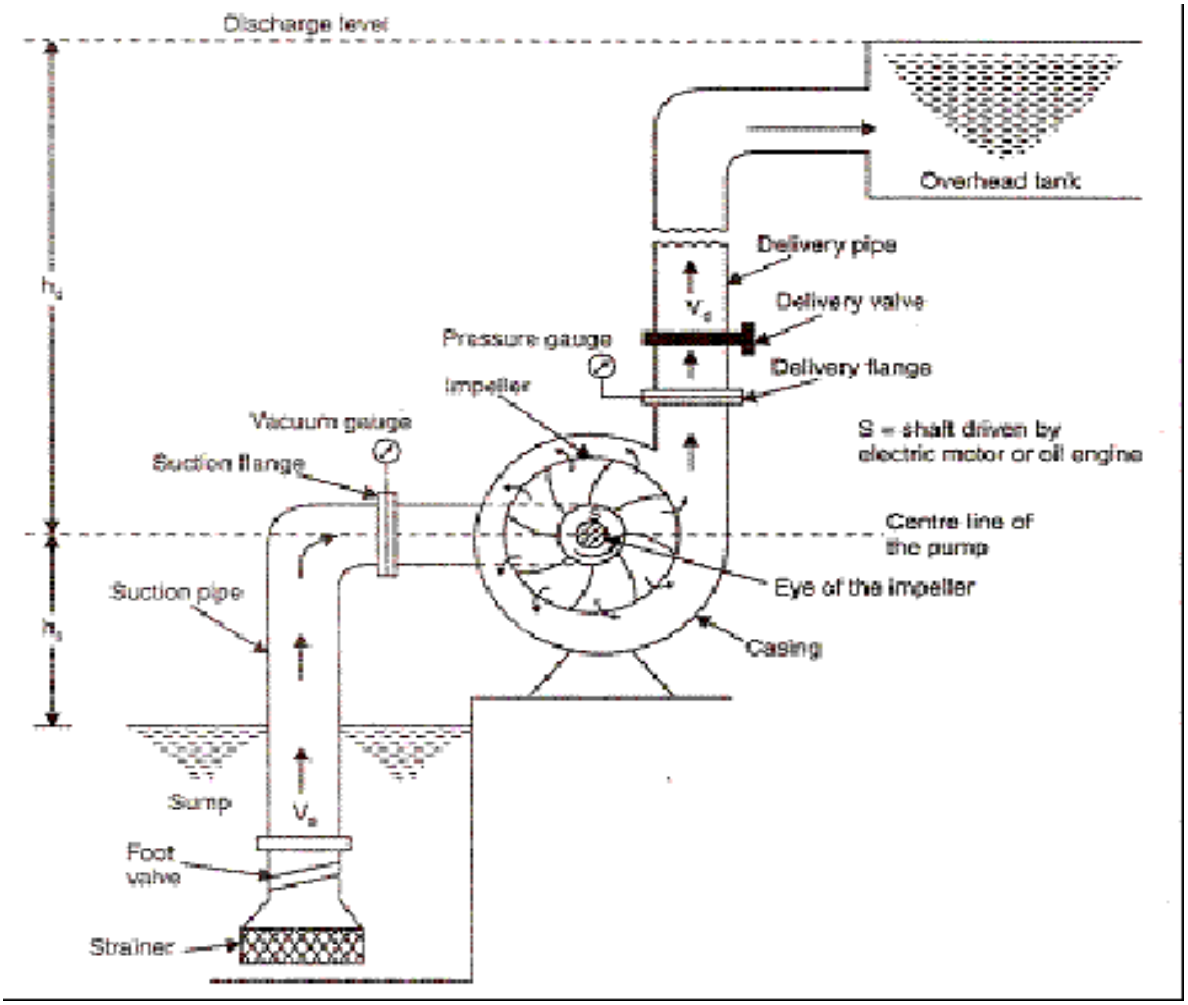

Fig: 1 Centrifugal Pump

A pump transfer mechanical energy from some external source to the liquid flowing through it and losses occur in any energy conversion process. The energy transferred is predicted by *the Euler Equation*. The energy transfer quantities are losses between fluid power and mechanical power of the impeller or runner. Thus, centrifugal pump may be taken losses of energy. The kinds of loss of centrifugal pumps can be differentiated in internal losses and external or mechanical losses. The internal loss is hydraulic losses or blade losses by friction, variations of the effective area or changes of direction losses of quantity at the sealing places between the impeller and housing at the rotary shaft seals. The external or mechanical loss is sliding surface losses by bearing friction or seal friction [2, 4].

Data of Centrifugal Pump:

For design calculation, the design parameters are taken as follows:

Flow rate, Q = 0.00293 m^3/s

Head, H = 10 m

Pump speed, n = 2900 rpm

density of water, ρ= 1000 kg/m^3

Specific Speed: $n_s = 3.65n\frac{\sqrt{Q}}{(10)^{3/4}}$(1)

The water power is determined from the relationship

$N= \rho gHQ$(2)

Shock Losses: The major loss considered is shock losses at the impeller inlet caused by the mismatch of fluid and metal angles. Shock losses can be found everywhere in the flow range of the pump. Shock Losses are given by following equation:

$h_s = k(Q_S-Q_N)^2$ (3)
Where k is the coefficient of leakage loss which value is assumed as 0.005.
Maximum flow rate: $Q_N = \pi D_1 b_1 V m_1$(4)

Table (a) - Shock Losses versus Flow Rate Graph

SL NO.	1	2	3	4	5	6	7	8	9	10	11	12	13	14	15
h_s	7.6	5.8	4.2	2.9	1.9	1.0	0.4	0.1	0	0.2	0.6	1.3	2.2	3.4	4.9
Q	0	0.0005	0.001	0.0015	0.002	0.0025	0.003	0.0035	0.004	0.0045	0.005	0.0055	0.006	0.0065	0.007

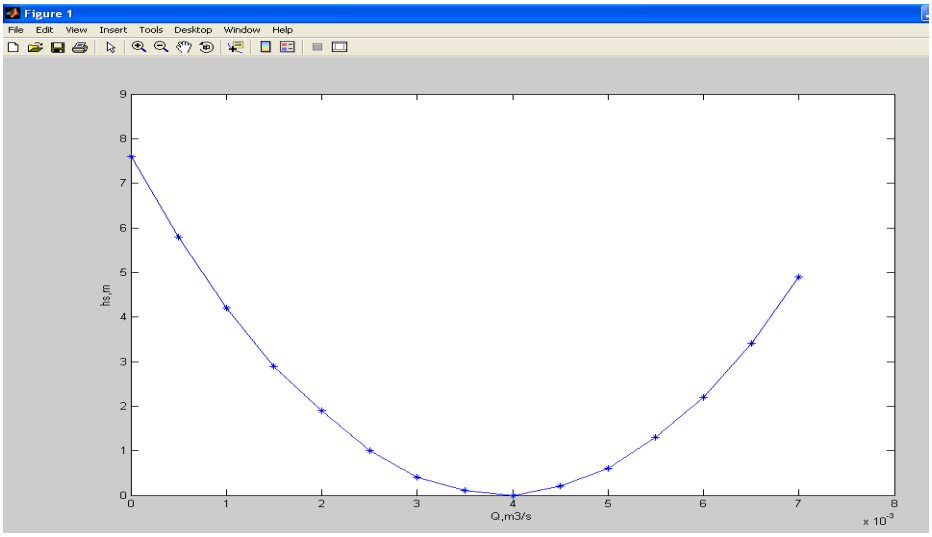

Fig. 2 Shock Losses versus Flow Rate Graph

Fig. 2 is the flow rate versus the shock loss of head. The shock loss of head increases when the flow rate decreases. Shock loss does not have in the design point condition. If this condition is over, the shock loss of head is high.

Impeller Friction Losses: The impeller was designed that the width of the impeller would become small and the friction loss at the flow passage would become large. Therefore to relive the increase in friction loss, radial flow passage on the plane of the impeller was adopted [3, 5]. The friction losses can be found for energy dissipation due to contact of the fluid with solid boundaries such as stationary vanes, impeller, casing, disk and diffuser, etc.
The impeller friction losses are:

$$h_1 = \frac{b_2(D_2-D_1)(V_{r_1}+V_{r_2})^2}{4gH_r \times 2\sin\beta_2} \quad (5)$$

Table (b) - Impeller Friction Losses versus Flow Rater Graph

SL NO.	1	2	3	4	5	6	7	8	9	10	11	12	13	14	15
h_1	0	0.01	0.02	0.03	0.04	0.05	0.07	0.09	0.12	0.16	0.19	0.23	0.27	0.33	0.38
Q	0	0.0005	0.001	0.0015	0.002	0.0025	0.003	0.0035	0.004	0.0045	0.005	0.0055	0.006	0.0065	0.007

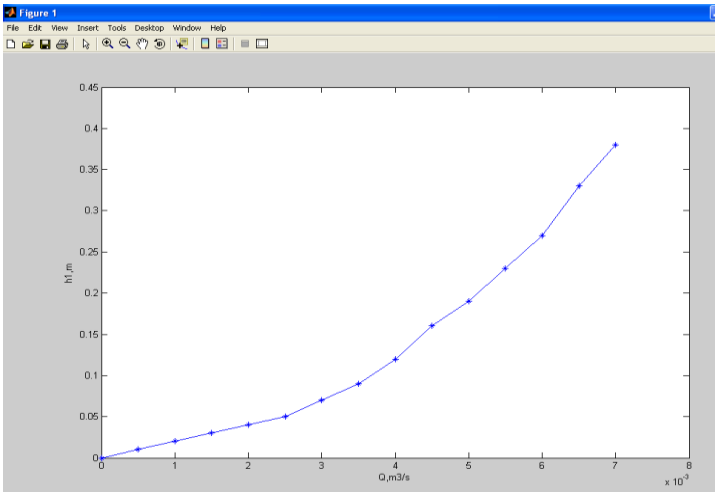

Fig. 3 Impeller Friction Losses versus Flow Rater Graph

The influence of the geometry of the impeller friction loss is obtained in Fig. 3. The analysis of the curves shows that small differences between the points for the flow rate versus theimpeller friction loss of head. The impeller loss of headincreases when the flow rate is increase.

Volute Friction Losses: This loss results from a mismatch of the velocity leaving the impeller and the velocity in the volute throat. If the velocity approaching the volute throat is larger than the velocity at the throat, the velocity head difference is less. The velocity approaching the volute throat by assuming that the velocity is leaving the impeller decreases in proportional to the radius because of the conservation of angular momentum. The volute friction losses:

$$h_2 = \frac{C_v V_3^2}{2g} \quad (6)$$

SL NO.	1	2	3	4	5	6	7	8	9	10	11	12	13	14	15
h_2	0	0.011 × 10^{-9}	0.033 × 10^{-9}	0.077 × 10^{-9}	0.12× 10^{-9}	0.17× 10^{-9}	0.25× 10^{-9}	0.4× 10^{-9}	0.6× 10^{-9}	0.9× 10^{-9}	1.2× 10^{-9}	1.6× 10^{-9}	2.0× 10^{-9}	2.5× 10^{-9}	3× 10^{-9}
Q	0	0.0005	0.001	0.0015	0.002	0.0025	0.003	0.0035	0.004	0.0045	0.005	0.0055	0.006	0.0065	0.007

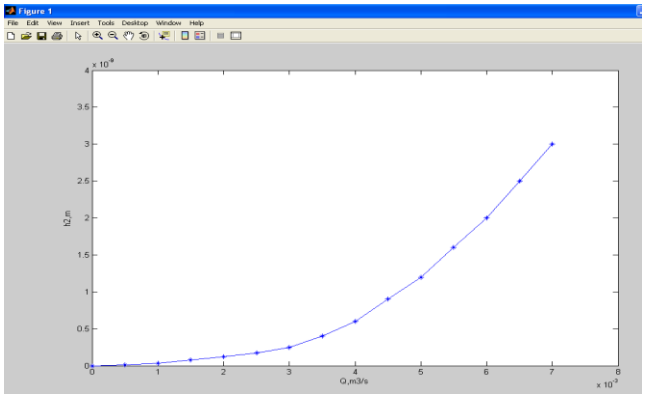

Fig. 4 Volute Friction Losses versus Flow Rate Graph

The volute friction losses versus flow rate graph are Fig. 4. The volute friction loss of head increases when the flow rate is increased. The volute friction coefficient decreases for smallvalues of the volute flow coefficient.

Disk Friction Losses: The impeller was designed to investigate the effect of disk friction on total power. The disk friction increases proportionally to the fifth power of disk diameter In order toexamine the relation between the height of disk friction lossesand the geometry of disks in real centrifugal pump housingdisks without and with modified outlet sections with variousnumbers, angles and widths are investigated. Disks withmodified outlet sections were examined to approach a realimpeller in real centrifugal pump housing. The disk friction power is divided by the flow rate and head to be added to the theoretical head when the shaft power demand is calculated [2, 6, 7].
The disk friction loss is;

$$h_3=\frac{f\rho\omega^3\left(\frac{D}{2}\right)^5}{10^9 Q_s} \qquad (7)$$

Loss coefficient of disk friction, f is assumed as 0.005.

$$h_3=\frac{f\times\rho\times\left(\frac{2\pi n}{60}\right)^3\left(\frac{D_2}{2}\right)^5}{10^9\times g\times Q} \qquad (8)$$

Table (d) Disk Friction Losses versus Flow Rate Graph

SL NO.	1	2	3	4	5	6	7	8	9	10	11	12	13	14
h_3	5.1×10^{-6}	2.5×10^{-6}	1.6×10^{-6}	1.2×10^{-6}	1.0×10^{-6}	0.8×10^{-6}	0.7×10^{-6}	0.6×10^{-6}	0.5×10^{-6}	0.45×10^{-6}	0.4×10^{-6}	0.35×10^{-6}	0.3×10^{-6}	0.25×10^{-6}
Q	0.0005	0.001	0.0015	0.002	0.0025	0.003	0.0035	0.004	0.0045	0.005	0.0055	0.006	0.0065	0.007

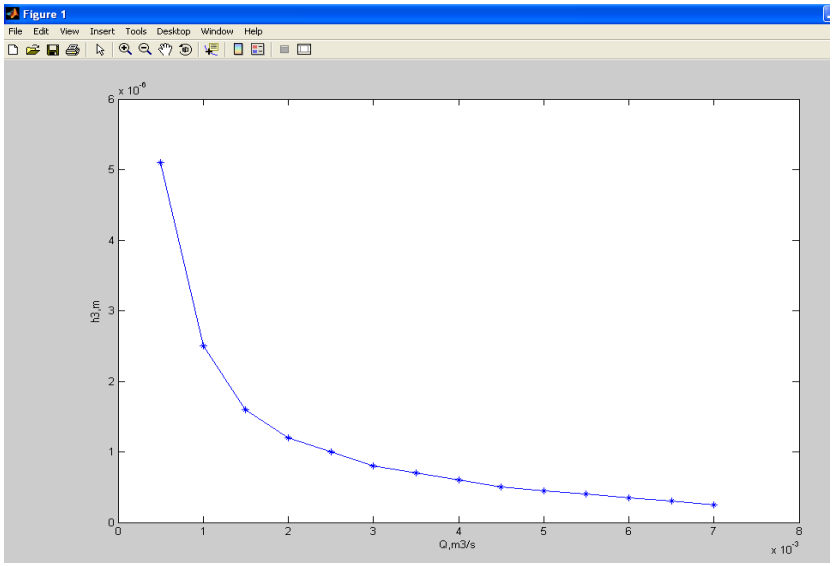

Fig. 5 Disk Friction Losses versus Flow Rate Graph

The disk friction coefficient increases with the increase the angle of the modified outlet sections of disks. The influence of geometrical parameters of disks means that affect the angular velocity of the developed [8]. When the low flow condition changes the other condition, the disk friction loss of head isimmediately high which is shown in Fig.5. If the flowaccelerates the loss of head changes about the normal rate.

Recirculation Losses: The recirculation loss coefficient depends on the piping configuration upstream of the pump in addition to the geometrical details of the inlet. The power of recirculation is also divided by the volume flow rate, like the disk friction power, in order to be converted into a parasitic head [3, 8].
The head of recirculation is;

$$h_4 = K\,\omega^3 D_1^2 \left(1 - \frac{Q_s}{Q_o}\right)^{2.5} \qquad (9)$$

Impellers with relatively large inlet diameters usually encountered in high-specific speed pumps are the most likely to re-circulate. The loss contains a default value of 0.005 for the loss coefficient. Coefficient of leakage loss K is assumed as 0.005.The pump speed is carried out with the value of specific speed because impeller with relatively large inlet diameters (usually encountered in high-specific-speed pumps) are the most likely to re-circulate. Coefficient of leakage loss K is assumed as 0.005[4, 7, 9].

Table (e) - Recirculation Losses versus Flow Rate Graph

SL NO	1	2	3	4	5	6	7	8	9	10	11	12	13	14	15
h_4	0.0145	0.009	0.005	0.0025	0.0009	0.0001	0	0	0	0	0	0	0	0	0
Q	0	0.0005	0.001	0.0015	0.002	0.0025	0.003	0.0035	0.004	0.0045	0.005	0.0055	0.006	0.0065	0.007

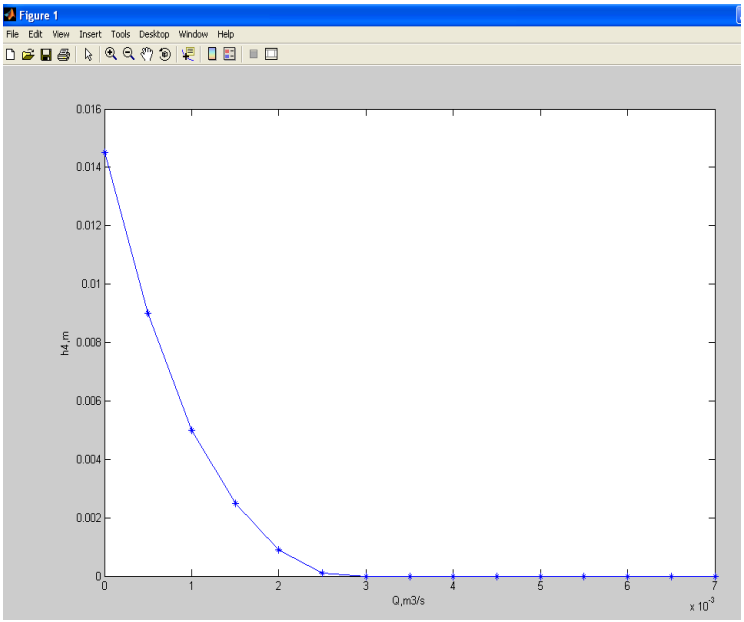

Fig. 6 Recirculation Losses versus Flow Rate Graph

The recirculation loss of head is high when the flow rate decreases. This graph is shown in Fig.6. If the flow rate is high, the recirculation loss of head is nearly zero.

Actual Head: The output of a pump running at a given speed is the flow rate delivered by it and the head developed. Thus a plot of head against flow rate at constant speed forms the fundamental performance characteristic of a pump. In order to achieve this actual head, the flow rate is required which involves efficiency of energy transfer.The actual pump head is calculated by subtracting from the net theoretical head all the flow losses which gives the actual head/flow rate characteristic provided it is plotted against [3, 9-12].
Therefore, the actual pump head is;

$$H_{act} = H_{thn} - (h_s + h_1 + h_2 + h_3 + h_4) \qquad (10)$$

Table (f) - Actual Pump Head Losses versus Flow Rate Graph

SL NO.	1	2	3	4	5	6	7	8	9	10	11	12	13	14	15
H_{act}	9.9	11.25	12.5	13.5	14.25	14.5	14.75	14.6	14.4	13.9	13.1	12	10.5	9	7
Q	0	0.0005	0.001	0.0015	0.002	0.0025	0.003	0.0035	0.004	0.0045	0.005	0.0055	0.006	0.0065	0.007

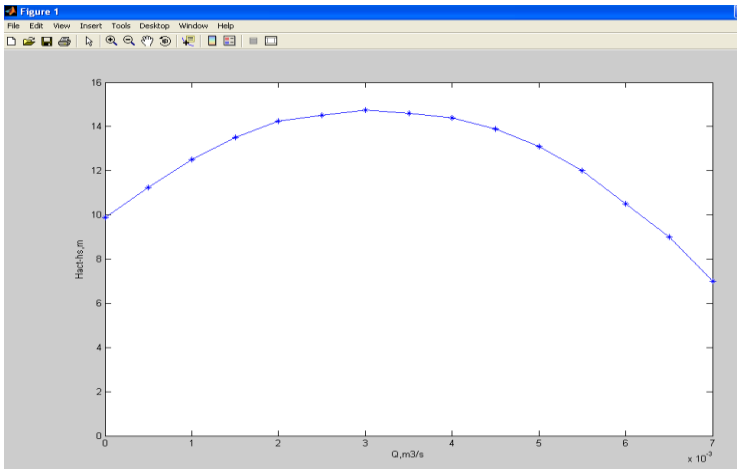

Fig. 7 Actual Pump Head Losses versus Flow Rate Graph

Actual head except head of recirculation:

$H_{act} - h_4 = H_{thn} - (h_s + h_1 + h_2 + h_3)$ (11)

Table (g) - Actual Head exceptHead of Recirculation versus Flow Rate Graph

SL NO.	1	2	3	4	5	6	7	8	9	10	11	12	13	14	15
$H_{act} - h_4$	9.8	11.3	12.5	13.5	14.3	14.5	14.8	14.6	14.4	13.9	13.2	12.0	10.5	9	7
Q	0	0.0005	0.001	0.0015	0.002	0.0025	0.003	0.0035	0.004	0.0045	0.005	0.0055	0.006	0.0065	0.007

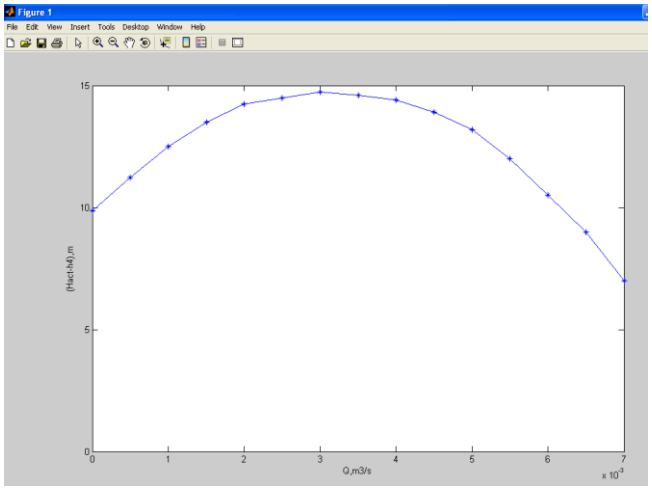

Fig. 8 Actual Head exceptHead of Recirculation versus Flow Rate Graph

disk friction loss:

$$H_{act} - h_3 = H_{thn} - (h_s + h_1 + h_2 + h_4) \quad (12)$$

Table (h) - Actual head except disk friction loss versus Flow Rate Graph

SL NO.	1	2	3	4	5	6	7	8	9	10	11	12	13	14	15
$H_{act} - h_3$	9.9	11.3	12.5	13.5	14.3	14.5	14.75	14.6	14.4	13.9	13.2	11.99	10.5	8.999	6.999
Q	0	0.0005	0.001	0.0015	0.002	0.0025	0.003	0.0035	0.004	0.0045	0.005	0.0055	0.006	0.0065	0.007

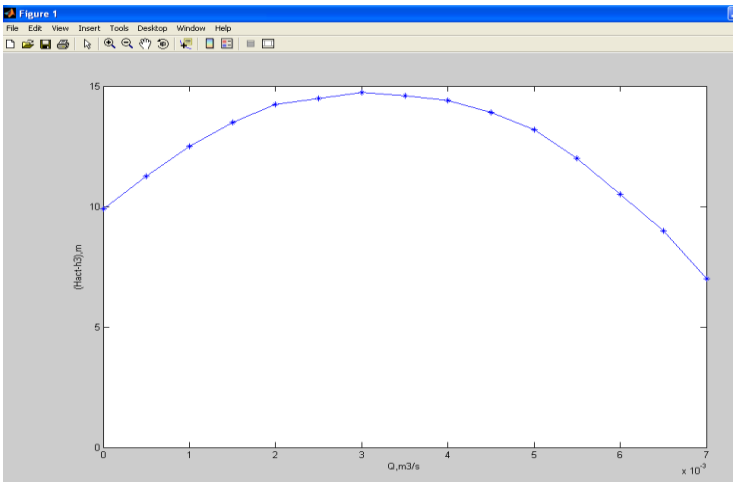

Fig. 9 Actual head except disk friction loss versus Flow Rate Graph

Actual head except volute friction losses:

$$H_{act} - h_2 = H_{thn} - (h_s + h_1 + h_3 + h_4) \quad (13)$$

Table (i) - Actual head except volute friction losses versus Flow Rate Graph

SL NO.	1	2	3	4	5	6	7	8	9	10	11	12	13	14	15
$H_{act} - h_2$	9.9	11.25	12.5	13.5	14.25	14.5	14.75	14.6	14.4	13.9	13.2	12.0	10.5	8.999	6.999
Q	0	0.0005	0.001	0.0015	0.002	0.0025	0.003	0.0035	0.004	0.0045	0.005	0.0055	0.006	0.0065	0.007

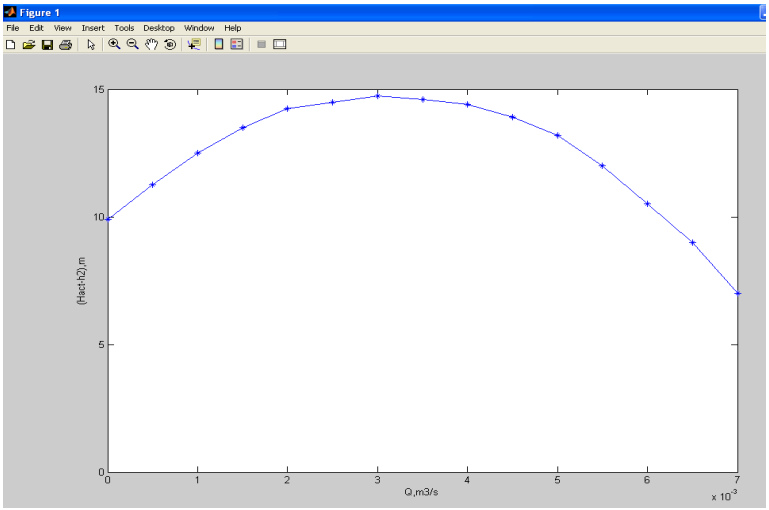

Fig. 10 Actual head except volute friction losses versus Flow Rate Graph

Actual head except impeller friction losses:

$$H_{act} - h_1 = H_{thn} - (h_s + h_2 + h_3 + h_4) \qquad (14)$$

Table (j) - Actual head except impeller friction losses versus Flow Rate Graph

SL NO.	1	2	3	4	5	6	7	8	9	10	11	12	13	14	15
$H_{act} - h_1$	9.99	11.24	12.48	13.47	14.21	14.45	14.68	14.51	14.28	13.74	13.01	11.77	10.23	8.67	6.62
Q	0	0.0005	0.001	0.0015	0.002	0.0025	0.003	0.0035	0.004	0.0045	0.005	0.0055	0.006	0.0065	0.007

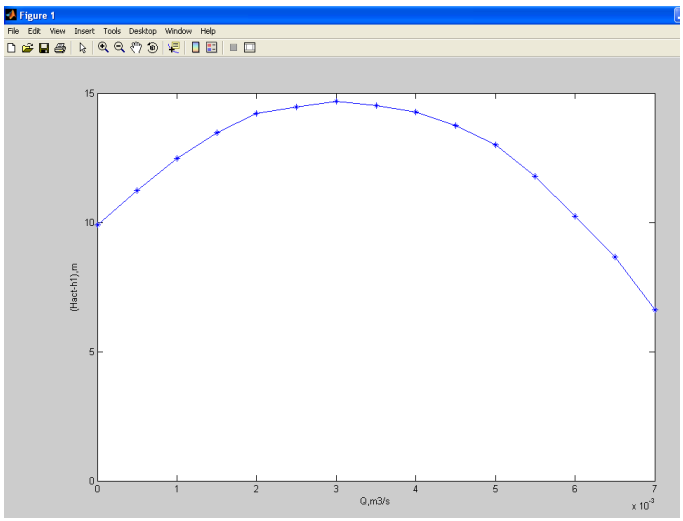

Fig.11 Actual head except impeller friction losses versus Flow Rate Graph

Actual head except shock losses:

$$H_{act} - h_s = H_{thn} - (h_1 + h_2 + h_3 + h_4) \qquad (15)$$

Table (k) - Actual head except shock losses losses versus Flow Rate Graph

SL NO.	1	2	3	4	5	6	7	8	9	10	11	12	13	14	15
$H_{act} - h_s$	2.9	6.45	9.8	12.6	14.3	15.7	16.4	16.7	16.1	15.3	13.9	12.1	9.3	6.2	2.5
Q	0	0.0005	0.001	0.0015	0.002	0.0025	0.003	0.0035	0.004	0.0045	0.005	0.0055	0.006	0.0065	0.007

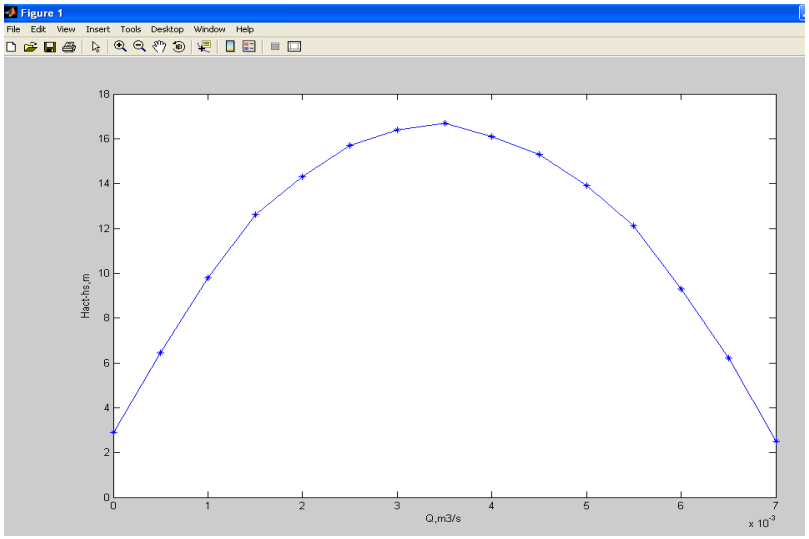

Fig. 12 Actual head except shock losses versus Flow Rate Graph

II. CONCLUSION

The analysis about losses of centrifugal pump is predicted in this paper. Theimpeller friction losses, volute friction losses and disk friction losses are considered to less the friction effect on centrifugal pump. Moreover, recirculation losses are also considered. And then, the actual performance curve of centrifugal pump is obtained. Afterthis curve subtracts each value of all losses from the value of actual pump head and calculated the new values. The performance curve of centrifugal pump is obtained from these new values. Thereafter we show all the losses subtracted from the actual head are approximately same except H_{act}-shock losses and H_{act}-impeller friction losses. The major loss considered is shock losses at the impeller inlet caused by the mismatch of fluid and metal angles. Shock losses can be found everywhere in the flow range of the pump.The performance of centrifugal pump is more effected by shock losses.

REFERENCES

[1] Khin Cho Thin, MyaMyaKhaing, and KhinMaung Aye (2008), Design and Performance Analysis of Centrifugal
[2] Pump, World Academy of Science, Engineering and Technology,Vol:2 -10-22.
[3] John Richards (1894). *Centrifugal pumps: an essay on their construction and operation, and some account of the origin and development in this and other countries* (http:/ / books. google. com/ books?id=013VAAAAMAAJ&pg=PA41). The Industrial Publishing Company.p. 40–41.
[4] Markus Reiner (14 April 1960). "A centripetal air pump" (http:/ / books. google. com/ books?id=9x-5Nx7OqHoC&pg=PA946). *New Scientist* 7 (178): 946. .
[5] Charles F. Conaway (1999). *The petroleum industry: a nontechnical guide* (http:/ / books. google. com/ books?id=sJ7BO1cCD20C&pg=SA8-PA52). PennWell Books. p. 200. ISBN 9780878147632.
[6] R. K. Bansal (2005). *A textbook of fluid mechanics and hydraulic machines* (http:/ / books. google. com/ books?id=nCnifcUdNp4C&pg=PA938) (9th ed.). Firewall Media. p. 938. ISBN 9788170083115.
[7] Pump handbook by Karassik.
[8] Energy Audit Reports of National Productivity Council.
[9] British Pump Manufacturers' Association, BEE (EMC) Inputs, PCRA Literature.

[10] F. MOUKALLED and A. HONEIN (1997,1998), Computer-aided analysis ofhydraulicpumps,International Journal of Mechanical Engineering Education Vol 27 No 4.
[11] D. Rajenthirakumar&K. A. Jagadeesh (2009), Analysis of interaction between geometry and efficiency of impeller pump using rapid prototyping, Int J AdvManufTechnol, 44:890–899.
[12] Mario Šavar, HrvojeKozmar, Igor Sutlović (2009), Improving centrifugal pump efficiency by impeller trimming, Desalination 249,654–659.
[13] LamloumiHedi, KanfoudiHatem, ZgolliRidha (2010), Numerical Flow Simulation in a Centrifugal Pump,International Renewable Energy Congress November 5-7,Sousse, Tunisia.

ISSN (e): 2250 – 3005 || Vol, 04 || Issue, 9 || September – 2014 ||
International Journal of Computational Engineering Research (IJCER)

Design Consideration of Different Volute Casing at Best Efficiency Point for Commercial

[1,]Ravi Shastri , [2,]Anjani Kumar Singh , [3,]Manish Kumar Singh

[1,] *Asst. Prof. Cambridge Institute of Technology, Tatisilway, Ranchi, Jharkhand, India*

[2,] *Ph.D. Scholar, Materials and metallurgical Engineering National Institute of Foundry and Forge Technology, Hatia, Ranchi, Jharkhand, India*

[3,] *M.Tech, Materials Science and Engineering, National Institute of Foundry and Forge Technology, Hatia, Ranchi, Jharkhand, India*

ABSTRACT:

The pump casing is to guide the liquid to the impeller, converts into pressure the high velocity kinetic energy of the flow from the impeller discharge and leads liquid away of the energy having imparted to the liquid comes from the volute casing. A design of centrifugal pump is carried out and analyzed to get the best performance point. The design consideration and performance of volute casing pump are chosen because it is the most useful mechanical rotodynamic machine in fluid works which widely used in domestic, irrigation, industry, large plants and river water pumping system.

KEY WORDS: *volute, pump,BEP*

I. INTRODUCTION

The word volute actually describes a specific type of pump casing that converts energy created by the impeller into pressure. The impeller pushes water into the volute which converts that energy into pressure and directs the flow toward the discharge point. In the picture on the right notice that the impeller is not located in the center of the volute. This is intentional. The portion of the volute that extends closest to the impeller is called the "cutwater". It is the point where the flow is forced to exit through the discharge point rather than continuing to swirl around the impeller[1,2]. The gradually increasing distance between the volute and casing and the direction of rotation of the impeller (noted by the arrow above the volute) combine to force the water around the volute in a counter-clockwise direction in the pump section shown, and once the flow reaches the cutwater it is forced to exit the volute. A volute is a curved funnel increasing in area to the discharge port. It is often used with impeller pumps. As the area of the cross-section increases, the volute reduces the speed of the liquid and increases the pressure of the liquid.

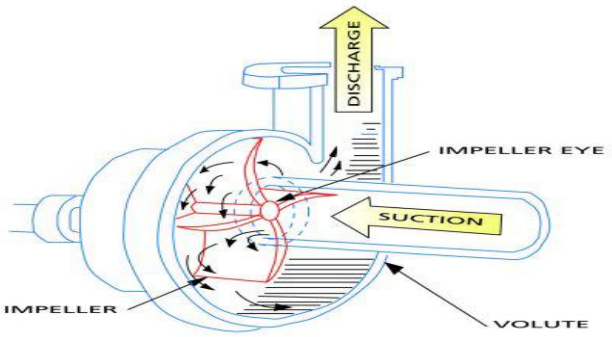

Fig: 1.volute casing pump

Types of volute Casing designs

- Single- Volute Casing Design
- Double- Volute Casing Design
- The Double- Volute Dividing Rib(Splitter)
- Triple-Volute Casings
- Quad- Volute Casings
- Circular- Volute Casings

Single- Volute Casing Design: Single-volute pumps have been in existence from Day One. Pumps designed using single- volume casings of constant velocity design are more efficient than those using more complicated volute designs. They are also less difficult to cast and more economical to produce because of the open areas around impeller periphery. Theoretically they can be used on large as well as small pumps of all specific speeds[3]. The single volute pump impeller will deflect either 60° or 240° from the cut water depending upon which side of the pump's best efficiency point (BEP) you are operating.

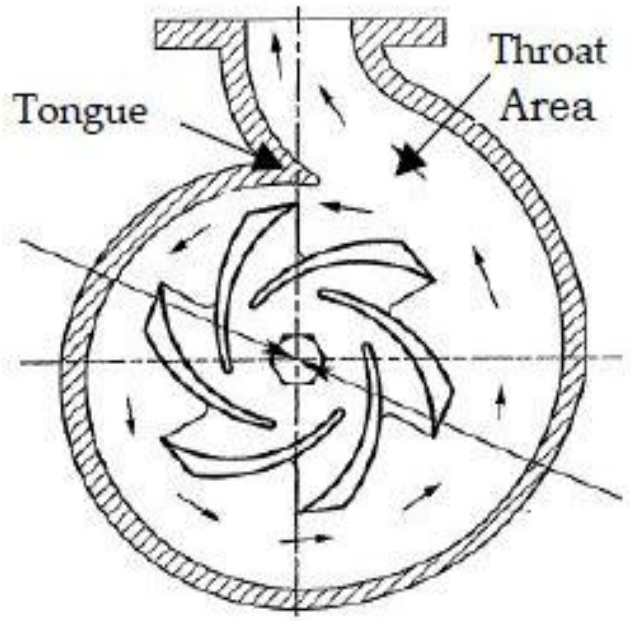

Fig. 2 Single-Volute Casing of pump

In all volute pumps the pressure distribution around the periphery of the impeller is uniform only at the best efficiency point (BEP). This pressure equilibrium is destroyed when the pump is operating on either side of the BEP, resulting in a radial load on the impeller. This load defects the pump shaft and can result in excessive wear at the wearing rings, seals, packing, or bearings. In extreme cases, shaft breakage due to fatigue failure can result.

The magnitude of this radial load is given by[4,5]:

$$\text{Radial load} = KHD_2b_2sp\ gr/2.31$$

where Radial force (lbs), H = Impeller head (ft), D_2 = Impeller diameter (in.), b_2 = Total impeller width including shrouds at D_2 (in.), K = Experimental constant, sp.gr = Specific gravity.

Values of the experimental constant K are given in bellow figure. For a specific single-volute pump it reaches its maximum at shutoff and will vary between 0.09 and 0.38 depending upon specific speed. The effect of force will be most pronounced on a single-stage pump with a wide b_2 or a large-sized pump. It is safe to say that with existing design techniques, single-volute designs are used mainly on low capacity, low specific speed pump or pump for special applications such as variables slurries or solids handling.

Double- Volute Casing Design: A double-volute casing design is actually two single-volute designs combined in an opposed arrangement. The total throat area of the two volutes is identical to that which would be used on a comparable single-volute design. Double-volute casings were introduced to eliminate the radial thrust problems that are inherent in single-volute designs. Test measurements, however, indicate that while the radial forces in a double volute are greatly reduced, they are not completely eliminated. This is because although the volute proper is symmetrical about its centerline, the two passages carrying the liquid to the discharge flange often are not. For this reason, the pressure forces around the impeller periphery do not precisely cancel, and a radial force does exist even in double-volute pumps.

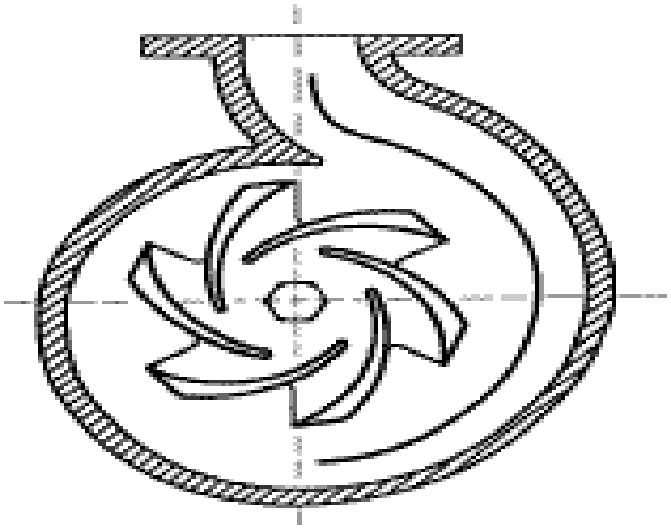

Fig. 3 Double-Volute Casing of pump

Values of the constant K have been established experimentally by actually measuring the pressure distributions in a variety of double-volute pumps. The data presented in above figure apply to conventional single stage double-volute pump and indicate substantial reductions in the magnitude of K. Tests on multistage pumps with completely symmetrical double-volute casings indicate that the radial thrust is nearly zero over the full operating range of the pump. The hydraulic performance of double-volute pumps is nearly as good as that of single-volute pumps. Tests indicate that double-volute pumps will be approximately one to one and one-half points less efficient at BEP, but will be approximately two points more efficient on either side of BEP than a comparable single-volute pump. Thus the double-volute casing produces a higher efficiency over the full range of the head-capacity curve than a single volute. Double-volute pump casings should not be used in low-flow (below 400 Gallons per Minute) single-stage pumps. The small liquid passages behind the long dividing rib make this type of casing very difficult to manufacture and almost impossible to clean. In large pumps double-volute casings should be generally used and single-volute designs should not be considered.

Triple-Volute Casings: Some pumps use three volutes symmetrically spaced around the impeller periphery. Total area of the three volutes is equal to that of a comparable single volute. The triple volute casing is difficult to cast, almost impossible to clean, and expensive to produce. We do not see any justification for using this design in commercial pumps.

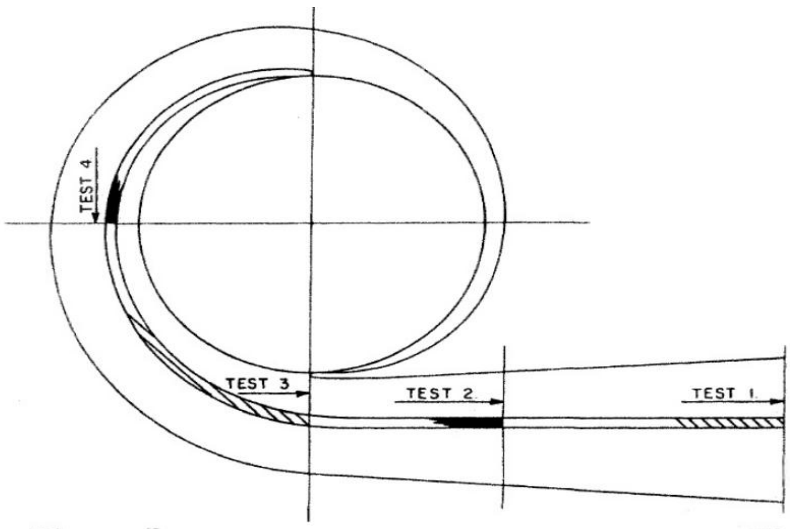

Fig. 4 Triple-Volute Casing of pump

Quad- Volute Casings: Approximately 15 years ago a 4-vane (quad) volute was introduced. Later this design was applied to large primary nuclear coolant pumps (100,000 GPM, to 10-15,000 HP). The discharge liquid passage of these pumps is similar to that of a multi-stage crossover leading to a side discharge. There is no

hydraulic advantage to this design.The only advantage of this design is its reduced material cost. The overall dimensions of quad-volute casing are considerably smaller than those of a comparable double-volute pump.

Circular- Volute Casings: Several pump manufacturers have conducted tests to evaluate the hydraulic performance of pumps with circular volutes. A study of the results of these tests reveals that circular volutes improve the hydraulic performance of small high head or low specific speed units and impair the performance of high specific speed pumps. Specifically, pump efficiency is improved below specific speeds of 600. For specific speeds above 600 the efficiency of circular-volute designs will be 95% of that possible with conventional volute designs. This can be explained by remembering that in a conventional volute a uniform pressure and velocity distribution exists around the impeller periphery only at the BEP. At off-peak capacities, velocities and pressures are not uniform. For circular volutes the opposite is true. Uniform velocity and pressure exist only at zero flow[6]. This uniformity is progressively destroyed as the capacity is increased. Therefore, at BEP the casing losses are generally greater than those of the conventional volute. For low specific speed pumps, however, there is some gain in efficiency due to a circular volute since the benefits of the improved surface finish in the machined volute outweigh the problems created by the non-uniform pressure distribution.

General Design Considerations: It was pointed out previously that the casing itself represents only losses and does not add anything to the total energy developed by the pump. In designing pump casings it is therefore important to utilize all available means of minimizing casing losses. However, commercial considerations dictate some deviations from this approach, and experience has shown that these do not have a significant effect on casing losses. The following designs rules have shown themselves to be applicable to all casing designs [1, 7, 8]:

- Constant angles on the volute sidewalls should be used rather than different angles at each volute section. Experience has shown that these two approaches give as good results and the use of constant wall angles reduces pattern costs and saves manufacturing time.
- The volute space on both sides of the impeller shrouds should be symmetrical.
- All volute areas should be designed to provide a smooth change of areas.
- Circular volutes should be considered for pumps below a specific speed of 600. Circular volutes should not be considered for multistage pumps.
- The total divergence angle of the diffusion chamber should be between 7 and 13 degrees. The final kinetic energy conversion is obtained in the discharge nozzle in a single-stage pump and in both the discharge nozzle and crossover in a multi-stage pump.
- In designing a volute, be liberal with the space surrounding the impeller. In multi-stage pumps in particular, enough space should be provided between the volute walls and the impeller shroud to allow one-half inch each way for end float and casting variations. A volute that is tight in this area will create axial thrust and manufacturing problems.

II. CONCLUSION

In a today competitive and sophisticated technology, centrifugal pump is more widely used than any other applications because the advantages of following factors are effect on the centrifugal pump.

- Its initial cost is low.
- Efficiency is high.
- Discharge is uniform and continuous flow.
- Installation and maintenance is easy.
- It can run at high speeds without the risk of separation of flow.

In this paper we show the what is design consideration of different volute casing at best efficiency point (BEP) for commercial aspect. In designing pump casings it is therefore important to utilize all exact dimensions as like volute throat area, volute mean diameter, volute circumferential length and minimizing casing losses. However, commercial considerations dictate some deviations from this approach, and experience has shown that these do not have a significant effect on casing. The following designs rules have shown themselves to be applicable to all casing designs.

REFERENCES

[1] B. V. Ukhin (2007), Effect of variation in the diameter of a centrifugal dredge impeller on its characteristics, Springer Science + Business Media, Inc,*Vol. 41, No. 1.*

[2] E.C. Bacharoudis, A.E. Filios2, M.D. Mentzos and D.P. Margaris (2008),Parametric Study of a Centrifugal Pump Impeller by Varying the Outlet Blade Angle,Bentham Open Mechanical Engineering Journal,2,75-83.

[3] D. Rajenthirakumar&K. A. Jagadeesh (2009), Analysis of interaction between geometry and efficiency of impeller pump using rapid prototyping, Int J AdvManufTechnol, 44:890–899.

[4] LamloumiHedi, KanfoudiHatem, ZgolliRidha (2010), Numerical Flow Simulation in a Centrifugal Pump,International Renewable Energy Congress November 5-7,Sousse, Tunisia.
[5] Beena D Baloni, S.A. Channiwala, V.K. Mayavanshi (2012) , Pressure recovery and loss coefficient variations in the two different centrifugal blower volute designs,Elsevier, Applied Energy 90(2012) 335-343.
[6] Pump handbook by Karassik
[7] Energy Audit Reports of National Productivity Council.
[8] British Pump Manufacturers' Association, BEE (EMC) Inputs, PCRA Literature

ISSN (e): 2250 – 3005 || Vol, 04 || Issue, 9 || September – 2014 ||
International Journal of Computational Engineering Research (IJCER)

Iterative Determinant Method for Solving Eigenvalue Problems

Owus M. Ibearugbulem[1], Osasona, E. S. and Maduh, U. J.[2]
[1,2] Civil Engineering Department, Federal University of Technology, Owerri, Nigeria

ABSTRACT:
This paper presents iterative determinant method for solving eigenvalue problems. A matlab program that operates iterative to evaluate the determinant of the problem was written. In the program, a trial eigenvalue is used in the program to compute the determinant. A small value (iterator) is added to trial eigenvalue to obtain a new trial eigenvalue, which is used to compute new determinant. The trial eigenvalue in the sequence that made the determinants to move from negative values to positive value or move from positive values to negative value becomes required eigenvalue. Some engineering problems were used to validate the eigensolver. Some of the data from the eigensolver and the corresponding exact data are 2.468 and 2.4678; 9.876 and 9.875; 60.001 and 60.00; 12.37 and 12.3695. Close look at

Key word: *eigensolver, iterative, determinant, eigenvalue, matlab program, iterator*

I. INTRODUCTION

According to Ibearugbulem et al (2013), the stiffness matrix [k], the geometric matrix [kg] and the mass (inertia) matrix [ki] are formulated using the assumed shape function. This shape function is usually assumed to approximate the deformed shape of the continuum. If the shape function assumed is the exact one, it means the solution will converge to the exact solution. The inertia matrix and the geometric matrix formulated using the assumed shape functions are called consistent mass matrix and consistent geometric matrix respectively (Paz, 1980 and Geradin, 1980). In the work of Ibearugbulem et al (2013), the dynamic equation in structural dynamic as:

$$[k] - \lambda[ki] = 0 \quad (1)$$

For static stability problem, the eigenvalue equation is given as:

$$[k] - Nc[kg] = 0 \quad (2)$$

Where K is the material stiffness matrix, k_i is the matrix of inertia, k_g is the geometric matrix λ is natural frequency parameter and N_c is the critical buckling load parameter. Of note here is that both k_g and k_i are consistent matrices (that is they are non-diagonal matrices). The difficulty posed by this type of eigenvalue problem led many researchers to transform the consistent matrices to diagonal matrices as:

$$[k] - \lambda A[I] = 0 \quad (3)$$

$$[k] - Nc\, A[I] = 0 \quad (4)$$

Here, A[I] is the transformed diagonal inertia or geometric matrix. In dynamics, the diagonal inertia matrix is often called lumped mass matrix. Many methods are adopted so far by researchers for solutions of eigenvalue problems of equation (3) and (4). According to Ibearugbulem et al, (2013), the methods include Jacobi method, Polynomial method, Iterative method and Householder's method were used by (Greenstadt, 1960; Ortega, 1967; and James, Smith and Wolford, 1977. Others are Power method, Inverse iterative (Wilkinson, 1965), Lanczos method (lanczos, 1950), Arnoldi method (Arnoldi, 1951; Demmel, 1997; Bai et al, 2000;Chatelin, 1993; and Trefethenand Bau, 1997), Davidson method, Jacobi-Davidson method (Hochstenback and Notay, 2004; and Sleijpen and Vander Vorst, 1996), Minimum residual method, generalized minimum residual method were used by Barrett et al, (1994), Multilevel preconditioned iterative eigensolvers (Arbenz and Geus, 2005), Block inverse-free preconditioned Krylov subspace method (Quillen and Ye, 2010), Inner-outer iterative method (Freitag, 2007), and adaptive inverse iteration method (Chen, Xu and Zou, 2010), Matrix iterative-inversion (Ibearugbulem et al, 2013). Sadly, of all these methods, only polynomial and iterative-inversion methods can handle the problems of equations (1) and (2). Other methods can only be used for equation (3) and (4). However, polynomial method also becomes very difficult to use when the size of the matrix exceeds 3x3. In the same way, iterative-inversion method is also difficult when the matrix size is large and the speed of computation is very slow.

The essence of this paper is to present a method that can be used in solving eigenvalue problems of equations (1), (2), (3), and (4) for any size of matrix with high speed and good accuracy

II. ITERATIVE DETERMINANT

In this method, a trial eigenvalue λ_0 or Nc_0 of default value of zero shall be substituted into the eigenvalue equation to obtain eigenvalue matrix as:

$$[k]- \lambda[ki] = [kk]_0 \quad (5)$$

The determinant of the eigenvalue matrix, $[kk]_0$ shall then be computed and the value kept. The value of this initial determinant, dt0 may be positive or negative. Now the value of the default eigenvalue shall be increased by adding iterator (say 1, 0.1, 0.01, 0.001 etc. as desired) to it to obtain new eigenvalue, λ_1. This shall be substituted into the eigenvalue equation to obtain $[kk]_1$. The determinant, dt_1 of $[kk]_1$ shall be computed. If dt_0 is negative and dt1 is also negative, then the actual eigenvalue has not been obtained and the iterator has to be added to λ_1 to obtain λ_2. This process has to be continued until we reach a stage where $\lambda_{n-1} > 0$ and $\lambda_n < 0$ or $\lambda_{n-1} < 0$ and $\lambda_n > 0$. Note here that the bigger the iterator, the faster the computation and less the accuracy, the smaller the iterator, the slower the computation and more the accuracy. To ease the use of this method, a general matlab program was written. The user is at will to modify the iterator, f and sub iterators ff (i) in the program, where is 1, 2, 3 … n and n is the size of the square matrix involved. For instance, if the order of the expected eigenvalue is 100, iterator and sub iterators of 1 or 0.1 can be used. In this case the expected accuracy shall be of the order of iterator, 1 or 0.1. In the same way, if the order of expected eigenvalue is 1, iterator of 0.001 can be used. The choice of iterator is guided by the speed and accuracy of the computation. In all, for high accuracy, iterators of 0.001 and below are advisable but the speed may be very slow. Thus, the level of accuracy and speed shall guide you in using your choice iterator in this program. The user is also at liberty to choose the range of eigenvalues to compute for by adjusting "for r = 1:3" to say "for r = 1:5" if the size of the matrix is 5x5. The stiffness matrix "prs" and the geometric matrix or inertia matrix "pri" in the program are to be entered by the user. The iterating count ceiling, "k" in the program can also be raised from 6260 to any higher value to suit the user. Number of sub iterators "ff(i) as we have them in the program is 7. The user is at liberty also to introduce more sub iterators say ff(8), ff(9) etc. as matches the size of the matrix. Some engineering problems were used to ascertain the adequacy of the method and the program.

III. NUMERICAL EIGENVALUE PROBLEMS

The program will be used to test the following problems.

1. $\left|\begin{bmatrix} 2 & 0 & 1 \\ -1 & 4 & -1 \\ -1 & 2 & 0 \end{bmatrix} - \lambda \begin{bmatrix} 1 & 0 & 0 \\ 0 & 1 & 0 \\ 0 & 0 & 1 \end{bmatrix}\right| = 0$ (Stroud, 1982)

2. $\left|\begin{bmatrix} 0.1 & 0.1 & 0.1 \\ 0.1 & 0.2 & 0.2 \\ 0.1 & 0.2 & 0.3 \end{bmatrix} - \lambda \begin{bmatrix} 1 & 0 & 0 \\ 0 & 1 & 0 \\ 0 & 0 & 1 \end{bmatrix}\right| = 0$ (James, Smith and Wolford, 1977)

3. $\left|\begin{bmatrix} 204.8 & -102.4 & 25.6 \\ -102.4 & 63.2 & -18.8 \\ 25.6 & -18.8 & 7.2 \end{bmatrix} - \lambda \begin{bmatrix} 4.8762 & -2.438 & 0.0762 \\ -2.438 & 2.419048 & -0.1381 \\ 0.0762 & -0.1381 & 0.0762 \end{bmatrix}\right| = 0$

4. $\left|\begin{bmatrix} 7.2 & -25.6 & -1.2 \\ -25.6 & 204.8 & 25.6 \\ -1.2 & 25.6 & 7.2 \end{bmatrix} - \lambda \begin{bmatrix} 0.07619 & -0.076 & 0.02381 \\ -0.07619 & 4.8762 & 0.07619 \\ 0.02381 & 0.0762 & 0.07619 \end{bmatrix}\right| = 0$

5. $\left|\begin{bmatrix} 204.8 & -102.4 & 25.6 \\ -102.4 & 63.2 & -18.8 \\ 25.6 & -18.8 & 7.2 \end{bmatrix} - \lambda \begin{bmatrix} 0.406349 & 0.0635 & -0.00635 \\ 0.0635 & 0.2063 & -0.01587 \\ -0.00635 & -0.016 & 0.001587 \end{bmatrix}\right| = 0$

6. $\begin{vmatrix} 126.4 & 18.8 & 18.8 & -102.4 & 0 & -102.4 \\ 18.8 & 14.4 & -1.2 & -25.6 & -25.6 & 0 \\ 18.8 & -1.2 & 14.4 & 0 & 25.6 & -25.6 \\ -102.4 & -25.6 & 0 & 204.8 & 0 & 0 \\ 0 & -25.6 & 25.6 & 0 & 204.8 & 0 \\ -102.4 & 0 & -25.6 & 0 & 0 & 204.8 \end{vmatrix} - \lambda \begin{vmatrix} 2.419048 & 0.138095 & 0.138095 & -2.4381 & 0 \\ 0.138095 & 0.15238 & 0.02381 & -0.07619 & -0.07619 \\ 0.138095 & 0.02381 & 0.15238 & 0 & 0.07619 \\ -2.4381 & -0.07619 & 0 & 4.87619 & 0 \\ 0 & -0.07619 & 0.07619 & 0 & 4.87619 \\ -2.4381 & 0 & -0.07619 & 0 & 0 \end{vmatrix} = 0$

IV. RESULT AND DISCUSSION

Table 1 shows result data from eigenvalue problems herein. Eigenvalues obtained from the program were compared with the exact eigenvalues. The exact eigenvalues were obtained by trial and error means using Microsoft excel worksheet. Any eigenvalue that made the determinant of the eigenvalue matrix [kk] to become zero is the exact eigenvalue. The data from the program compared very well with the values from Microsoft excel worksheet with high degree of accuracy. As said earlier, it was observed that with small iterators say 0.01, we obtained more accurate eigenvalues with slow computing speed. We also confirmed that with big iterators say 1.0 we obtained less accurate eigenvalues with fast computing speed.

Table 1: Result data from the Eigenvalue Problems

	Eigenvalues									
	From iterative Determinant method					**Exact Eigenvalues**				
Problems	1st	2nd	3rd	4th	5th	1st	2nd	3rd	4th	5th
1	1	2	3			1	2	3		
2	0.0308	0.0644	0.5049			0.0308	0.0644	0.5049		
3	2.468	23.392	109.143			2.4678	23.3912	109.1422		
4	9.876	60.001	170.128			9.875124	60	170.1276		
5	12.37	494.266				12.3695	494.2658			
6	15.1	27	42.1	83.1	133.8	15.075832	26.95929142	42	83.07804	133.72546

V. APPENDIX A (MATLAB PROGRAM)

```
nn = input('enter size of matrix');nn = nn*1;
p=0;m=1;k=6260;j=1;f=0.1;ff(1)=0.1;ff(2)=0.01;ff(3)=0.001;ff(4)=0.001;ff(5)=0.001;ff(6)=0.001;ff(7)=0.001;
for r = 1 : 3
while p < k
prs = [43.2 0   0   ;0  6.400093    0   ;0  0   6.4];
pri = [0.54824  0   0   ;0  0.01268 0   ;0  0   0.01268];
a = prs - p*pri;
for x = 1:nn
for y = 1:nn
c(x,y)= a(x,y) ;
end
end
d = det(c);
if (m < 1.1); t1 = d;end
m = m + 1;
if (j >nn); break; end
if ((d >= 0)&& (t1 <= 0));py(j) = p;j = j + 1;t1 = d;end
if ((d <= 0)&& (t1 >= 0));py(j) = p;j = j + 1;t1 = d; end
p = p + f;
end
p = p-f; f =ff(r);m=1;
end
```

REFERENCES

[1] Arnoldi, W. E. (1951). The principle of minimized iteration in the solution of the matrix eigenvalue problem, Quarterly of Applied Mathematics, vol. 9, pp. 17– 29.

[2] Arbenz, P. andGeus, R. (2005). Multilevel preconditioned iterative eigensolvers for maxwell eigenvalue problems. Applied numerical mathematics.Vol. 54 , issue 2 .pp 107 – 121

[3] Bai, Z. Demmel, J., Dongarra, J. Ruhe, A., and van der Vorst, H. (2000). Templates for the Solution of Algebraic Eigenvalue Problems - A Practical Guide, SIAM, Philadelphia, PA,

[4] Barrett, R., Berry, M., Chan, T. F., Demmel, J., Donato, J., Dongarra, J., Eijkhout, V., Pozo, R., Romine, C.and van der Vorst, H. A. (1994). Templates for the Solution of Linear Systems: Building Blocks for Iterative Methods, 2nd Edition, SIAM, Philadelphia, PA,

[5] Chatelin, F. (1993).Eigenvalues of matrices,JohnWiley&SonsLtd,Chichester,West Sussex, England, Originally published in two separate volumes by Masson, Paris: Valeurspropres de matrices (1988) and Exercises de valeurspropres de matrices (1989).

[6] Demmel, J. W. (1997). Applied Numerical Linear Algebra, SIAM, Philadelphia, PA A.

[7] Freitag, M. (2007).Inner-outer Iterative Methods for Eigenvalue Problems - Convergence and Preconditioning.PhD Thesis submitted to University of Bath
[8] Fullard, K. (1980). The Modal Method for Transient Response and its Application to Seismic Analysis. In J. Donea (Ed.), Advanced Structural Dynamics (pp.43-70)
[9] Geradin, M. (1980).Variational Methods of Structural Dynamics and their Finite Element Implementation. In J. Donea (Ed.), Advanced Structural Dynamics (pp.1-42)
[10] (Greenstadt, J. (1960). Mathematical Methods for Digital Computers. Vol. 1, ed. A. Ralston and H. S. Wilf (New York: John Wiley & sons). Pp. 84-91.
[11] Hochstenbach, M. E. andNotay, Y. (2004). The Jacobi-Davidson method, GAMM Mitt.,
[12] Ibearugbulem, O. M., Ettu, L. O., Ezeh, J.C., and Anya, U.C. (2013).Application of Matrix Iterative – Inversion in Solving Eigenvalue Problems in Structural Engineering. International Journal of Computational Engineering Research, vol.3. pp: 17-22
[13] James, M. L., Smith, G. M. and Wolford, J. C. (1977). Applied Numerical Methods for Digital Computation: with FORTRAN and CSMP. Harper and Row Publishers, New York.
[14] Key, S. W. (1980). Transient Response by Time Integration: Review of Implicit and Explicit Operators. In J. Donea (Ed.), Advanced Structural Dynamics.
[15] Key, S. W. and Krieg, R. D. (1972) Transient Shell Response by numerical Time Integration.2nd US-JAPAN Seminar on Matrix Methods in Structural Analysis. Berkeley, California.
[16] Lanczos, C. (1950). An iterative method for the solution of the eigenvalue problem of linear differential and integral operators, Journal of Research of the National Bureau of Standards, vol. 45 , pp. 255–282.
[17] [Ortega, J. (1967). Mathematical Methods for Digital Computers. Vol. 2, ed. A. Ralston and H. S. Wilf (New York: John Wiley & sons). Pp. 94-115.

ISSN (e): 2250 – 3005 || Vol, 04 || Issue, 9 || September – 2014 ||
International Journal of Computational Engineering Research (IJCER)

Efficient Query Evaluation of Probabilistic Top-k Queries in Wireless Sensor Networks

P.Supriya[1] ,M.Sreenivasulu, Me[2]
[1]PG student, SITE,[2]assist. Professor, SITE

ABSTRACT:

Indecisive data arises in a number of domains, including data addition and sensor networks. Top-k queries that grade results according to some user-defined score are an significant tool for exploring large indecisive data sets. So, we introduce the ordered query evaluation of the Enough set-based (ESB), necessary set-based (NSB), and boundary-based (BB) algorithm for distributed processing in Top-K queries in wireless sensor networks, for inter cluster query processing with delimited rounds of communications and in responding to dynamic changes of data giving out in the network, we build up an adaptive algorithm that dynamically switches between the three proposed algorithms to diminish the transmission cost. The general method to evaluate the reliability of a data robotically retrieved from the web. Finally results given that the proposed algorithms decrease data transmissions drastically and acquire only small constant rounds of data communications for reliability. The investigational results also demonstrate the superiority of the adaptive algorithm, which achieves a near-optimal performance under various conditions.

***Index Terms**: Distributed data management, network topologies, probabilistic databases*

I. INTRODUCTION

In Wireless sensor networks are revolutionizing the ways to gather and use information from the physical world. This new technology has resulted in momentous impacts on a wide array of applications in a variety of fields, including army, science, industry, commerce, transportation, and health-care. However, the quality of sensors varies significantly in terms of their sensing exactness, accuracy, tolerance to hardware/external noise, and so on. For example, studies show that the distribution of noise varies widely in different photo voltaic sensors, precision and accuracy of readings usually vary significantly in humidity sensors, and the errors in GPS devices can be up to several meters. Thus, sensor readings are inherently uncertain. On the contrary, our proposal is a general approach which is applicable to probabilistic top-k queries with any semantic. Furthermore, instead of repeatedly requesting data which may last for several rounds, our protocols are guaranteed to be completed within no more than two rounds. These differences uniquely differentiate our effort from. Our previous work as the initial attempt only includes the concept of sufficient set. In this paper, besides of sufficient set, we propose another important concept of necessary set. With the aid of these two concepts, we further develop a suite of algorithms, which show much better performance than the one. Probabilistic ranked queries based on uncertainty at the attribute level are studied. Finally, uncertain top-k query is studied under the setting of streaming databases where a compact data set is exploited to support efficient slide window top-k queries. Armed with sufficient set and necessary set, we develop a suite of algorithms for processing probabilistic top-k queries in two-tier hierarchical wireless sensor networks with PT- Topk as a case study, including 1) sufficient set-based (SSB) algorithm, 2) necessary set-based (NSB) algorithm, and 3) boundary-based (BB) algorithm. Moreover, we developed an adaptive algorithm that dynamically switches among the three proposed algorithms to minimize the communication and energy overhead, in responding to changing data distribution in the network. Furthermore, we discuss how to apply sufficient set and necessary set to devise a series of algorithms, namely SSB-T, NSB-T, and optimized NSB-T (NSB-T-Opt), for processing probabilistic top-k in a sensor network with tree topology. Finally, we evaluate the proposed algorithms both in two-tier hierarchy (i.e., SSB, NSB,BB) and tree topology(i.e.,SSB-T,NSB-T,NSB-T-Opt) in comparison with two baseline approaches.

The Existing paper is the full version of our preliminary work published as a short paper in Probabilistic top-k query processing in Distributed Sensor Network, where we introduce the targeted problem and propose the idea of employing sufficient set to develop the SSB algorithm for distributed processing of probabilistic top-k queries.

In this paper, we extend the idea of sufficient set with the notion of necessary set and sufficient/necessary boundaries; develop new distributed processing algorithms; and demonstrate the extend of our ideas to a sensor network with tree topology. The Experimental result validates our ideas and shows that the proposed algorithms reduce data transmissions significantly without incurring excessive rounds of communications

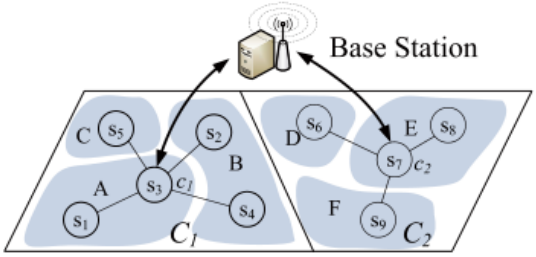

Fig- 1 : Wireless sensor network. These are 6 zones, denoted as A,B,..F which are organized into two clusters C1 & C2 with the corresponding cluster heads.

II. DISTRIBUTED DATA MANAGEMENT

2.1 Distributed Database

In Distributed Data Management, The DDBMS synchronizes all the data periodically and, in cases where multiple users must access the same data, ensures that updates and deletes performed on the data at one location will be automatically reflected in the data stored elsewhere. A centralized distributed database management system (DDBMS) manages the database as if it were all stored on the same computer. In this paper, we assume that a wireless sensor network consisting of a base station and N sensor nodes is deployed in a monitoring field. The base station serves as the data collection and processing center to the external users and applications. We assume M clusters are formed and a cluster head is selected for each cluster. The whole sensor network can be logically treated as a distributed uncertain database. Sensor readings are collected by cluster heads and transformed into uncertain data, then set of uncertain tuples are distributed in cluster heads within the sensor network

Definition 1 (Top-k Probability). Let Na denote the top-k answer set in a possible world A. Given a tuple t € T, the top-k probability of t is the aggregate probability of t being in the top-k answers over all A €A , i.e.,

$$Ptopk(t) = \sum_{Aea,teNa} P(A)$$

Definition 2 (Probabilistic Threshold Top-k Query (PT- Topk)). Given a probability threshold p(0<p<1), PT- Topk finds the set of tuples whose top-k probabilities are at least p.

2.2 Centralized PT-Topk Query Processing

In this section, we present a general approach for processing PT-Topk queries in a centralized uncertain database, which provides a good background for the targeted distributed processing problem.

Given an uncertain table T, we first sort T in accordance with the ranking function f such that t1<f t2<f … <f tn. The query answer can be obtained by examining the tuples in descending ranking order from the sorted table (which is still denoted as T for simplicity). We can easily determine that the highest ranked k tuples are definitely in the answer set as long as their confidences are greater than p since their qualifications as PT-Top k answers are not dependent on the existence of any other tuples. Nevertheless, the qualification of tuple tkþ1 as a PT-Top k answer is dependent on

1) Whether there exist some possible worlds where the tuples in front of tk+1 belong to less than k x-tuples; and

2) Whether the aggregated confidence of tk+1 over these possible worlds are greater than p. If the answer is positive, then tuple tk+1 is included in the answer set and tuple tK+2 is examined. This process continues until there are no more qualified tuples left to be examined

III. INTRACLUSTER DATA PRUNING

In a cluster-based wireless sensor network, the cluster heads are responsible for generating uncertain data tuples from the collected raw sensor readings within their clusters.

To answer a query, it's natural for the cluster heads to prune redundant uncertain data tuples before delivery to the base station in order to reduce communication and energy cost. The key issue here is how to derive a compact set of tuples essential for the base station to answer the probabilistic top-k queries. This is a very challenging issue for the following reasons: 1) the interplay of probability and ranking due to the semantic of probabilistic top-k queries; and 2) the lack of global knowledge to determine the probability and ranking of

candidate tuples locally at cluster heads. In this section, we propose the notion of sufficient set and necessary set, and describe how to identify them from local data sets at cluster heads. Next, we use the PT-Top k query as a test case to derive sufficient set and necessary set and show that the top-k probability of a tuple t obtained locally is an upper bound of its true top-k probability. Thus, data tuples excluded from the sufficient sets and necessary sets in local clusters will never appear in the final answer set.

3.1 Definition of Sufficient and Necessary Sets

It would be beneficial if cluster heads are able to find the minimum sets of their local data tuples that are sufficient for the base station to answer a given query. Ideally, sufficient set is a subset of the local data set. Data excluded from the sufficient set, no matter which clusters they reside, will never be included in the final answer set nor involved in the computation of the final answer set. Here, we define the sufficient set more formally as follows:

Definition 3 (Sufficient Set). Given an uncertain data set Ti in cluster Ci, if there exists a tuple tsb€Ti (called sufficient boundary) such that the tuples ranked lower than tsb are useless for query processing at the base station, then the sufficient set of Ti, denoted as S(T), is a subset of Ti as specified below:
S(Ti)={t|t=ftsbort<ftsb}
Where f is a given scoring function for ranking. Note that a sufficient boundary may not exist for a given data set; then we consider the whole data set as a sufficient set and will discuss it in more detail later.

Definition 4 (Necessary Set). Given a local data set Ti in cluster Ci, assume that Ai is the set of locally known candidate tuples for the final answer and tnb (called necessary boundary) is the lowest ranked tuple in Ai. The necessary set of Ti, denoted as N(Ti), is
N(Ti)= {t|t€ Ti, t <f <tnb}
Note that, at the base station, for a given cluster, the probability computation of some candidate tuples from other clusters may still require data tuples outside its necessary set. In other words, while the data tuples in the necessary sets include the final answer set, they may not be sufficient to determine the final answer set. In the following theorem, we depict a relationship between the sufficient set and necessary set.

IV. INTER CLUSTER QUERY PROCESSING

Response time is another important metrics to evaluate query processing algorithms in wireless sensor networks. All of those three algorithms, i.e., SSB, NSB, and BB, perform at most two rounds of message exchange there is not much difference among SSB, NSB, and BB in terms of query response time, thus we focus on the data transmission cost in the evaluation. Finally, we also conduct experiments to evaluate algorithms, SSB-T, NSB-T, and NSB-T-Opt under the tree-structured network topology.

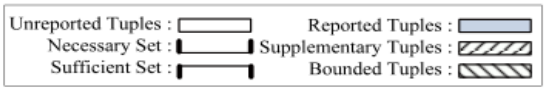

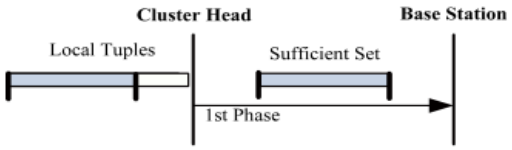

(a) Sufficient Set-based (SSB) Algorithm

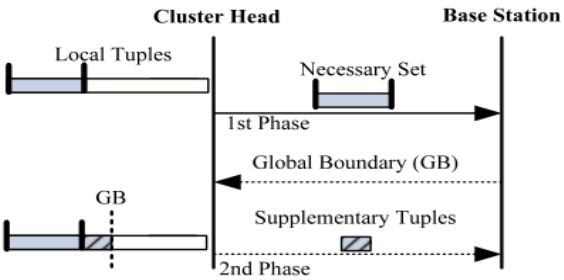

(b) Necessary Set-based (NSB) Algorithm

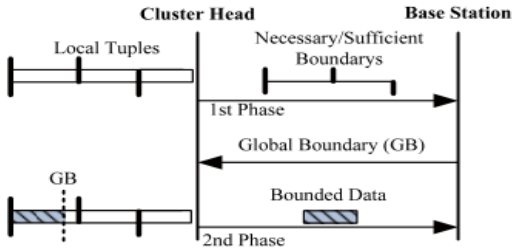

(c) Boundary-based (BB) Algorithm

Fig–2:Algorthim for inter cluster query processing.

V. ADAPTIVE QUERY PROCESSING

In this section, we first perform a cost analysis on data transmission of the three proposed methods. Since their performance is affected by factors such as the skewness of data distribution among clusters which may change continuously over time, we propose a cost-based adaptive algorithm that keeps track of the estimated cost for all methods in order to switch as appropriate.

5.1 Cost Analysis

We develop a cost model on communication cost of the three proposed algorithms. Accordingly, we propose a cost-based adaptive algorithm that dyna-mically switches among the three algorithms based on their estimated costs. Let M denote the no. of clusters in the network, and Cq, Cb and Cd be the sizes of query messages, boundary messages, and data messages, respectively. Also let |C(Ti)| and |N(Ti)| denote the cardinalities of the sufficient set and necessary set of the data set Ti in a cluster Ci(1< i <M), respectively.

VI. PERFORMANCE EVALUATION

In this section, we first conduct a simulation-based performance evaluation on the distributed algorithms for processing PT-topk queries in two-tier hierarchical cluster- based wireless sensor monitoring system. As discussed, limited energy budget is a critical issue for wireless sensor network and radio transmission is the most dominate source of energy consumption. Thus, we measure the total amount of data transmission as the performance metrics. Notice that, response time is another important metrics to evaluate query processing algorithms in wireless sensor networks. All of those three algorithms, i.e., SSB, NSB, and BB, perform at most two rounds of message exchange, thus clearly outperform an iterative approach which usually needs hundreds of iterations. Note that, there is not much difference among SSB, NSB, and BB in terms of query response time, thus we focus on the data transmission cost in the evaluation. Finally, we also conduct experiments to evaluate algorithms, SSB-T, NSB-T, and NSB-T-Opt under the tree-structured network topology.

6.1 Simulation Model

Here we describe our simulation model. We assume a wireless sensor field consisting of I zones. Each zone is deployed with an average of λ sensor nodes. Here, I can also be seen as the number of x-tuples in the global database and λ is the average size of an x-tuple. The confidence values for sensor readings in an area are assigned randomly. The clusters in the network is realized by a simple grid partition. There are M clusters, which is varied in our experiments. The simulator models sensor mote behavior at a coarse level, similar to the TAG simulator in which time is divided into units of rounds. At the beginning of each round, users may issue PT-Topk queries at the base station and the query messages are passed to cluster heads and sensor nodes without delay since transmission latency is not our main concern in this evaluation.

6.2 Experimental Model

A series of experiments is conducted to evaluate the proposed algorithms for a two-tier network in the following aspects: 1) overall performance, 2) sensitivity tests, and 3) adaptiveness. Additionally, overall performance under the tree topology is evaluated.

6.2.1 Overall Performance

We first validate the effectiveness of our proposed methods in reducing the transmission cost against two baseline approaches, including 1) a naive approach, which simply transmits the entire data set to the base station for query processing; 2) an iterative approach devised based on the processing strategy explored. The iterative

approach runs as follows: in each round, each cluster head delivers a single data tuple with the highest score in its local data set and the information of current local highest score (after removing the delivered data) to the base station. In response, the base station derives necessary set upon the data collected so far. One important reason that our approaches outperform the Iterative approach is due to the small and constant query processing rounds in our approaches. In our experiment, our algorithms complete within two rounds; while the iterative approach incurs about 60-200 rounds. Note that the experiments on adaptive algorithm are conducted on a setting that exhibits dynamic changes with certain temporal locality. Since the algorithm dynamically adapts to the changes by switching to appropriate methods, it provides an additional saving over the other algorithms.

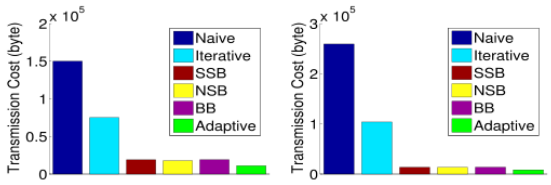

(a) Synthetic Data (b) Real Data

Fig -3 : Performance Evaluation

6.2.2 Sensitivity Tests

Next, we examine the impact of a variety of query and system parameters on the performance of the proposed algorithms. In the plots, we do not show there result of baseline approaches for clarity of presentation. We also omit the plots of experiments on real traces due to space limitation.

Here we first show the impact of query parameters, i.e., k and p, on performance. It shows the trend of transmission cost by varying k from 2 to 10. At the transmission cost increases for all algorithms because the number of tuples needed for query processing is increased. Among the SSB, NSB, and BB algorithms, BB does not perform as well as others when k is small but it becomes a good choice when k becomes larger.

6.2.3 Adaptiveness

The adaptive algorithm reaches our expectation by achieving the least transmission cost under all circumstances. In this section, we further test its adaptiveness to dynamic sensor network environments. One important factor that has an impact on the adaptive algorithm is the size of tuning window. To figure out the optimal setting of tuning window size, additionally, we conduct an experiment to show the behaviors of algorithms under a dynamic environment. We simulate shows that the adaptive algorithm switches timely to match the best algorithms. The adaptive algorithm switches from the NSB algorithm to the BB algorithm at about time 10, then returns back to NSB at about time 20, and finally switches to the BB algorithm again at about time 30. While the different algorithms may outperform each other at different time, the adaptive algorithm adapts to the dynamic changes to achieve the least transmission cost.

VII. IMPLEMENTATION RESULTS

Implementation is the most crucial stage in achieving a successful system and giving the user's confidence that the new system is workable and effective. This type of conversation is relatively easy to handle, provide there are no major changes in the system. Each program is tested individually at the time of development using the data and has verified that this program linked together in the way specified in the programs specification, the computer system and its environment is tested to the satisfaction of the user.

The system that has been developed is accepted and proved to be satisfactory for the user. The final stage is to document the entire system which provides components and the operating procedures of the system. Systems implementation is the construction of the new system and the delivery of that system into production (that is, the day-to-day business or organization operation).

Implementation is the carrying out, execution, or practice of a plan, a method, or any design for doing something. As such, implementation is the action that must follow any preliminary thinking in order for something to actually happen. In an information technology context, implementation encompasses all the processes involved in getting new software or hardware operating properly in its environment, including installation, configuration, running, testing, and making necessary changes. The word deployment is sometimes used to mean the same thing. Generally implementation of the software is considered as the actual creation of the software.

VIII. CONCLUSION

In this paper, we propose the notion of sufficient set and necessary set for efficient in-network pruning of distributed uncertain data in probabilistic top-k query processing. Accordingly, we systematically derive sufficient and necessary boundaries and propose a suite of algorithms, namely SSB, NSB, and BB algorithms,

for in-network processing of PT-Topk queries. Additionally, we derive a cost model on communication cost of the three proposed algorithms and propose a cost-based adaptive algorithm that adapts to the application dynamics. Although our work in this paper is based mainly under the setting of two-tier hierarchical network, the concepts of sufficient set and necessary set are universal and can be easily extend to a network with tree topology. The performance evaluation validates our ideas and shows that the proposed algorithms reduce data transmissions significantly. While focusing on PT-Topk query in this paper, the developed concepts can be applied to other top-k query variants.

IX. FUTURE ENHANCEMENTS

Every web application has its own merits and demerits. The project has covered almost all the requirements. Further requirements and improvements can easily be done since the coding is mainly structured or modular in nature. Changing the existing modules or adding new modules can append improvements. Further enhancements can be made to the application, so that the web site functions very attractive and useful manner than the present one. We plan to develop algorithms to support other probabilistic top-k queries in the future.

REFERENCES

[1] V. Bychkovskiy, S. Megerian, D. Estrin, and M. Potkonjak, "A Collaborative Approach to in-Place Sensor Calibration," Proc.Second Int'l Conf. Information Processing in Sensor Networks (IPSN), pp. 301-316, 2003.

[2] M. Hua, J. Pei, W. Zhang, and X. Lin, "Ranking Queries on Uncertain Data: A Probabilistic Threshold Approach," Proc. ACM SIGMOD Int'l Conf. Management of Data (SIGMOD '08), 2008.

[3] D. Zeinalipour-Yazti, Z. Vagena, D. Gunopulos, V. Kalogeraki, V. Tsotras, M. Vlachos, N. Koudas, and D. Srivastava, "The Threshold Join Algorithm for Top-k Queries in Distributed Sensor Networks," Proc. Second Int'l Workshop Data Management for Sensor Networks (DMSN '05), pp. 61-66, 2005.

[4] X. Lian and L. Chen, "Probabilistic Ranked Queries in Uncertain Databases," Proc. 11th Int'l Conf. Extending Database Technology (EDBT '08), pp. 511-522, 2008.

[5] Y. Xu, W.-C.Lee, J. Xu, and G. Mitchell, "Processing Window Queries in Wireless Sensor Networks," Proc. IEEE 22nd Int'l Conf. Data Eng. (ICDE '06), 2006.

[6] S. Madden, M.J. Franklin, J. Hellerstein, and W. Hong, "TAG: A Tiny AGgregation Service for Ad-Hoc Sensor Networks," Proc. Fifth Symp. Operating Systems Design and Implementation (OSDI '02), 2002.

[7] M. Wu, J. Xu, X. Tang, and W.-C.Lee, "Top-k Monitoring in Wireless Sensor Networks," IEEE Trans. Knowledge and Data Eng., vol. 19, no. 7, pp. 962-976, July 2007.

[8] D. Wang, J. Xu, J. Liu, and F. Wang, "Mobile Filtering for Error- Bounded Data Collection in Sensor Networks," Proc. 28th Int'l Conf. Distributed Computing Systems (ICDCS '08), pp. 530-537, 2008.

[9] K. Yi, F. Li, G. Kollios, and D. Srivastava, "Efficient Processing of Top-k Queries in Uncertain Databases with X-Relations," IEEE Trans. Knowledge and Data Eng., vol. 20, no. 12, pp. 1669-1682, Dec. 2008.

[10] J. Li, B. Saha, and A. Deshpande, "A Unified Approach to Ranking in Probabilistic Databases," Proc. Int'l Conf. Very Large Data Bases (VLDB), vol. 2, no. 1, pp. 502-513, 2009.

ISSN (e): 2250 – 3005 || Vol, 04 || Issue, 9 || September – 2014 ||
International Journal of Computational Engineering Research (IJCER)

Effect of sintering time on the particle size and dielectric properties of La-doped $PbTiO_3$ ceramic nanoparticles

A. A. Abd El-razek[*1], E. M. Saed[1], M. K. Gergs[1]
[1]*Ferroelectric Lap, Physics Department, Faculty of science, South Valley University, Qena-83523, Egypt*

ABSTRACT

Nanoparticles of [$Pb_{0.7}$ $La_{0.2}$] TiO_3 ceramics were prepared by conventional combust technique from the oxides of PbO, La_2O_3 and TiO_2 with different sintering time (t_s) (2, 6, 10, 12, 16 c 20h) while keeping the calcination temperature at 1200 ^oC. Particle size of the samples was estima between 25 to 65 nm through Scherrer formula and was found to increase with increasing sintering ti (t_s). Microstructural analysis of the samples was carried out using scanning electron microscope wh showed that grain boundary increased with increasing sintering time (t_s) while dislocations were reduc The dielectric constant and Curie temperature of the samples was increased with increasing sintering ti (t_s), but the activation energy in both of ferroelectric and paraelectric (E_a) decreased with increasing The diffusion coefficient (γ) decreased with increasing t_s. In other words the optimum sintering ti conditions was found.

KEYWORDS: *- A. Ceramics, B. Crystal growth, C. X-ray diffraction, D. Dielectric properties*

I. INTRODUCTION

In recent years, lead titanate ($PbTiO_3$) ceramics have attracted lot of attention due to its high Curie temperature (490 ^oC) and low dielectric constant (200), which makes it suitable for high-temperature and high-frequency transducer applications than that of PZT ceramic system [1,2]. However, pure lead titanate ceramics are very difficult to be sintered because of its large lattice anisotropy (c/a = 1.064). On cooling through Curie temperature, the large anisotropy of ceramic material becomes fragile. In addition, it's difficult to pole the ceramics with low resistivity ($10^7 – 10^8$ Ω cm).

By substitution of isovalent (Ca^{2+}, Ba^{2+}, Cd^{2+}, ……etc) or off-valent (Sm^{3+}, Gd^{3+}, La^{3+}, Y^{3+}, ……etc) ions into the Pb sites, the lattice anisotropy is reduced [3], and the samples become more dense. Mn doped $PbTiO_3$ produces a material with high mechanical strength, low dielectric losses and low dielectric constant reliable for piezoelectric resonator applications [4].

M.K. Gerges and et al. studied effect of preparation conditions (pressure, sintering time and temperature) on the ferroelectric properties of $(Pb_{0.1825}La_{0.125})TiO_3$ ceramics, where the optimum pressure was 40 MPa and they summarized that the sintering time and sintering temperature are considered to be the essential factor for improving quality of ceramics [5].

La- and Zr-doped lead titanate (PLT, PLZT) powder ceramics and thin films are known to have interesting dielectric, pyroelectric, electro-optic and piezoelectric properties [6-9], and so have a wide range of applications such as infrared sensors [10], capacitors [11], ferroelectric memories (dynamic random access memory (DRAM) and non-volatile random access memory (NVRAM)) [12], shutters [7], optical modulators [13], etc.

PLT and PLZT belong to the family of ferroelectric relaxors, and so show anomalies in their properties in a relatively extended interval around a temperature, T_m at which the permittivity, ε_r, reaches a maximum. The corresponding phase transition is called diffuse phase transition.

Piezoelectric ceramics are commonly used as sensors. These materials have good detection and output characteristic, and can operate over a wide range of frequencies. However, pure piezoelectric ceramics are often too stiff and brittle to be used as embedded sensors in polymeric composites.

In the present work, ferroelectric and piezoelectric properties have been investigated for nanoparticles of PLT ceramics synthesized through conventional ceramic preparation technique.

Corresponding author*1: Tel: +20966904409; Fax: +20965211273
E-mail address: abdelrazek.mahmoud@sci.svu.edu.eg; abdophy2010@yahoo.com

II. EXPERIMENTAL PROCEDURE

Nanoparticles of the PLT were prepared with conventional ceramic method where stoichiometric ratios of oxide powders of PbO, La_2O_3 and TiO_2 were mixed together, and pressed into disc shaped pellets of 2 cm diameter and about 1 cm thickness by applying a pressure of 20 MPa. These discs were calcined for 2 h at a temperature of 700 °C. These discs were further sintered at different sintering times (t_s) 2, 6, 10, 12, 16 and 20 h at 1200 °C. Finally, the disks were rushed and grinded mechanically to produce samples with 7.5 mm diameter and about 1.5mm thickness and were coated with on opposite face with aluminum thin films to study the electrical properties. Compositional analysis and lattice parameters of the samples were carried out through X-ray diffraction (XRD) and microstructure analysis was done using scanning electron microscope (SEM) (JEOL, JSM-5500LV). The dielectric properties were measured using LCR meter (TH2826) The Curie temperature was calculated by measuring the dielectric behavior as a function of temperature.

III. RESULTS AND DISCUSSIONS

a. *Structural properties*

The X-ray diffraction patterns of ceramic nanoparticles of $[Pb_{0.7}\ La_{0.2}]\ TiO_3$ sintered under different times (2, 12 and 20h) at sintering temperature 1200 ^oC are shown in Fig. 1. The X-ray analysis indicated that the La-doped $PbTiO_3$ ceramic nanoparticles have major peaks at (101), and all of them are tetragonal in phase. The average grain size (D) of the samples was calculated using Debye-Scherrer method from the broadening of the diffraction line using the expression [14]:

$$\mathbf{D = 0.94\lambda/\beta\cos(\theta)} \qquad \mathbf{(1)}$$

Where λ is the wave length of the CuKα radiation, β is the full width at half maximum (FWHM) of the diffraction peak and θ is the Bragg diffraction angle. Fig. 2 shows the variation of grain size as a function of sintering time (t_s), and it was found that with increasing t_s, grain size increases. The behavior can be explained according to the phenomenological kinetic grain growth equation expressed as [15]:

$$\mathbf{\log G = (1/n) \log t + (1/n) [\log K_o - 0.434 (Q/RT)]} \qquad \mathbf{(2)}$$

Where G is the average grain size at the time sintering, n is the kinetic grain growth exponent, K_o a constant, Q the apparent activation energy, R the gas constant, and T is the absolute temperature. The average grain size of all the studied samples has been found increased with increasing of sintering time (t), where the average grain size increased from 25 nm to 65 nm, if the sintering time increased from 2h to 20 h are respectivelly between 25 to 65 nm. The growth in grain size as a function of sintering time can be observed in [16].

Fig. 3(a) and (b) shows the lattice constant and lattice anisotropy of La-doped $PbTiO_3$ ceramic nanoparticles as a function of sintering time (t_s) at sintered temperature 1200 ^oC, respectively. It is seen that the lattice constant c-axis decreases correspondingly with increasing the sintering time, while the a-axis changes little, so that the lattice anisotropy (c/a) decreases with increasing sintering time. This results indicate that the system is approaching towards cubic structure. The increasing of sintering time it will assist the modified Lead titanate ceramics in sintering process and improve the crystal structure of the samples. This behavior can be observed in [17,18]. According to Arlt's model [19], the lattice anisotropy (c/a) is inverse proportional to the partical size.

The microstructural analysis of La doped $PbTiO_3$ ceramic nanoparticles were carried out using scanning electron microscope (SEM). Fig.4 (a-c) presents the SEM micrographs of 20% doped $PbTiO_3$ sample sintered at 1200 ^oC and at different sintering time (2, 10, 16 and 20h). It can be seen that the diameter of grain boundary increased with increasing sintering time of the sample.

b. Dielectric properties

Figs. 5(a) presents the variation of dielectric constant with sintering temperature 1200 ^0C for three sintering times 2, 12 and 20h under an applied field of 100 kHz. While Fi.5 (b) presents the variation of dielectric constant with respect to the sintering time at two fixed frequencies, 10 KHz and 100 KHz, respectively., Fig. 5(a) shows that for each sample, the general mode of (ε) variation against (T) yields a bell curve, where the dielectric constant increases with increasing temperature and reaches to a maximum value (ε_{max}) at Curie temperature (T_c), then it decreases with further increase of sintering temperature. Further, it is also seen that ε_{max} increases with increasing sintering time, where if the sintering time is increased from 2h to 20h, the ε_{max} increases from 5367 to 8217. This increase in dielectric constant is due to increasing grain size corresponding to the increase in sintering time. Similar behavior has been reported by M. Dongle et al. where they report that the dielectric constant increases with increasing sintering time [5]. From Fig.5(b) it can be seen that the Curied temperature (T_c) for all the studied samples is independent of frequency and the ε_{max} decreases with increasing frequency of the applied field, where in low-frequency region, the dielectric constant has high value, which can be attributed to various polarization effects. At higher frequencies, electronic polarization contribution dominates over ionic and orientation polarization and hence the dielectric values are less [20-22].

Fig.6 shows the variation of Curie temperature with respect to the sintering time. It is seen that the Curie temperature increases with increasing sintering time, where if the sintering time is increased from 2 to 20h, the T_c increases from 423 to 453 ^oK. This increase in T_c can be related to the configuration of new dipole moments.
Fig. 7 presents plot of activation energy (Ea_f, Ea_p) versus the sintering time (t_s), where Ea_f and Ea_p are the activation energy in ferroelectric and paraelectric phases, which can be calculated from the equation [23].

$$\mathbf{Ln\ (\tau^{-1}) = Ln\ (\tau_\circ^{-1}) - (E_a/k)(1/T)} \qquad \mathbf{(3)}$$

Where, τ and $\tau_\circ$ represents the relaxation and critical relaxation times at T_c, respectively. E_a is the activation energy and k is the Boltzmann constant. The slope of $\ln(\tau^{-1})$ versus (1/T) gives the value of E_a. From Fig.7, it is seen that in whole range of sintering time the value of Ea_p is higher than that of Ea_f. The behavior can be related with crystal structure which is tetragonal before the Curie temperature T_c and cubic after it. The rate of decrease for both values of Ea is rapid at low sintering time t_s while it is slowed down at higher values and both the values of Ea reach to a minimum at $t_s \geq 20$ h. These results can indicate the behavior of maximum value for dielectric constant according to the following equation [24]

$$\mathbf{\mu = \mu_o\ exp\ (-E/KT)} \qquad \mathbf{(4)}$$

Where μ the mobility of dipole moment, E is the activation energy, K is the Boltzmann constant and T is the temperature. The last equation show that the mobility of dipole moment and consequently the maximum value of dielectric constant is inverse proportional to the activation energy, and as the sample was sintered at t_s = 20h posses minimum value for activation energy, so that it posses maximum value for dielectric constant.

c. Sintering time effect-induced diffused phase transition

The broadening of the dielectric peak of nanocrystalline PLT suggests a typical non-relaxor behavior with diffuse phase transition. A quantitative estimate of the diffuseness parameter (γ) of the ferroelectric-paraelectric phase transition can be obtained using the equation [25]:

$$\mathbf{(1/\varepsilon - 1/\varepsilon_{max}) = 1/C(T - T_c)^\gamma,\ (T > T_c),} \qquad \mathbf{(5)}$$

Where γ and C are modified constants with $1 < \gamma < 2$. The value of γ determines the degree of diffuseness of the phase transition. The value of γ is equal to 1 for a system with a completely ordered transition. On the basis of a local compositional fluctuation model, the value of γ is equal to 2 for a completely diffuse system. The value $\gamma > 1$ suggests diffused transition [26]
The plots of $\ln(1/\varepsilon - 1/\varepsilon_{max})$ versus $\ln(T - T_c)$ corresponding to the samples for sintering time = 2, 12 and 20h, respectively, are shown in Fig. 8 at an applied field of 10 kHz.
According to Eq (4) the slope of $\ln(1/\varepsilon - 1/\varepsilon_{max})$ versus $\ln(T - T_c)$ gives the value of γ. From the plot, it can noted that value of γ decrease from 1.3 to 1.11 when the sintering time is increased from 2 to 20h, indicating that the ferroelectric transition becomes less diffuse and the quality of the samples is more. These results are in agreement with the results reported by S.K.S. Parashar et al [27,28]. The values of γ calculated from the fitting of curve in Fig.8 are listed in Table 1.

IV. CONCLUSIONS

We have successfully grown the nanoparticles of $(Pb_{0.7}La_{0.2})TiO_3$ ceramic and studied the effect of sintering time on the samples sintered at 1200 ^oC which show that the sintering time cannot only reduce the lattice anisotropy (c/a), but also keep good dielectric properties, where the value of ε_{max} increased from 6010 to 18200 if the sintering time is increased from 2 to 20h at a frequency 10 kHz of the applied field. For all the ceramics samples, the values of ε_{max} at 10 kHz were more than that at 100 kHz at the same sintering time. Also the phase transition increased with increasing sintering time and it is independent of the frequency of applied electric field. The grain sizes of the samples were increased with increasing sintering time which means that the dislocations were reduced and the samples became harder. The γ coefficient decreased with increasing sintering time which means that the sample quality was further improved and the bell curve was sharper with increasing sintering time. We can conclude that the sintering time is considered to be the essential factor for improving the quality of the ceramics samples.

REFERENCES

[1]. S. Ikegami, I. Ueda, T. Nagata, Electromechanical properties of $PbTiO_3$ ceramics containing La and Mn, J. Acoust. Soc. Am. 50 (1971) 1060-1066.
[2]. T. Takahashi, Lead titanate ceramics with large piezoelectric anisotropy and their application, Ceram. Bull. 69 (1990) 691-695.
[3]. Te-Yi Chen, Sheng-Yuan Chu, Yung-Der Juang, Sensors and Actuators A 102 (2002) 6-1.
[4]. D. Hennings, H.Pomplum, J. Amer. Ceram. Soc. 57, 527, (1974).
[5]. M.Dongl, M.K. Gerges, H.A. Aly, J. Sol, 19 (2) (1996) 319-332.
[6]. G.H. Haerling, C.E. Land, J. Am. Ceram. Soc. 54 (1) (1971) 1.
[7]. C.E. Land, P.P. Thacher, Proc. IEEE 57 (1969) 751.
[8]. J.S. Wright, L.F. Francis, J. Maker. Res. 8 (1993) 1712.
[9]. G.H. Haerling, J. Am. Ceram. Soc. 82 (4) (1999) 797-818.

[10]. K. Ijima, Y. Tomita, R. Takayama, I. Veda, J. Appl. Phys. 60 (1986).
[11]. D. Bersani, P.P. Lottici, A. Montenero, S. Pigoni, Mater. Sci. 31 (1996) 3153-3157.
[12]. S.J. Lee, K.Y. Kang, S.K. Han, M.S. Jang, B.G. Chae, Y.S. Yang, S.H. Kim, Appl. Phys. Lett. 72 (3) (1998) 299-300.
[13]. M. Ishida, H. Mastsurami, T. Tanka, Appl. Phys. Lett. 31 (1977) 433.
[14]. P.Scherrer, Gottinge Nachichten, 2, 98, (1918)..
[15]. T. Senda, R.C. Bradt, Grain growth in sintered ZnO and ZnO-Bi_2O_3 ceramics, J. Am. Ceram. Soc. 73 (1) (1990) 106-114.
[16]. Xingang Wang, Maolin Wang, Hua Song, Bingiun Ding, Materials Letters 60 (2006) 2261-2265.
[17]. Sarabjit Singh, O.P. Thakur, Chandra Prakash, K.K. Raina, Material Letters 61(2007) 1082-1085**.**
[18]. Sheng-Yuan Chu, Te-Yi Chen, J. Sensors and Actuators A 107 (2003) 75–79.
[19]. Grace King, Edward K. Goo, Effect of the c/a ratio on the domain structure in [Pb_{1-x}, Ca_x]TiO_3, J. Am Ceram. Soc. 73[6] (1990) 1534-1539.
[20]. M.K.Gergs, G.A.Gamal, M.A.Massaud, Dielectric properties, Deby relaxation time and activation energy of [$(Pb_{1-x}$ $Sr_x)_{1-1.5z}La_z$]TiO_3. Ceramics, Egypt. J. Solid, 30(2) (2007) 20-35.
[21]. M. Kellati, S. Sayouri,, N.El Moudden, M. Elaatmani, A. Kaal, M. Taibi, Material Research Bulletin 39 (2004) 867-872.
[22]. Ravender Tickoo, R.P. Tandon, K.K. Bamzai, P.N. Kotru, Materials Science and Engineering B103 (2003) 145-151.
[23]. A. Ziel, " Solid State Physical Electronics" Secind Edition, Prentice- Hall of India Private Limited, New Delhi, (1971) 489
[24]. E.V. Bursian, Ferroelectrizitat (KTB), 2, (1981) 47.
[25]. S.M. Piligrim, A.E. Sutherland, S.R. Winzer, J. Am. Ceram. Soc. 73 (1990) 3122.
[26]. K. Kuchnio, S. Nomura, Ferroelectric Lett. 44 (1982) 55.
[27]. S.K.S. Parashar, R.N.P. Choudhary, B.S. Murty, Material Science and Engineering B 110 (2004) 58-63.
[28]. K. Prasad, Indian J. Eng. Mater. Sci. 7 (2000) 446.

Table Caption

Table.1. Comparison of lattice parameter (nm), dielectric data, grain size (nm), diffusivity and activation energy (eV) for the sample ($Pb_{0.7}$ La $0_{.2}$□$_{0.1}$)TiO_3 ceramics, with different sintering time.

Parameter	2	6	10	12	16	20h
c (A^o)	4.1	4.09	4.075	4.065	4.05	4.045
a (A^o)	3.9	3.901	3.9015	3.9018	3.902	3.9022
c/a	1.05	1.048	1.044	1.041	1.037	1.035
ε_{max} (10 kHz)	6010	9153	13308	15427	17500	18200
ε_{max} (100 kHz)	5367	7149	7305	7650	7966	8217
T_c (K)	423	427	433	440	447	453
partical size (nm)	25	38	50	57	61	65
γ	1.3	1.24	1.19	1.16	1.13	1.11
E_{af} (eV)	1.6	1.18	1.07	0.983	0.903	0.853

Figure caption

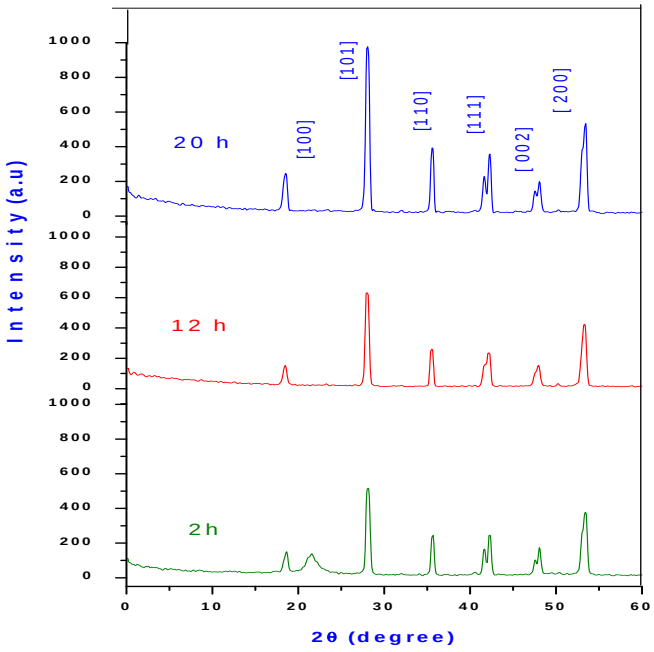

Fig. 1. Shows XRD patterns of variation sintering time for the sample [($Pb_{0.7}$ $La_{0.2}$ □$_{0.1}$)] TiO_3 ceramics sintered at 1200 ^oC.

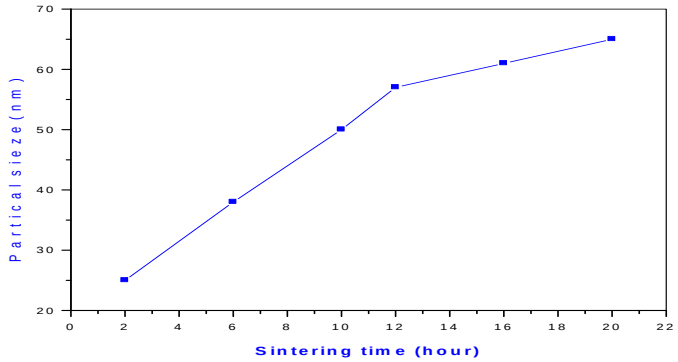

Fig. 2. Shows variation of average grain size for the sample [($Pb_{0.7}La_{0.2}\square_{0.1}$)] TiO_3 ceramics with sintering time sintered at 1200 ^oC.

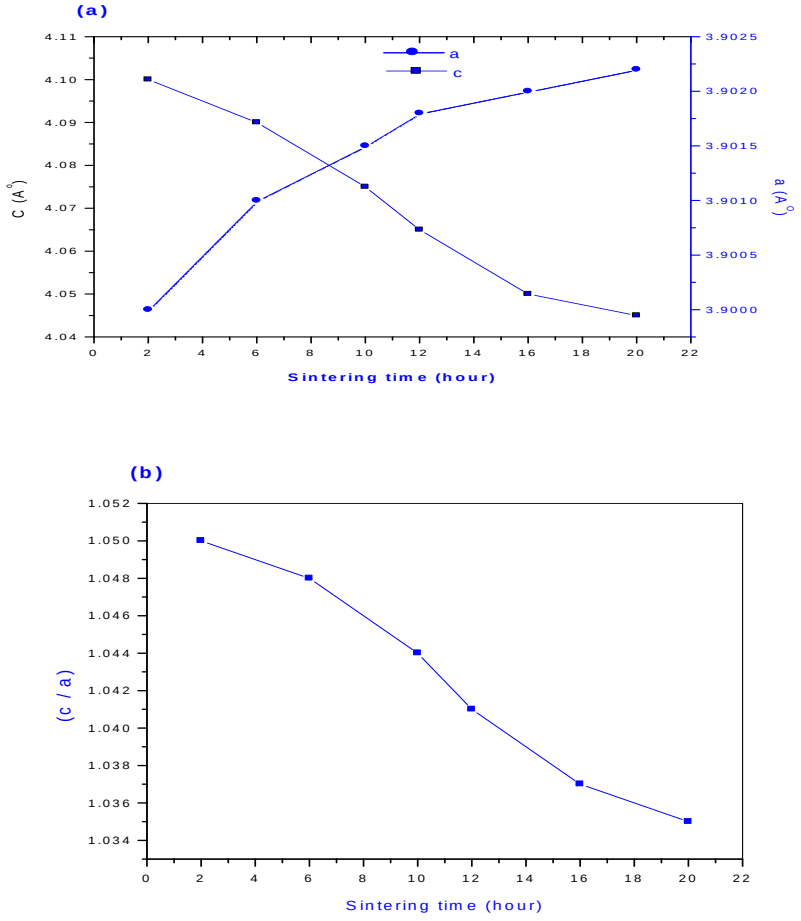

Fig.3. Dependence of the (a) lattice constant and (b) lattice anisotropy (c/a) of [($Pb_{0.7}La_{0.2}\square_{0.1}$)] TiO_3 ceramics on the sintering time.

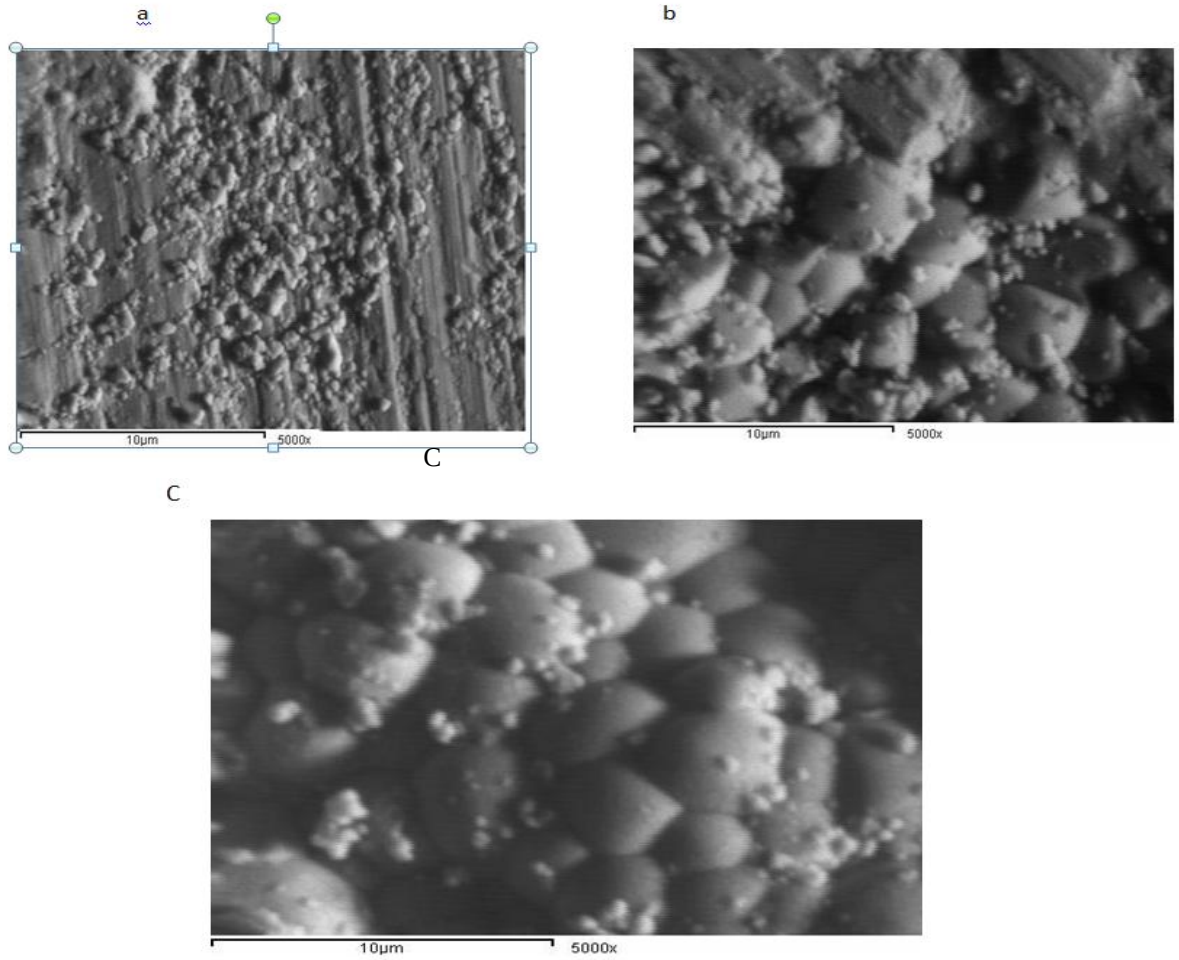

Fig. 4. SEM photographs of (a), (b) and (c) represented the sample [($Pb_{0.7}La_{0.2}$ □$_{0.1}$)] TiO_3 ceramics sintered at 1200 ^{0}C on the sintering time 2, 12 and 20h are respectively.

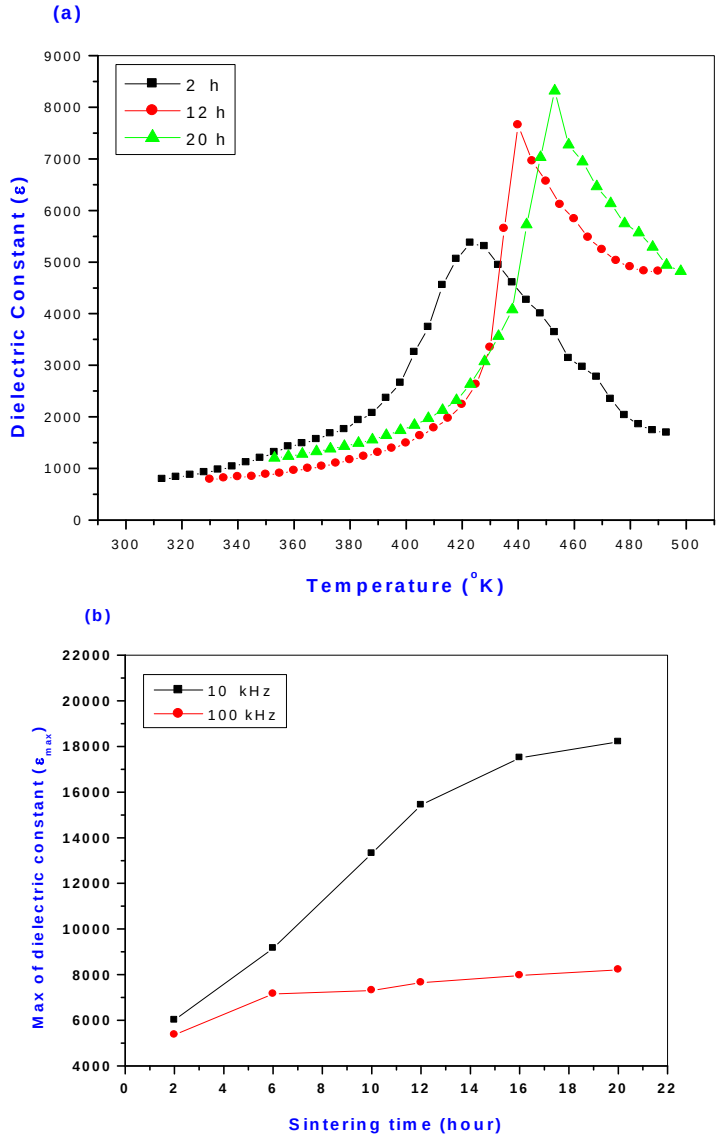

Fig. 5. (a) Variation of dielectric constant with temperature for the sample PLT ceramics sintered at 2, 12 and 20h. (b) Depending (ε_{max}) with two various frequencies (10 and 100 kHz) for all studied the samples

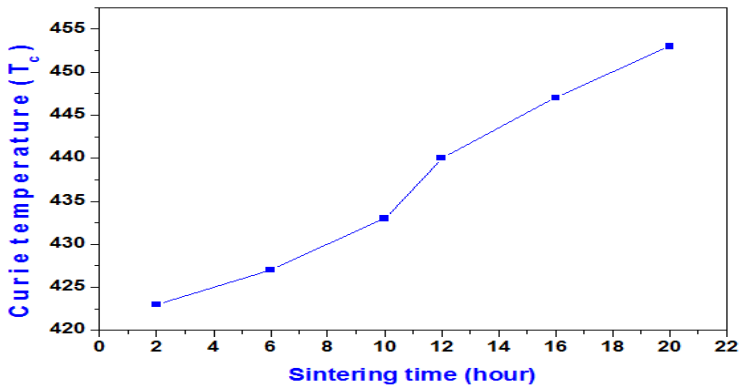

Fig.6. Depending Curie temperature for the sample [$(Pb_{0.7}La_{0.2}\square_{0.1})$] TiO_3 ceramics sintered at 1200 ^{0}C as a function of the sintering time.

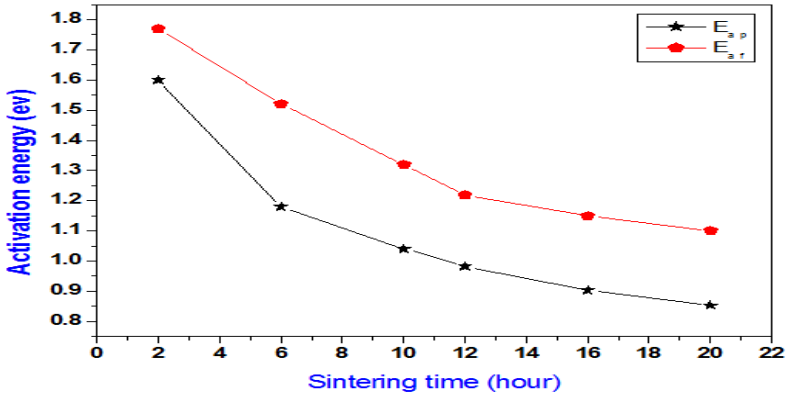

Fig. 7. A plot of activation energy at the ferroelectric (E_{af}) and paraelectric phases (E_{ap}) for the sample $(Pb_{0.7}La_{0.2}\square_{0.1})TiO_3$ ceramics versus with the sintering time.

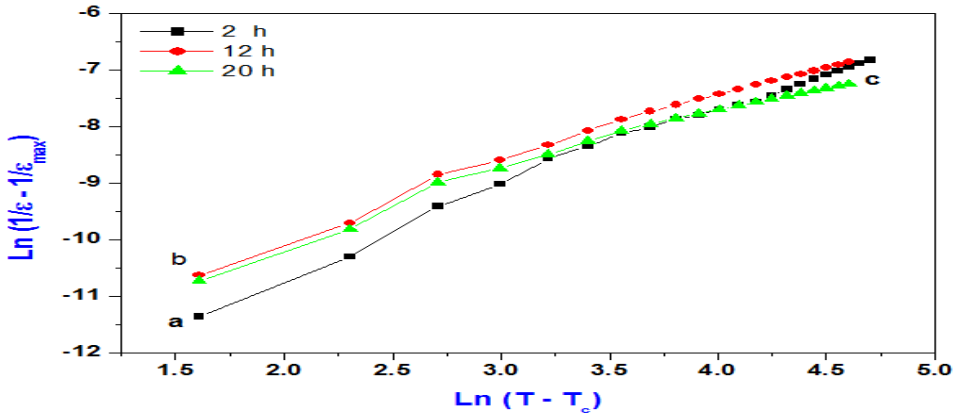

Fig. 8. A plot of ε_{max} versus the $\ln(1/\varepsilon - 1/\varepsilon_{max})$ versus $\ln(T - T_c)$ for $(Pb_{0.7}La0_{.2}\square_{0.1})TiO_3$ ceramics, with sintering time (a) = 2h, (b) = 12h, and (c) = 20h.

ISSN (e): 2250 – 3005 || Vol, 04 || Issue, 9 || September – 2014 ||
International Journal of Computational Engineering Research (IJCER)

Can Digital Drawing Tools Significantly Develop Children's Artistic Ability and Creative Activity?

Aber Salem ABOALGASM[1], Rupert WARD[2]
[1]*Huddersfield University, Queensgate, Huddersfield, HD1 3DH, United Kingdom*
Tel: 01484471286 +0044, 014, Fax: 148441106

ABSTRACT:
This study aims to investigate how the new digital art tools can significantly improve children's artistic ability and creative activity. This particular research tested 16 students aged 9-10 years old in art classes, with the intention of presenting a model for the development and measurement of technological creativity. It uses a modified TAM technology acceptance model to assess the usefulness of digital art tools. The children were provided with appropriate subjects and techniques to improve their performance with the tools, and the relationship between art, technology and creativity was explored. The results of the project show a general improvement in pupils' artistic ability and inventiveness through the development of their technological skills, as well as greater ability to express themselves visually.

KEYWORDS: *Artistic ability, creative activity, children, ease of use of digital art tools, TAM technology acceptance model, usefulness of digital art tools, visual art*

I. INTRODUCTION

Many new digital methods of drawing using computers and software have become available recently. These techniques are now even available in primary schools. They include laptops, iPads, tablets, smart boards and special software such as Photoshop, 3D, Premier Illustrator and others. This hasexpanded the boundaries of traditional drawing and made it possible and much easier to re-arrange, select, add, delete, add colours, store and transmit work, since these digital tools are now part of modern technology. Children are encouraged to use them and this is a way to both improve children's cognitive skills and enhance their creativity. However, some researchers argue that such technology destroys artistic creativity because it puts mechanical processes between the artist and the finished work of art. This is related to concerns about the use of 'instant art' [1]and the attraction of easy reproduction by using programs such as those mentioned above. It is feared that exposure to so many electronic images might have a negative impact on pupils' imaginations. It is also claimed that technology produces an over-sanitized result: for example, the Disney studios [2] decided this may be the case, and returned to traditional methods. In contrast, Davis [3] demonstrates that digital tools are a good method of building artistic creativity, as well as being easier to use in circumstances where great flexibility is needed in terms of source materials and techniques. A number of studies have found that digital tools can offer the user more choice and variety than traditional methods, as"Students can manipulate drawing tools with ease, and can perform subsequent revision and dynamic linkage of ideas and concepts" [4].

In order to answer the questionposed in the title, regarding whether digital tools can help to develop children's artistic ability, further information is needed. Much research has been focusedon the use of technology in schools, and the subject of children's artistic abilities has been extensively discussed, but there is little published information on the topic of art combined with technology and virtually none on this topic in relation to children of 7-11 years old. Until recently, the use of computers in schools was primarily focused on older students, but as the equipmenthas become less expensive,its use has spread to all schools. Now computer technology is readily available for educational purposes in many parts of the world. In addition, with the spread of home computers, children of a younger age generally have some experience of using them.
Many world-famous artists are experimenting with the new technological capabilities that are currently available. Artistic creativity and development is becoming increasingly important in the modern world, where visual information is essential.When trying to collect data for the present research,

it was found to be impossible to carry out a large-scale survey of junior school art practice.Even though computers are present in all English schools, there is no information available to say which schools, or how many, are practising the use of digital tools in art classes. Information was needed on certain main topics, which canbe expressed most simply as a series of questions. Do digital tools help children to express themselves visually? Do they promote and develop artistic ability?Do children find the digital tools satisfactory to use?How easy or difficult are they to use?Does ease of use affect the children's usage and motivation,and thus their ability?Which digital tools are best and why?Due to limitations regarding time and space, the research was restrictedto collecting data from schools only.

II. PREVIOUS RESEARCH

Opinions about the value of digital tools vary. Some studies find that the use of technology in art is positive as an aid to creativity, whereas others find it has a negative effect. This question is tested and researched in daily practice in the fields of commerce, education and fine art. One of the concerns raised is the risk of'spoon-feeding' [5].In addition, according to Papadimitriou [6], exposure to too many electronic images might prevent the pupil's own imaginations working. It is feared that 'Instant art' and the temptations of easy reproduction, such as those that Adobe Illustrator and Photoshop provide, can destroy creativity [1].However, there appears to be more favourable than unfavourable research opinion. As researcher [7] indicates, theeffective use of computers to express creativity also depends on how imaginative the user is. Faber [8] demonstrates that new technology can give a greater understanding of how we express the world through drawing, and this can strengthen the use of traditional tools. Gan [9] favours the use of technological tools to strengthen children's manipulative skills and help them to understand complex ideas. Other studies show how extremely useful digital drawing methods can be as teaching aids, for speed and clarity.

III. METHODOLOGY

It was decided that a case study would be the best choice of strategy for collecting information. This flexible approach allows mixed methods to be used effectively. Data has been collected from a sample of 16 students, in an art workshop using both digital and traditional drawing tools. The 16 students comprised 11 males and 5 females in a classroom art workshop. The agerange chosen was 9-10 year olds, and they were given traditional tools such as paper, pencils, erasers and colours to use first. The aim of the testwas to show how students can be equally creative using digital and traditional drawing tools. Tamazight fonts were used as an art designand the intention was to teach the students to use this font in avisual way. They were asked to draw Tamazight fonts on different themes using traditional drawing tools, and then to draw and paint the same ideas using digital tools. The students worked as individuals and as groups. The traditional Tamazight font drawings were incorporated into the computer via utilisation of the art software known as 'Tux Paint'.

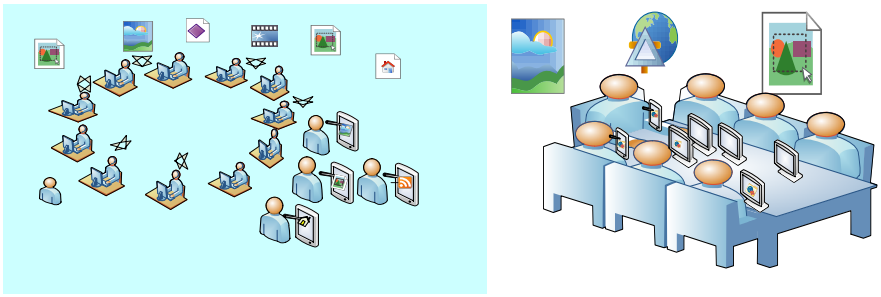

Fig 1. Graphic illustrating children working both independently and in a group

The art tools available in the ICT room were'Tux paint'software and iPads; few pupils had access to Tablets and iPads at home, which may have affected their abilities. They startedby working with traditional tools and then pursued the use of digital tools.

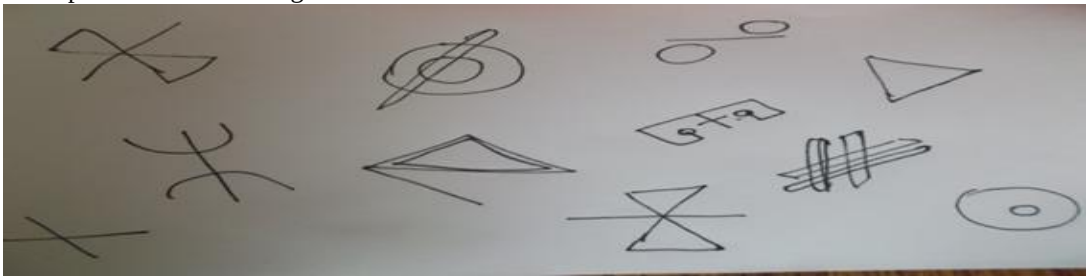

Fig 2. Picture illustrating Tamazight fonts

To answer the research questions, the data from the case study was analysed and placed into categories. Three techniques were used to collect information: narrative observation, semi-structured interview and a questionnaire.

2.1 Information obtained by observation and semi-structured interviews

The study concentrates on three topics: the enhancement of artistic creativity in using the fonts, the pupils 'motivation, and assessment of the digital tools and how well pupils use them. At first, the pupils drew with traditional methods to involve them in the project. They then drew the same things using digital software techniques. At the beginning, they had no knowledgeof these tools and no clear idea of what to do. However, there was good progressin their technical skills and artistic ability. By the end of the project, they were almost all using the tools correctly and completing their work using most of the software available. They showed continuity of ideas, a clear idea/message in their work and definite self-expression. Working as a group is also a powerful means of helping pupilsexplore possibilities and become more creative. The work involved the children in the whole design process. It was possible to observe how different tools motivated them to create more and better art work. Only two or three pupils were unable to continue or complete work, and had to find alternative ways to achieve their ideas, or even change their subject completely. Most pupils solved any difficulties and showed great persistence in doing so. Their motivation to overcome difficulties was very strong. There appeared to be a general improvement in artistic creativity in the class, shown by the usage of more complex ideas and better and increased use of shape, colour and space, as well as improved ability to complete projects. The semi-structured interview data was obtained using grounded theory to provide greater depth and accuracy. The three topics exploredwithin the information obtained fromsemi-structuredinterviews were againenhancement of artistic creativityin using the fonts, pupil's motivation, and assessment of the digital tools and how well pupils use them.

Pupil's motivation and assessment of digital tools and how well pupils use them: questions and researcher's analysis of answers

Table 1. Interview questions and analysis of answers

Question	*Answer*	*Observer'snotes*
Which tool was most useful to carry your project?	*All the students find that 'Magic' is the best tool because it makes good art; it gives more than they expect. The Magic tool has many different functions. It can give students the opportunity to create different forms of work. 6 of the 16 students also add 'Stamp'as a preferred tool. They say it gives good results for their art work, is more realistic and has big effects.One student says, "Magic makes big effects for my work". 3 students like the graphic tool as well.*	*Students explore the ease and usefulness of digital tools*
Which tool was easiest to use? Can you say why?	*All students find that the tools which are easy to use are not always the most useful. Some tools are difficult to use but useful, while some of them, such as brushes, are very useful but are difficult to use. In contrast, lines are difficult to use and are also not useful. One of the students says, "I switch on the software then I use the tools".*	*Ease of use in relation to usefulness*
How do you tell the computer you want to draw?	*Students start giving actual detail about how and which buttons are used to start their work. All of them start with basic tools first,such as pencil and rubber to draw the idea.*	*Here students know how to start working*
What if you make a mistake?	*Some of them say that it is easy to solve problems by using a rubber, or to cover mistakes by putting another picture over it or deleting the picture and doing it again. A student says, "I can go back two steps to delete the mistake". Another says "I will ask the teacher to help me to correct the mistake".*	*All of them know how to solve problems*
Do you think that you do better drawings using digital or has using them made	*About 13 of the 16 think drawing by using digital tools makes better art. The rest say they prefer to touch and feel with the tools to do creative art work. One student says, "I like to touch my art work and my tools, then I feel that is my creativity". That is, they prefer traditional tools.*	*Preference depends on the student's interest*

your work less good?		
What did you learn from doing your project?	*They say they have learned how to use the tools, developed skillsin using them and understand each tool's function, and know how to use the tools perfectly.*	*Understand each tool's function*
Do you know how to choose colours for project?	*All the students say, yes, they know how to choose colours, because they find it easy, useful and enjoyable to use.*	*Colours used tobuild artistic creativity*
My screen is full how do I make the space bigger?	*Some of the students find the digital screen too small. They like to draw on a big space such as smart board.*	*Space is important to develop their cognitive ability*
Did you find it more pleasant or easier to use the traditional and the digital tools?	*Some of the pupils support the digital method.A student says, "Digital tools have more effects". Another student prefers traditional methods: "It is easy and I can control the tools and it's very flexible". Another student says "Both tools have advantages and disadvantages and both are useful". The more you work, the more you build your talent with both types.*	*Both tools (D and T) haveadvantages and disadvantages*
In which subject do you like to use digital tools?	*Some students say, "We like some school topics. Drawing helps me to understand the topic more clearly, such as geography, history and others". Most say it is useful in all subjects.*	*Clear understanding*
What the advantages and disadvantages of digital and traditional tools?	*Some students say "Traditional tools make me closer to my project and are more feeling, sensitive and interesting. Both tools have advantages and disadvantages."Other students say that the digital tools add more than they expected. They can add things such as animation, sound and sound effects, as well as more colours. One student says, "Digital is a little bit strict, I can't control them, whereas traditional is easy to control".*	*T methods allow more feeling, sensitivity and interest*
Is there anything can make digital art work different and more attractive?	*Adding more pictures in the ICT room and providing more tables for drawing will offer more stimulation for art and creative activity.*	*The design of the place has a big impact for the child*

It appears from the interviews that in general, the children found the digital tools very useful. They are young children, however, and although it seems they appreciate the usefulness of these tools, at this stage of development they still find some difficulties in using them compared to simple traditional tools. On the other hand, their skill is improving all the time and clearly, thepupils enjoyed these sessions. Working as a group is also a powerful means of helping pupils investigate possibilities and become more creative. The children were involved in the work throughout the whole design process.

2.2Modification of the technology acceptance TAM model for the purposes of the current research

The Technology Acceptance Model (TAM) is an information systems theory that shows how users come to accept and use a technology [10].It appears that the basic TAM theory sometimes needs adjustment for different purposes. This would be necessary in the present research. The modified TAM model can help the teacher to assess the usefulness and ease of use of different digital art tools in producing creative art work with imagination and ability. Digital tools can be a support for children in their creative work. Evaluation of children's performance in a classroom project such as this enables a clear assessment of the children's capabilities, and can also determine which tools can motivate children to create a good piece of art.

This research has summarized the criticism of previous studies that TAM is too simple and does not explain the connections between intention and behaviour, or the pressures caused by having an ultimate goal. There can also be a danger of pre-determined action, or that PU and PEU are not sufficiently investigated. However, research also suggests that the TAM theory should work in more than one situation. Itcan be flexible and is able to adapt particularly well to children's personalities; thus, in an attempt to combine the social element with the technical element,it should be possible to assess both aspects using the Technology Acceptance Model.

Two of the most important factors affecting child learning and creativity are intrinsic, artistic motivation, which arises from within the person, and extrinsic motivation, which comes when a child is obliged to do something because of factors external to him or her, such as rewards like good grades, prizes and competitions. The child's attitude and motivation can be greatly affected by providing tools, by giving praise and by stimulation of ideas, for example, a drawing to complete, a pretend identity change or an imaginary situation. Possibly the main factor in building a child's artistic creativity is intrinsic motivation, because when children are motivated to do art work it either brings them pleasure, or they feel that what they are doing is significant.

The proposed framework for practical research

The modified TAM framework is based on input from the data collected from the case study. The exploration of results from the observation test, questionnaire and interviewswith pupils in the art classroom is also based on a literature review and diverse theories in the area of motivation and the effectiveness of digital art tools in developing children's artistic ability and promoting creative activity that could be used in the art classroom.

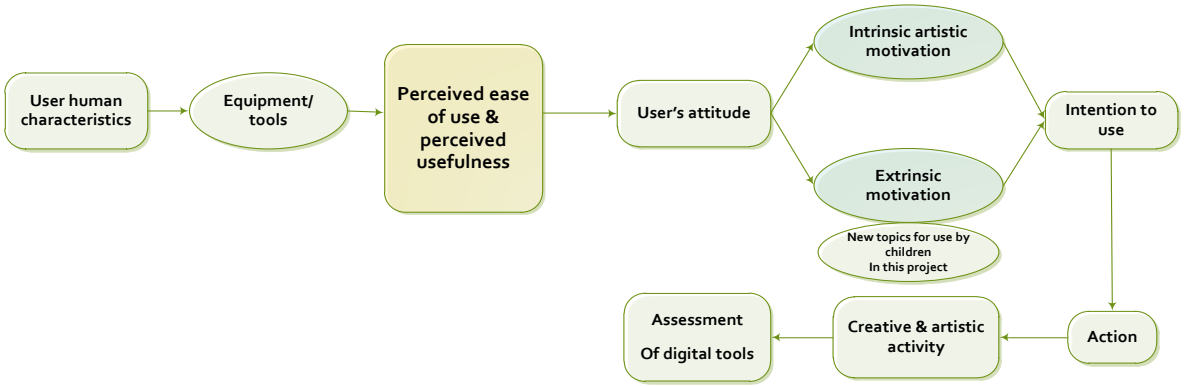

Fig4. Framework of modified TAM theory model for classroom project

Benefits of modified TAM theory for use in the present research:

- The present research suggests that the child's motivation and enjoyment are important,and the wish to create good artwork enhances the desire to use digital drawing tools perfectly and improve their performance. Thus, when a pupil understands how to use digital tools, and understands which are easy and which difficult to use, this leads to the child grasping the usefulness of digital tools.
- This new framework model helped to assess artistic ability and creativity to a limited extent. The results proved that ease of use is not important in developing artistic powers; satisfaction with the final product, whether its creation was easy or difficult, was far more important.
- This could be useful for both pupils and teachers as the use of digital tools in art increases within education at all levels.
- The new model of working enables the identification of relationships between art, technology and ability.
- The model must provide children with suitable tools and techniques to improve their performance by means of their attitudes, intentions and actions.

IV. CONCLUSIONS

Based on information from observation and interviews, the children (with one exception) felt that digital tools improved their creative ability. They were quite strongly motivated to use them by a wish to create art works, and also by the wish to improve their technological skills. There was also some understanding of the value of these tools in learning other subjects. It appears that the method of teaching art is important in promotingpupils'artistic ability and creative activity, and also in revealing students' talent. The teacher should encourage the students in order to stimulate and motivate them.

It seems that, in general, ease of use was not the main motivation when the children used digital tools. They found more ease and enjoyment, generally, when using traditional methods. The most popular digital methods were sometimes the easiest to use, but according to their own statements, it was not the ease of use, but the successful effects the tools provided which motivated the children to use them. It seems, therefore, that enjoyment and artistic satisfaction is more significantfor pupils than ease of use. Usefulness is more valuable than ease. The pupils all showed independence and initiative after an early lack of confidence. The researcher's opinion is that creative abilities and skills have been increased by the project. Surprisingly, although girls are traditionally regarded as less adventurous than boys, the girls showed more signs of acceptance of digital methods than the boys. The TAM method showed itself to be very useful in assessing the value of traditional and digital tools. It was also useful in documenting the children's progress in learning to use digital software, and it helped to assess the effect of the tools in motivating the children. In the researcher's opinion, the digital tools did improve the children's artistic expression and creativity.

V. ACKNOWLEDGEMENTS

I would like to thank best friend Julia Bridge continuous support in my research; she always encouraging me to press on. Massive gratitude also goes to my parents and my husband for their motivation and encouragement.

REFERENCES

[1] P.Hawks. "The relevance of traditional drawing in the digital age"Thames Valley University 33 St Peters Road Reading RG6 1NT phil.hawks@gmail.com. 2010.
[2] M.I.Pinsky. The gospel according to Disney: Faith, trust, and pixie dust. Westminster John Knox Pr.2004.
[3] F.D. Davis, R. Bagozzi, P. Warshaw. User acceptance of computer technology: A comparison of two theoretical models, Management Science 35: 982–1003- 1989.
[4] D. Hods. Digital drawing exploring the possibilities of digital technology as an essential tool and component in contemporary drawing, Department of Art, University of Minnesota. Minneapolis USA. 2008.
[2] R. S. Johansson. G. Westling, A. Bäckström, J. R. Flanagan. Eye–hand co-ordination in object manipulation, Journal of Neuroscience 21 (17): 6917–6932. PMID 11517279. 2001.
[5] S.Bråten. Intersubjective Communication and Emotion in Early Ontogeny, Cambridge University Press. Online book.2006.
[6] M.Papadimitriou. "The Impact Images have on children's Learning in a Hypermedia Environment". Journal of Hypermedia in Education. Downloaded in October 2012.1997
[7] C. Hodes Computer as catalyst. Pub. Printmaking Today, Vol. 6 No. 2, p. 26.1997.
[8] C.H. Faber. Digital Drawing Tablet to Traditional Drawing on Paper: A Teaching Studio Comparison. In Proc. IASDR 2009
[9] Y.Gan. "The Effect of Drawing Generated by Students on Idea Production and Writing in Grade 4". Ontario Institute for Studies in Education, University of Toronto, 252 Bloor Street West. Toronto, Ontario, M5S 1V6. Canada yongcheng.gan@utoronto.ca. 2008.
[10] F.D. Davis, A technology Acceptance Model for Empirically Testing New End-User Information Systems: Theory and Result, Doctoral dissertation. Sloan School of Management, Massachusetts Institute of Technology. pp.1-291 Available at: http://dspace.mit.edu/handle/1721.1/15192,1986.

Aber Salem Sasi Aboulgasem is a PhD student in school of Computing Engineering and department of informatics, studying "How art digital tools can develop students aged 9-10 years old in classroom". Her researches interests include enhance artistic ability and promote creative activity by using digital tools on students of primary school. She received her B.C. in Journalism in 1993 from Faculty of Fine Art and Media. M.A in Graphics (2005) in Faculty of Fine Art from VUT University, technique university Brno, Czech Republic. She had both teaching undergraduate and postgraduate in Fine art department and in Media department. Some experience in primary school. She previously worked as research assistant at Faculty of Art and Media in Tripoli University in Libya. She had some publications in Art digital tools. She has a several experience in art "graphic, painting, drawing and visual Media" now she is concentrating on art using digital tools.

ISSN (e): 2250 – 3005 || Vol, 04 || Issue, 9 || September – 2014 ||
International Journal of Computational Engineering Research (IJCER)

Some Other Properties of Fuzzy Filters on Lattice Implication Algebras

Priyanka Singh[1], Amitabh Banerjee[2], Purushotam Jha[3]
[1]Department of Engineering, ITM University Raipur(C.G)
[2]Department of Mathematics, Govt. D.B.Girls P.G.College Raipur(C.G)
[3]Department of Mathematics, Govt. J.Y.C.G.College Raipur(C.G)

ABSTRACT
In this paper we discuss several properties of fuzzy filters are given in lattice implication algebra, the new equivalent conditions for fuzzy filters are also discuss in lattice implication algebra.

KEYWORDS- *Lattice implication algebra, fuzzy implication, filter, fuzzy implicative filter.*

I. INTRODUCTION

The concept of fuzzy set was introduced by zadeh[6]. Since then this concept has been Applied to other algebaric structure such as group, semigroup, ring, modules, vector space and topologies. With the development of fuzzy set, it is widely used in many fields. In order to research the logical system whose propositional value was given in a lattice , Xu. proposed the concept of lattice implication algebra and discussed their properties in [1]. Xu and Qin introduced the concept of filters and implicative filters in lattice implication algebra and investigate their properties in[2]. In [3] Xu. applied the concept of fuzzy sets to lattice implication algebra and proposed the notions of fuzzy filters and fuzzy implicative filters. In [7] [8] the notions of implicative filters, positive implicative and associative filters were studied. In[9][10] fuzzy filters, fuzzy positive implication and fuzzy associative filters were presented. In [11] Qin and Liu introduced a new class of filters known as v-Filters and they generated relation between v-filters and filters. Filter theory play an important role in studying the structure of algebra. In this paper we discuss several equivalent conditions for fuzzy filters are proved in lattice implication algebra. At the same time we discuss the relations of fuzzy filters and fuzzy implicative filters.

II. PRELIMANARIES

Definition 2.1. [5] A binary operator

$$I : [0, 1] \times [0, 1] \to [0, 1]$$

is said to be an implication function or an implication if it satisfies;
i) $I(x, y) \geq I(y, z)$ when $x \leq y$, $\forall z \in [0, 1]$.
ii) $I(x, y) \leq I(x, z)$ when $y \leq z$, $\forall x \in [0, 1]$.
iii) $I(0, 0) = I(1, 1) = I(0, 1)$ and $I(0, 1) = 0$ etc.

Definition 2.2. [1] Let $(L, \vee, \wedge, O, I)$be a bounded lattice with an order-reversing involution $'$, I and O the greatest and smallest element of L respectively, and
$\to: L \times L \to L$ be a mapping. $(L, \vee, \wedge, ', O, I))$ is called a quasi-lattice implication algebra if the following conditions hold for any $x, y, z \in L$
(I1) $x \to (y \to z) = y \to (x \to z)$;
(I2) $x \to x = I$;
(I3) $x \to y = y \to x$;
(I4) $x \to y = y \to x = I$ implies $x = y$
(I5) $(x \to y) \to y = (y \to x) \to x$

Definition 2.3. [1] A quasi-lattice implication algebra is called a lattice implication algebra, if (I1) and (I2) hold for any $x, y, z \in L$
(I1) $(x \vee y) \to z = (x \to z) \wedge (y \to z)$;
(I2) $(x \wedge y) \to z = (x \to z) \vee (y \to z)$;

Theorem 2.1. [1] Let L be a quasi-lattice implication algebra, then for any x, y, x ∈ L
1. If I → x = I, then x = I;
2. I → x = x and x → O = x;
3. O → x = I and x → I = I;
4. (x → y) → ((y → z) → (x → z)) = I

Theorem 2.2. [1] Let L be a lattice implication algebra, then for any x, y ∈ L, x ≤ y if and only if x → y = I.

Theorem 2.3. [1] Let L be a lattice implication algebra, then for any x, y, z ∈ L, x ≤ y ,
1. (x → z) → (y → z) = y → (x ∨ z) = (z → x) → (y → x)
2. (z → x) → (z → y) = (x ∧ z) → y = (x → z) → (x → y).

Theorem 2.4. [1] Let L be a lattice implication algebra, then for any x, y, z ∈ L,
1. z → (y → x) ≥ (z → y) → (z → x);
2. z ≤ y → x if and only if y ≤ z → x.

Theorem 2.5. [1] Let L be lattice implication algebra then the following statements are equivalent;
1. For any x, y, z ∈ L, x → (y → z) = (x ∧ y) → z;
2. For any x, y ∈ L, x → (x → y) = x → y;
3. For any x, y, z ∈ L,
   (x → (y → z)) → ((x → y) → (x → z)) = I

In lattice implication algebra L, we define binary operations ⊕ and ⊗ as follows: for any x, y ∈ L;
x ⊗ y = (x → y′)′ ;
x ⊕ y = x → y;

Theorem 2.6. [1] Let L be a lattice implication algebra, then for any x, y, z ∈ L,
1. x ⊗ y = y ⊗ x, x ⊕ y = y ⊕ x;
2. x → (x ⊗ y) = x ∨ y = (x ⊕ y) → y;
3. (x → y) ⊗ x = x ∧ y;
4. x → (y → z) = (x ⊗ y) → z;
5. x → (y → z) if and only if x ⊗ y ≤ z;

Definition 2.4. [2] A non-empty subset F of lattice implication algebra L is called a filter of L if it satisfies
(F1) I ∈ F
(F2) (∀x ∈ F)(∀y ∈ L)(x → y ∈ F ⇒ y ∈ F)

Definition 2.5. [3] A fuzzy set A of lattice implication algebra L is called a fuzzy filter of L if it satisfies
(F3) (∀x ∈ L)(A(I) ≥ A(x))
(F4) (∀x, y ∈ L)(A(y) ≥ min{A(x), A(x → y)})

Definition 2.6. [3] Let L be a lattice implication algebra. A is a non-empty fuzzy set of L . A is called a fuzzy implicative filter of L if it satisfies:
(F5) A(I) ≥ A(x) for any x ∈ L;
(F6) A(x → z) ≥ min{A(x → y), A(x → (y → z))} for any x, y, z ∈ L

Theorem 2.7. [3] Let L be a lattice implication algebra and A a fuzzy filter of L, then for any x, y ∈ L, x ≤ y implies A(x) ≤ A(y)

III. PROPERTIES OF FUZZY FILTERS

Theorem 3.1. [9] Let A be a fuzzy set of L. A is a fuzzy filter of L if and only if it satisfies the following conditions; for any x, y, z ∈ L
1. A(x) ≤ A(I);
2. A(x → z) ≥ min{A(x → y), A(y → z)}.

Theorem 3.2. [9] Let A be a fuzzy set of L. A is a fuzzy filter of L if and only if it satisfies the following conditions; for any x, y, z ∈ L
1. $A(x) \leq A(I)$;
2. $A(z) \geq \min\{A(x), A(y), A(x \to (y \to z))\}$.

Theorem 3.3. [9] Let A be a fuzzy set of L. A is a fuzzy filter of L if and only if it satisfies the following conditions; for any x, y, z ∈ L
1. $A(x) \leq A(I)$;
2. $A(z \to x) \geq \min\{A((z \to y) \to x), A(y)\}$.

Theorem 3.4. [9] Let L be a lattice implication algebra and A be a fuzzy set of L, if A is a fuzzy implicative filter, the following statements are satisfied and equivalent:
1. A is a fuzzy filter for any x, y ∈ L,
$A(x \to y) \geq A(x \to (x \to y))$;
2. A is a fuzzy filter and for any x, y, z ∈ L,
$A((x \to y) \to (x \to z)) \geq A(x \to (y \to z))$
3. $A(x) \leq A(I)$ and for any x, y, z ∈ L
$A(x \to y) \geq \min\{A(z \to (x \to (x \to y))), A(z)\}$

Theorem 3.5. [9] Let A be a fuzzy filter of L if $x \leq y \to z$for any x, y, z ∈ L then
$A(z) \geq \min\{A(x), A(y)\}$
Corollary 3.1. [9] Let A be a fuzzy filter of L. If $(x \otimes y) \to z = I$ for any x, y, z ∈ L, then

$$A(z) \geq \min\{A(x), A(y)\}.$$

Theorem 3.6. [9] Let A be a fuzzy set of L. A is a fuzzy filter of L iff it satisfies the following conditions: for any x, y ∈ L.

1. If $x \leq y$, then $A(x) \leq A(y)$;
2. $A(x \otimes y) \geq \min\{A(x), A(y)\}$

IV. SOME OTHER PROPERTIES OF FUZZY FILTERS

Theorem 4.1. Let A be a fuzzy set of L. A is a fuzzy filter of L iff it satisfies the following conditions, for any x, y, z ∈ L
1. $A(x) \leq A(I)$;
2. $A(y \to (x \vee z)) \geq \min\{A(x \to z), A(x \to z) \to y))\}$
Proof: Assume that A is a fuzzy filter of L. then (1) is trivial and for any x, y, z ∈ L
$(y \to (x \vee z)) \geq \min\{A(x \to z), A(x \to z) \to y)\}$
by theorem 2.2 it can suffices to prove that
$(x \to (x \vee z)) \to ((x \to z) \to y) = I$
for this
$= (y \to (x \vee z)) \to ((x \to z) \to y)$
$= ((z \to x) \to (y \to x)) \to ((x \to x) \to y)$
$= ((z \to y) \to (z \to y)) = I$ if $x = I$
then $(y \to (x \vee z)) \geq ((x \to z) \to y)$
Then form theorem 2.6 hence
$A(y \to (x \vee z)) \geq \min\{A(x \to z), A((x \to z) \to y)\}$ conversely by (1) and (2) it follows that $A(x) \leq A(I)$ and for any x ∈ L
By (2) it follows that for any x, y, z ∈ L if we take $x = I$ then
$A(y) \geq \min(A(z), A(z \to y))$
Hence A is a fuzzy filter of L.

Theorem 4.2. Let A be a fuzzy set of L. A is a fuzzy filter of L iff it satisfies the following conditions for any x, y, z ∈ L
1. $A(y) \leq A(I)$
2. $A(y \to z) \geq \min\{A(x), A(y), A(x \to (y \to z))\}$
Proof: Assume that A is a fuzzy filter of L, then (1) is trivial and for any x, y, z ∈ L
$A(y \to z) \geq \min\{A(x), A(y), A(x \to (y \to z))\}$
By theorem 2.2 it can suffices to prove that

$((x \to (y \to z)) \to (y \to z)) = I$
For this we have
$= ((x \to (y \to z)) \to (y \to z))$
$= ((x \to z) \to z$ if $y = I$
$= (x \to (z \to z)$
$= (x \to I) = I$
Then $((x \to (y \to z)) \leq (y \to z)$
Then form theorem 2.6 hence
$A((x \to (y \to z)) \leq A(y \to z)$
It follows that
$A(y \to z) \geq \min\{A(x), A(y), A(x \to (y \to z)\}$
conversely by (1) and (2) it follows that $A(x) \leq A(I)$ and for any $x \in L$
By (2) it follows that for any $x, y, z \in L$ if we take $y = I$ then
$A(z) \geq \{A(x), A(x \to z))\}$
Hence A is a fuzzy filter of L.

Theorem 4.3. Let A is a fuzzy filter of L, if $x \leq y$ for any $x, y \in L$ then
1. $A(x) \leq A(I)$
2. $A(x \vee y) \geq \min\{A(x), A(x \oplus y)\}$
Proof:Suppose that A is a fuzzy filter of L then (1) is trivial any for any $x, y \in L$
$A(x \vee y) \geq \min\{A(x), A(x \oplus y)\}$
for this we have to show that
$(x \to (x \oplus y)) \to (x \vee y) = I$
By theorem 2.2 . Hence
$= (x \oplus y) \to (x \to (x \vee y))$
$= (x \oplus y) \to ((y \to x) \to (x \to x))$
By theorem 2.3, and
$= (x \oplus y) \to ((y \to x) \to I)$
$= (x \oplus y) \to (y \to (x \to I))$
$= (x \oplus y) \to (y \to I)$
By theorem 2.1 and
$= (x \oplus y) \to I$ by theorem 2.5 and
$= (x \to y) \to I$ because $x \leq y$ hence
$(x \to (x \oplus y)) \to (x \vee y) = I$
this implies that
$(x \oplus y) \leq (x \to (x \vee y))$ Then by theorem 2.2 we get
$A(x \oplus y) \leq A(x \to (x \vee y))$
$A(x \to (x \vee y)) \geq \min\{A(x \oplus y)\}$ by theorem 2.7
Hence
$A(x \vee y) \geq \min\{A(x), A(x \oplus y)\}$.

V. CONCLUSION

In this paper we define some other equivalent conditions for fuzzy filters in lattice implication algebra.The relation between fuzzy filters and fuzzy implicative filters are also defined, and we also prove that fuzzy implicative filters are fuzzy filters in lattice implication algebra.

REFERENCES

[1] Y.Xu, Lattice implication algebra, J.Southwest Liaotong Univ. 1, pp. 20-27,1993.
[2] Y.Xu, K.Y.Qin, On filters of lattice implication algebras, J. Fuzzy Math. 1:251-260, 1993.
[3] Y.Xu, K.Y.Qin, Fuzzy lattice implication algebras, J. Southwest Jiaotong Univ. 30:121-127,1995.
[4] Lukasiewicz, J : Interpretaejaliczbowateoriizda'n Ruchfilzoficzny 7:92-98,1923.
[5] Benjam'In C. Bedregal et.al. : Xor-implications and E- implications b: classes of fuzzy implications based on fuzzy xor,2008.
[6] Zadeh, L.A. : Fuzzy sets. Infor and Control 8:94-102,1965.
[7] Y.B.Jun, Implicative filters of lattice implication algebra, Bull. Korean Math. Soc.34(2):193-198, 1997.
[8] Y.B.Jun, Y.Xu, K.Y.Qin, Positive implicative and associative filters of lattice impli- cation algebras, Bull. Korean Math. Soc 35(1):53-61,1998.
[9] K.Y.Qin, Y.Xu, On some properties of fuzzy filters of lattice implication algebra, Liu. Y.M.(Ed.)Fuzzy set Theory and its Application. Press of Hebi University, Baoding, China,179-182,1998.
[10] Y.B.Jun, Fuzzy positive implicative and fuzzy associative filters of lattice implication algebras, Fuzzy sets an systems. 121:353-357,2001.
[11] Y.Qin, Y.Liu, v-Filters on Lattice Implication Algebras,Journal of Emerging Trends in Computing and Information Sciences.3(9):1298-1301,2012.

ISSN (e): 2250 – 3005 || Vol, 04 || Issue, 9 || September – 2014 ||
International Journal of Computational Engineering Research (IJCER)

Global Domination Set in Intuitionistic Fuzzy Graph

R. JahirHussain [1] ,S. Yahya Mohamed [2]

[1]P.G and Research Department of Mathematics, Jamal Mohamed College (Autonomous), Tiruchirappalli-620 020, India

[2]P.G and Research Department of Mathematics, Govt. Arts College, Trichy-22, India

ABSTRACT

In this paper, We define global Intuitionistic fuzzy domination set and its number of IFGs. Also connected Intuitionistic fuzzy domination number of IFGs are discussed. Some results and bounds of global Intutionistic fuzzy domination number of IFGs are established.

KEYWORDS: *Intuitionistic fuzzy graph, connected Intuitionistic fuzzy dominating set, global Intuitionistic fuzzy dominating set, effective degree.*

2010Mathematics Subject Classification: *05C69, 03F55, 05C72, 03E72.*

I. INTRODUCTION

Atanassov [1] introduced the concept of intuitionistic fuzzy (IF) relations and intuitionistic fuzzy graphs (IFGs). Research on the theory of intuitionistic fuzzy sets (IFSs) has been witnessing an exponential growth in Mathematics and its applications. R. Parvathy and M.G.Karunambigai's paper [7] introduced the concept of IFG and analyzed its components. Nagoor Gani, A and Sajitha Begum, S [5] defined degree, Order and Size in intuitionistic fuzzy graphs and extend the properties. The concept of Domination in fuzzy graphs is introduced by A. Somasundaram and S. Somasundaram [8] in the year 1998. Parvathi and Thamizhendhi[6] introduced the concepts of domination number in Intuitionistic fuzzy graphs. Study on domination concepts in Intuitionistic fuzzy graphs are more convenient than fuzzy graphs, which is useful in the traffic density and telecommunication systems. The Global domination number of a Graph was discussed by E. Sampathkumar [10] in 1989.In this paper, We define global Intuitionistic fuzzy domination set of IFG and discuss the situation of this concept used in network. Also some thereoms and bounds of global Intuitionistic fuzzy domination number of IFGs are established.

II. PRELIMINARIES

Definition 2.1: An Intuitionistic fuzzy graph is of the form G = (V, E) where

(i) V={v1,v2,….,vn} such that μ_1: V→[0,1]and γ_1: V →[0,1] denote the degree of membership and non-membership of the element vi ϵV, respectively, and

$0 \le \mu_1(vi) + \gamma_1(vi) \le 1$ for every vi ϵV, (i = 1,2, ……. n),

(ii) E $\subseteq$ V x V where μ_2: VxV →[0,1] and γ_2: VxV →[0,1] are such that

$\mu_2(vi, vj) \le \min[\mu_1(vi), \mu_1(vj)]$ and $\gamma_2(vi, vj) \le \max[\gamma_1(vi), \gamma_1(vj)]$

and $0 \le \mu_2(vi, vj) + \gamma_2(vi, vj) \le 1$ for every (vi ,vj) ϵ E, (i, j = 1,2, ……. n)

Definition 2.2 An IFG H = < V', E' > is said to be an Intuitionistic fuzzy subgraph (IFSG) of the IFG, G = < V, E > if V' $\subseteq$V and E' $\subseteq$ E. In other words, if $\mu_{1i}' \le \mu_{1i}$; $\gamma_{1i}' \ge \gamma_{1i}$ and $\mu_{2ij}' \le \mu_{2ij}$; $\gamma_{2ij}' \ge \gamma_{2ij}$ for every i, j = 1,2…….n.

Definition 2.3: Let G = (V,E) be a IFG. Then the cardinality of G is defined as

$$|G| = \left| \sum_{vi \in V} \frac{1+\mu_1(vi)-\gamma_1(vi)}{2} + \sum_{vi,vj \in E} \frac{1+\mu_2(vi,vj)-\gamma_2(vi,vj)}{2} \right|$$

Definition 2.4: The vertex cardinality of IFG G is defined by

$$|V| = \left| \sum_{vi \in V} \frac{1+\mu_1(vi)-\gamma_1(vi)}{2} \right| = p \text{ and}$$

The edge cardinality of IFG G is defined by $|E| = \left| \sum_{vi,vj \in E} \frac{1+\mu_2(vi,vj)-\gamma_2(vi,vj)}{2} \right| = q$.

The vertex cardinality of IFG is called the order of G and denoted by O(G). The cardinality of G is called the size of G, denoted by S(G).

Definition 2.5: An edge e = (x, y) of an IFG G = (V, E) is called an effective edge if $\mu_2(x, y) = \mu_1(x) \wedge \mu_1(y)$ and $\gamma_2(x, y) = \gamma 1(x) \vee \gamma 1(y)$.

Definition 2.6: An Intuitionistic fuzzy graph is complete if $\mu_{2ij} = \min(\mu_{1i}, \mu_{1j})$ and $\gamma_{2ij} = \max(\gamma_{2i}, \gamma_{2j})$ for all (vi , vj) $\in$ V.

Definition 2.7: An Intuitionistic fuzzy graph G is said to be strong IFG if $\mu_2(x, y) = \mu_1(x) \wedge \mu_1(y)$ and $\gamma_2(x, y) = \gamma 1(x) \vee \gamma 1(y)$ for all (vi , vj) $\in$ E. That is every edge is effective edge.

Definition 2.8 : The complement of an IFG G = < V, E > is denoted by $\bar{G}$ = ($\bar{V}$, $\bar{E}$) and is defined as i) $\bar{\mu}_1(v) = \mu_1(v)$ and $\bar{\gamma}_1(v) = \gamma_1(v)$

ii) $\bar{\mu}_2(u,v) = \mu_1(u) \wedge \mu_1(v) - \mu_2(u,v)$ and $\bar{\gamma}_2(u,v) = \gamma_1(u) \vee \gamma_1(v) - \gamma_2(u,v)$ for u,v in V

Definition 2.9: Let G = (V,E) be an IFG. The neighbourhood of any vertex v is defined as N(v) = ($N_\mu(v)$, $N_\gamma(v)$), Where $N_\mu(v) = \{w \in V : \mu_2(v,w) = \mu_1(v) \wedge \mu_1(w)\}$ and $N_\gamma(v) = \{w \in V : \gamma_2(v,w) = \gamma_1(v) \vee \gamma_1(w)\}$. N[v] = N (v) $\cup$ {v} is called the closed neighbourhood of v.

Definition 2.10: The neighbourhood degree of a vertex is defined as $d_N(v) = (d_{N\mu}(v), d_{N\gamma}(v))$ where $d_{N\mu}(v) = \sum_{w \in N(v)} \mu_1(w)$ and $d_{N\gamma}(v) = \sum_{w \in N(v)} \gamma_1(w)$.

The minimum neighbourhood degree is defined as $\delta_N(G) = (\delta_{N\mu}(v), \delta_{N\gamma}(v))$, where $\delta_{N\mu}(v) = \wedge \{ d_{N\mu}(v) : v \in V\}$ and $\delta_{N\gamma}(v) = \wedge \{ d_{N\gamma}(v) : v \in V\}$.

Definition 2.11: The effective degree of a vertex v in a IFG. G = (V, E) is defined to be sum of the effective edges incident at v, and denoted by $d_E(v)$. The minimum effective degree of G is $\delta_E(G) = \wedge \{d_E(v)/v \in V\}$

Definition 2.12: Let G= (V, E) be an IFG. Let u, v $\in$ V, we say that u dominated v in G if there exist a strong arc between them. A Intuitionistic fuzzy subset D $\subseteq$V is said to be dominating set in G if for every v$\in$ V-D, there exist u in D such that u dominated v. The minimum scalar cardinality taken over all Intuitionisitc fuzzy dominating sets is called Intuitionistic fuzzy domination number and is denoted by γ. The maximum scalar cardinality of a minimal domination set is called upper Intuitionistic fuzzy domination number and is denoted by the symbol Γ .

Definition 2.13: A Intuitionistic fuzzy dominating set D$\subseteq$V of IFG G is said to be a Intutitionisitc fuzzy connected dominating set of G if the subgraph <D> induced by D is connected. The minimum cardinality taken over all minimal Intuitionistic fuzzy connected dominating sets is called Intuitionistic fuzzy domination number of G and it is denoted by $\gamma_c(G)$.

Definition 2.14: An independent set of an Intuitionistic fuzzy graph G = (V, E) is a subset S of V such that no two vertices of S are adjacent in G.

Definition 2.15: A Bipartite IFG, G= (V,E) is said to be complete Bipartite IFG, if $\mu_2(v_i, v_j) = \mu_1(v_i) \wedge \mu_1(v_j)$ and $\gamma_2(v_i, v_j) = \gamma_1(v_i) \vee \gamma_1(v_j)$ for all $v_i \in V_1$ and $v_j \in V_2$. It is denoted by $K_{v1i, v2j}$.

III. GLOBAL INTUITIONISTIC FUZZY DOMINATION SET IN IFG

Definition 3.1: Let G = (V, E) be an IFG. A Intuitionistic fuzzy dominating set S $\subseteq$ V is said to be global Intuitionistic fuzzy dominating set of G if S is also a Intuitionistic fuzzy dominating set of $\bar{G}$.

The minimum cardinality of global Intuitionistic fuzzy dominating sets is global Intuitionistic fuzzy domination number and is denoted by $\gamma_g(G)$.

Example:

In case of transportation and road networks, the travel time is mostly used as weight. The travel time is a function of the traffic density on the road and/or the length of the road. The length of a road is a crisp quantity but the traffic density is fuzzy. In a road network, we represent crossings as nodes and roads as edges. The traffic density is mostly calculated on the road between adjacent crossings. These numbers can be represented as intuitionistic fuzzy numbers. Road network represented as an intuitionistic fuzzy graph $R^* = (C, L)$, where C is an intuitionistic fuzzy set of crossings at which the traffic density is calculated and L is an intuitionistic fuzzy set of roads between two crossings. The degrees of membership, $\mu_L(xy)$, and non membership, $\nu_L(xy)$, are calculated as $\mu_L(xy) = \min(\mu_C(x), \mu_C(y))$, $\gamma_L(xy) = \max(\gamma_C(x), \gamma_C(y))$.

Some essential goods are being supplied to some crossings from supplying stations located some other crossings. It may happen that the roads(edges of G) may be closed for some reason or the other. So, we have to think of maintaining the supply of goods to various crossing uninterrupted through secret links (i.e. edges of the complement of network). We have to find minimum number of supplying stations(crossings) needed which is called global Intuitionistic fuzzy domination number.

Example 3.2: Let G = (V,E) be IFG be defined as follows

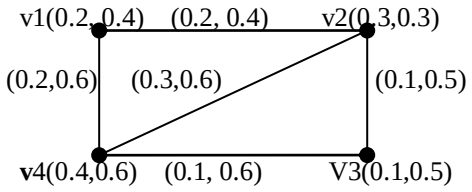

Fig- 1: Intuitionistic fuzzy graph(G)

Here |v1| = 0.4 , |v2| = 0.5, |v3| = 0.3, |v4| = 0.4 and minimum γ_g-set is { v2, v3, v4} and therefore $\gamma_g(G) = 1.2$.

Observations 3.3:

(i) $\gamma_g(Kn) = \gamma_g(\bar{K}_n) = p$

(ii) $\gamma_g(K_{V1i\,,V2j}) = \text{Min } \{|vi|\} + \text{Min } \{|vj|\}$, where $v_i \in V_1$ and $v_j \in V_2$.

Proposition 3.4: The global Intuitionistic fuzzy dominating set is not singleton.

Proof: Since gifd-set contain dominating set for both G and G^{sc} then at least two vertices are in the set.
i.e) The gifd-set containing at least two vertices.

Theorem 3.5: For any IFG G= (V, E) with effective edges, $\text{Min}\{|V_i|+|V_j|\} \leq \gamma_g(G) \leq p$, $i \neq j$

Proof: We know that global Intuitonistic fuzzy dominating set has at least two vertices. Let {vi, vj} are the vertices, then $\text{Min}\{|Vi|+|Vj|\} = \gamma_g(G)$
If the set contains other than {vi, vj} then $\text{Min}\{|Vi|+|Vj|\} < \gamma sg(G)$, $i \neq j$
If the given G is complete IFG then gifd-set contains all the vertices of the G, that is $\gamma_g(G) \leq O(G) = p$
i.e.) We get, $\text{Min}\{|Vi|+|Vj|\} \leq \gamma_g(G) \leq p$.

Theorem 3.6: Let G = (V, E) be the IFG and the Intuitionistic fuzzy dominating set S of G is global Intuitionistic fuzzy dominating set if and only if, for each v ∈ V-S, there exists a u ∈S such that u is not adjacent to v.

Proof: Let S is global dominating set and also dominating set.
Suppose u is adjacent to v then we get S is not a dominating set.
Which is contradiction. That is u is not adjacent to v.
Conversely, for each v ∈ V-S and u is not adjacent to v then the set S is dominating both G and $\bar{G}$. That is S is global Intuitionistic fuzzy dominating set.

Theorem 3.7: Let G = (V, E) be an IFG then (i) $\gamma_g(G) = \gamma_g(\bar{G})$ (ii) $\gamma(G) \leq \gamma_g(G)$

Proof: G is connected IFG and γ_g-set dominating vertices of G and $\bar{G}$. Clearly $\gamma_g(G) = \gamma_g(\bar{G})$.
Suppose D is the γ-set of G then the number of vertices in the dominating set is less than or some time equal to γ_g-set. That is $\gamma(G) \leq \gamma_g(G)$.

Theorem 3.8: Let S be the minimum Intuitionisitc fuzzy dominating set of IFG G containing t vertices. If there exist a vertex v ∈ V-S adjacent to only vertices in S then γ_g-set contain atmost t+1 vertices.

Proof: Since S is the γ-set and v ∈ V-S adjacent to only vertices in S then we get S∪{v} is a global Intuitionistics fuzzy dominating set.
That is γ_g-set contain atmost t+1 vertices.

Theorem 3.9: Let G = (V, E) be strongly connected IFG then, at least one of the following holds.
(i) $\gamma_c(G) \leq \gamma_g(G)$. (ii) $\bar{\gamma}_c(G) \leq \gamma_g(G)$.

Proof: Since γ_c-set also dominating set and induced Intuitionistic fuzzy subgraph is connected then the Gc may be disconnected and it is less than or equal to γ_g-set.
That is $\gamma_c(G) \leq \gamma_g(G)$. Similarly, we have $\bar{\gamma}_c(G) \leq \gamma_g(G)$.

Definition 3.10: G = (V, E) be a connected IFG with effective edges which is said to be semi complete IFG, if every pair of vertices have a common neighbor in G .

The IFG G is said to be purely semi complete IFG if G is semi complete IFG but not complete IFG.

Example 3.11:

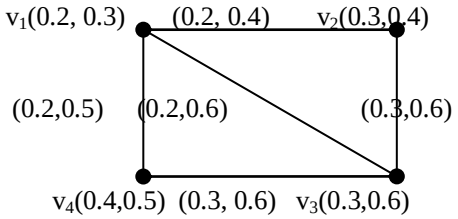

Fig-2: Purely Semi complete IFG

Theorem 3.12: Let G =(V, E) be the purely semi complete IFG. Then γg-set contains at least three vertices.

Proof: Since G is purely semi complete IFG then it contains triangles with common vertex.

Let v be the common vertex then, In G^c , the vertex v is isolated vertex. Also global Intuitionistic dominating set contains Intuitionistic fuzzy dominating vertices of G and G^c.

Suppose gifd-set contains less than three vertices

We know that gifd-set not a singleton. i.e) gifd-set contains at least two vertices

Let D = { v_1, v_2} be a gifd-set in G.

Case 1: <D> is connected in G

Then v_1v_2 is an effective edge in G. By the definition of semi complete IFG, there is a v_3 in G such that $<v_1v_2v_3>$ is triangle in G, i.e) D is not a Intuitonistic fuzzy domination set in G^c.

Which is contradiction to D is a gifd-set in G.

Case 2: <D> is disconnected in G. i.e.) There is no effective edge between v_1 and v_2 .

Since G is semi complete IFG, there is v_3 in G such that $v_1v_3$and v_3v_2 are the effective edges in G

Therefore, In G^c, v_3 is not dominated by a vertex in D.

Which implies, D is not a gifd-set in G

Which is contradiction to our assumption.

That is γ_g-set contains at least three vertices

Theorem 3.13: Let G = (V, E) be the IFG with effective edges . $\gamma_g(G)$ = Min{|Vi|+|Vj|} i ≠j if and only if there is an effective edge uv in G such that each vertex in V – {u, v} is adjacent to u or v but not both.

Proof: Suppose $\gamma_g(G)$ = Min{|Vi|+|Vj|} i≠j, We assume D = {u, v} be the gifd-set in G

Let <D> is connected in G, then uv is an effective edge in G.

If any vertex w in V-{u, v} is adjacent to both u and v.

Which implies D is not a dominating set for G^c. which is contradiction to our assumption. i.e) effective edge uv in G such that each vertex in V – {u, v} is adjacent to u or v but not both.

Conversely, each vertex in V – {u, v} is adjacent to u or v but not both, then we get γg(G) = Min{|Vi|+|Vj|} i≠j.

IV. CONCLUSION

Here ,We defined global Intuitionistic fuzzy domination set of IFG and discussed the situation of this concept used in network. Also some theorems and bounds of global Intuitionistic fuzzy domination number of IFGs are established. Further we going to establish more results and bounds on this gifd number with other domination parameters.

REFERENCES

[1]. Atanassov. KT. Intuitionistic fuzzy sets: theory and applications. Physica, New York, 1999.
[2]. Bhattacharya, P. Some Remarks on fuzzy graphs, Pattern Recognition Letter 5: 297-302,1987.
[3]. Harary,F., Graph Theory, Addition Wesley, Third Printing, October 1972.
[4]. Kulli,V.R., Theory of domination in graph, Vishwa International Publications, 2010.math. Phys. Sci., 13 (1979), 607-613.
[5]. Nagoor Gani. A and Shajitha Begum.S, Degree, Order and Size in Intuitionistic Fuzzy Graphs, International Journal of Algorithms, Computing and Mathematics, (3) 3 (2010).
[6]. Parvathi,R., and Thamizhendhi, G. Domination in Intuitionistic fuzzy graphs, Fourteenth Int. conf. on IFGs, Sofia, NIFS Vol.16, 2, 39-49, 15-16 May 2010.
[7]. Parvathi, R. and Karunambigai, M.G., Intuitionistic Fuzzy Graphs, Computational Intelligence,Theory and applications,International Conference in Germany, Sept 18 -20, 2006.
[8]. Somasundaram, A and Somasundaram, S., Domination in Fuzzy graph-I, Patter Recognition Letter 19(9), 1998, 787-791.
[9]. Sampathkumar.E, and Walikar.H.B., The connected domination number of a graph, J. math. Phys. Sci., 13 (1979), 607-613.
[10]. Sampathkumar. E., The Global Domination number of a Graph, Jour. Math. Phy. Sc., vol. 23, No. 5, pp. 377-385.
[11]. Tamizh Chelvam. T and Robinson Chelladuari. S, Complementary nil domination number of a graph, Tamkang Journal of mathematics, Vol.40, No.2 (2009),165-172.